Mineral Res. Expl. Bull., 143, 1-12, 2011

THE USE OF TILT ANGLE IN GRAVITY AND MAGNETIC METHODS

Uður AKIN*, Betül IÞIKDENÝZ ÞERÝFOÐLU* and Mehmet DURU**

ABSTRACT.- Tilt angle method, which has been recently used in investigating the boundaries of structures, reveals useful information on deep and shallow structures. Tilt angle is expressed as the arctan value of the ratio of the vertical derivative of the potential field to its horizontal derivative. The method was applied to Kýrþehir-Ý31 sheet. As a result, the presence of volcanites buried under terrestrial sediments was demonstrated.

Key words: Magnetic, gravity, tilt angle, volcanic rocks, Kýrýkkale.

INTRODUCTION

Tilt Angle Method was applied to 1: 100.000 scale Kýrþehir-Ý31 map sheet which is situated between 33°30'-34°00' longitudes and 39°30'-40°00' latitudes in the vicinity of Kýrýkkale (Figure 1). The objective was to determine the subsurface location of the Late Cretaceous aged volcanic rocks in the study area using this method.

In potential field methods (gravity and magnetic) in the determination of the structural boundary of the body causing anomaly, there are a lot of methods such as analytic signal, horizontal derivative, first and second vertical derivatives, Euler deconvolution, artificial gravity, Normalized Full Gradient (NFG). Cordell and Grauch (1982, 1985) studied the magnetization or horizontal variations in density of the upper crustal rocks. Blakely and Simpson (1986) improved the works of Cordell and Grauch and carried out a study which reveals the boundaries of the source body by means of magnetic and gravity anomalies.

Hood and Teskey (1989) and Roest et al. (1992) investigated vertical boundaries of body using horizontal and vertical derivatives. Thompson (1982) made depth estimation applying Euler equation to magnetic data.

With the aim of detection of oil deposits NFG method (Normalized Full Gradient Method) was applied to gravity data for the first time by Berezkin and Buketov (1965). In following years, the application of this method to magnetic data was realized by Berezkin et al. (1994). And in Turkey, Aydýn et al. (1997) and Aydýn (2000, 2007) applied this method to gravity and magnetic data. Furthermore, the method was used in seismic studies by Karslý (2001), in electromagnetic studies by Dondurur (2005) and in SP studies by Sýndýrgýet al. (2008).

Miller and Singh (1994) compared tilt angle with horizontal derivative, second vertical derivative and analytic signal techniques. Salem et al. (2008) developed new techniques to interpret magnetic data. By means of linear correlation, similar to 3D Euler equation, they evaluated tilt angle derivatives and calculated horizontal locations and vertical depths of bodies without using structural index.

TILT ANGLE

Tilt angle is defined as the arctan value of the ratio of the vertical derivative of the potential field to its horizontal derivative (Miller and Singh, 1994; Verduzco at al., 2004) as seen in figure 2.

* Maden Tetkik ve Arama Genel Müdürlüðü, Jeofizik Etütleri Dairesi, 06800 - Balgat/Ankara
** Maden Tetkik ve Arama Genel Müdürlüðü, Jeoloji Etütleri Dairesi, 06800 - Balgat/Ankara

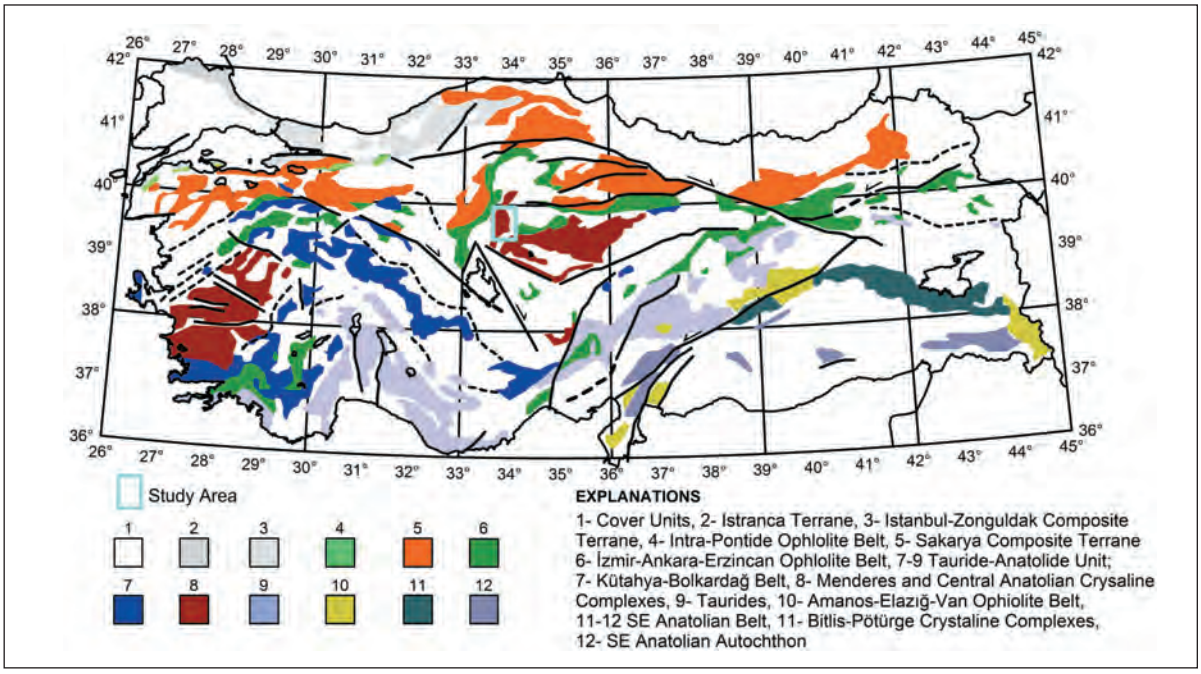

Figure 1- The location map and geological position of the study area in Turkey (Modified after Göncüoðlu et al. 1996).

Tilt angle;

$$\theta = tan^{-1}\frac{\left(\frac{\partial T}{\partial z}\right)}{\left(\frac{\partial T}{\partial h}\right)}$$

where

$$\frac{\partial T}{\partial h} = \left[\left(\frac{\partial T}{\partial x}\right)^2 + \left(\frac{\partial T}{\partial y}\right)^2\right]^{1/2}$$

and ∂T/∂x, ∂T/∂y, ∂T/∂z are first - order derivatives of the potential field in the *x, y*, and *z* directions; ∂T/∂h is total horizontal derivative, *θ* is tilt angle, *T* is potential field.

Horizontal derivatives of potential field data were computed using finite differences relations. For example, at a grid point i,j ; the derivatives of a total magnetic field measurement value T (i,j) in the x and y directions are given as

$$\frac{\partial T}{\partial x} = \frac{T_{i+1,j} - T_{i-1,j}}{2\Delta X}$$

$$\frac{\partial T}{\partial y} = \frac{T_{i,j+1} - T_{i,j-1}}{2\Delta y}$$

The derivatives of the potential field data in the vertical direction can be computed in the frequency environment using the equation below (Gunn, 1975).

$$\frac{\partial^n T}{\partial z^n} = T(f)|f|^n$$

Here, T(f) shows the amplitude value in the f frequency, and n shows order of the derivative. In this study first-order derivatives in the vertical direction were computed (using n=1).

The advantage of the tilt angle method comparing to the other methods is that there is

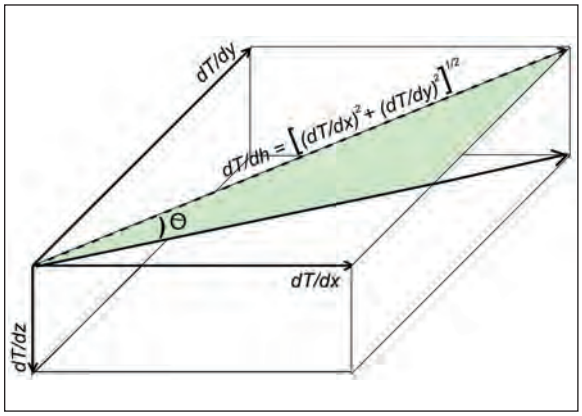

Figure 2- Geometric delineation of tilt angle (θ)

no need for parameters (density, magnetic susceptibility, inclination and deflection angles, permanent magnetization, structural index, etc.). An estimation can be made about the depth of the source from the contours of the tilt angle. Due to the nature of the arctan trigonometric function, all tilt amplitudes are restricted between -90° and +90°.

Miller and Singh (1994) showed the boundaries of the source body by means of tilt angle. As the part where the contours of the tilt angle are positive defines the source itself, the part where the contours are negative represents the outside of the source and the zero contour represents the vertical boundary of the source. For this reason, Miller and Singh (1994) stated that it is possible to obtain reliable results about structural boundaries by means of tilt angle method.

Salem et al. (2007, 2008) expressed the relationship between the upper depth (z_c) and horizontal location (h) of the source by means of a simple drawing.

According to Nabighian (1972) the horizontal and vertical derivatives of the magnetic field over contacts located at a horizontal location of h=0 and at a depth of z_c are given by the equations

$$\frac{\partial T}{\partial h} = 2KF_c\, sind\, \frac{z_c\, \cos(2I-d-90)+h\, \sin\,(2I-d-90)}{h^2+z_c^2}$$

$$\frac{\partial T}{\partial z} = 2KF_c sind\, \frac{hcos(2I-d-90)-z_c \sin\,(2I-d-90)}{h^2+\, z_c^2}$$

where

(K) is the susceptibility contrast at the contact, (F) the magnitude of the magnetic field,

c=1-cos²$i$sin²A,

(A) the angle between the positive h-axis and magnetic north,

(i) the ambient field inclination,

tanI=tani/cosA,

(d) the dip (measured from the positive h-axis) and all trigonometric quantities are in degrees.

Under certain assumptions such as when the contacts are nearly vertical and the magnetic field is vertical or reduced to the pole, last two equations can be written as

$$\frac{\partial T}{\partial h} = 2KF_c\, \frac{z_c}{h^2+z_c^2}$$

$$\frac{\partial T}{\partial z} = 2KF_c\, \frac{h}{h^2+z_c^2}$$

Substituting equations and then we get

$$\theta = tan^{-1}\left(\frac{h}{z_c}\right)$$

then indicates the value of the tilt angle above the edges of the contact is 0° (h=0) (Figure 3) and equal to 45° when h=z_c and -45° when h=-z_c. Half the distance between the contours (± 45°) of the magnetic tilt angle gives the depth (Salem et al., 2007).

The important advantages of this method are its simplicity both in its theoretical derivation and

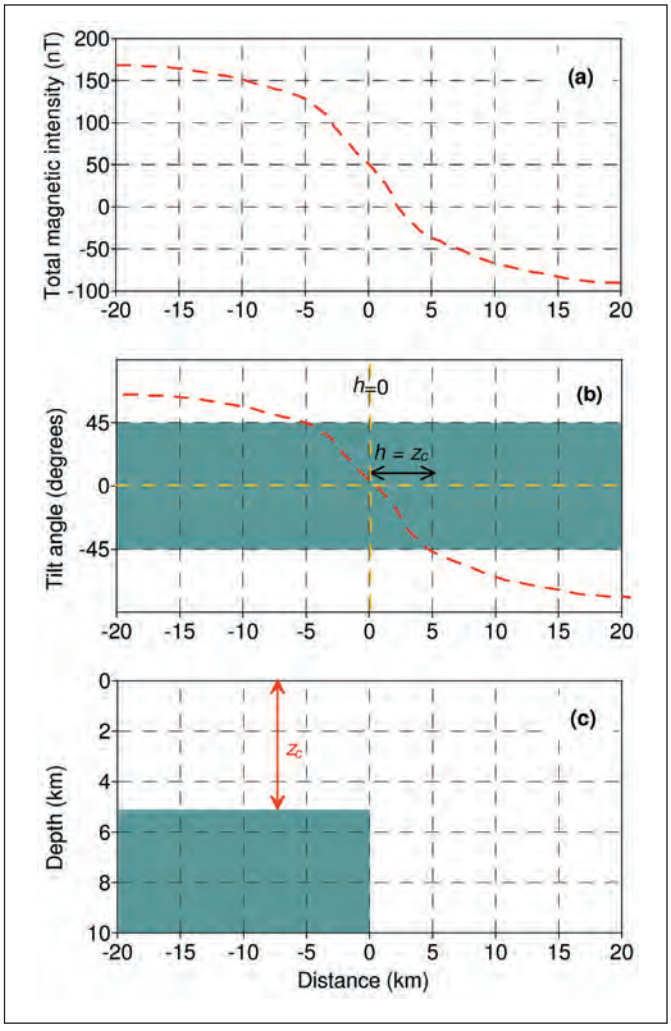

Figure 3- Vertical 2D contact model; a) Total magnetic anomaly, b) The tilt derivative over a vertical contact for reduced-to-pole data. Tilt values are restricted to within ± 90°. The point of coincidence of the part of the tilt derivative between ± 45° with the 0° gives the vertical contact, c) Model structure (Salem et al., 2007).

in its practice application and it provides both a qualitative and quantitative approach for the interpreter about location and depth, there is no need for parameters in calculations, and it is potentially less sensitive to noise comparing to the other methods using higher order derivatives.

THE GEOLOGY OF THE STUDY AREA

For the field application 1/100.000 scale KIRÞEHÝR-Ý31 map sheet, which covers an area of about 2250 km^2 over the Central Anatolian Metamorphic Massif, was selected (Figure 1).

Exploratory geological map of the sheet Ý31 was prepared by Dönmez et al. (2005) from the 1/500.000 scale Geological Map of Turkey (MTA, 2002) (Figure 4). Metamorphic rocks of Kýrþehir Massif constitute the basement lithology of Kýrþehir-Ý31 sheet. Palaeozoic aged metamorphic rocks, affected from low-medium grade regional metamorphism, are generally composed of schist, gneiss and marbles. In the study area these metamorphic basement rocks are represented by marbles and recrystallized limestones (Seymen, 1982; Dönmez et al., 2005). Metamorphic basement rocks are covered by volcanic and sedimentary rocks of Late Cretaceous such as basic volcanites, volcanoclastic and pelagic deposits (Ketin, 1955; Ayan, 1963; Seymen, 1982; Kara and Dönmez, 1990). Volcanics are diabase dikes, basalts, spilitic basalts, alternating with pelagic limestone, mudstone and radiolarite at the bottom, and sandstone and siltstone having volcanic material on the top.

Metamorphic and volcanic rocks are cut by Late-Cretaceous-Paleocene aged plutonic rocks (Ayan, 1963; Ataman, 1972; Seymen, 1982). These plutonic rocks are mainly represented by granite, granodiorite, quartz diorite and syenite. In addition, volcanic and subvolcanic rocks (rhyolite, rhyodacite, trachite, etc) which are closely associated with these plutonic rocks were mapped together with plutonic rocks.

Early Tertiary aged marine sedimentary rocks unconformably overly all these units. These units, consist of a sequence of alternating red-colored terrestrial conglomerate, sandstone and mudstone at the bottom and shallow marine clastics and highly fossiliferous neritic limestones on the top deposited by Eocene transgression (Ketin, 1963; Birgili et al., 1975; Norman, 1972; Oktay, 1981; Kara, 1991; Dönmez et al., 2005). The marine units, which have a thickness of 500-800 m in the mapped area, are of Early-Middle Eocene age. With the regression which started in Late Eocene, the terrestrial-lacustrine units of Oligo-Miocene age, which widely outcrop in the north and east of the region, were deposited. These terrestrial units are represented by a sequence of alternating red-colored conglomerate, sandstone, mudstone at the bottom and by a sequence of alternating variegated lacustrine sandstone, claystone, limestone on the top. Evaporites (gypsum, anhydrite and salt) and ignimbritic tuffs are also observed commonly within these sequences (Pasquare, 1968; Birgili et al., 1975; Uygun et al., 1981; Kara and Dönmez, 1990; Dönmez et al., 2005). Overlying these terrestrial units, which have a thickness of around 100-1500 m, are Quaternary aged alluviums which outcrop in stream and valley bottoms.

FIELD APPLICATION

In this study regional gravity and aeromagnetic data were used. Magnetic data of the study area were taken from the aeromagnetic works of the General Directorate of Mineral Research and Exploration (MTA), conducted during the years of 1978-1989. In this work of MTA, which covered all over Turkey, the flights were carried out by taking into consideration the topography and geological trends. Flight altitude was tried to be maintained at around 625 meters.

The regional gravity data were first started to be taken in the year 1973 by MTA and completed in 1988 through a work lasted 15 years. The regional gravity data of Turkey were taken at intervals of approximately 3 and 5 km.

Tilt angle maps are very useful in that they facilitate the work of the interpreters. The field application was carried out making use of the model shown in figure 3 which shows the relationship between tilt angle and source depth. On the maps of gravity and magnetic tilt angle, the angles are shown in degrees (Figure 5c and 6c). The part between 45 contours is shown in yellow color. Half the vertical distance between these contours gives information about the depth of the body. The contours between 0° and +90°, shown

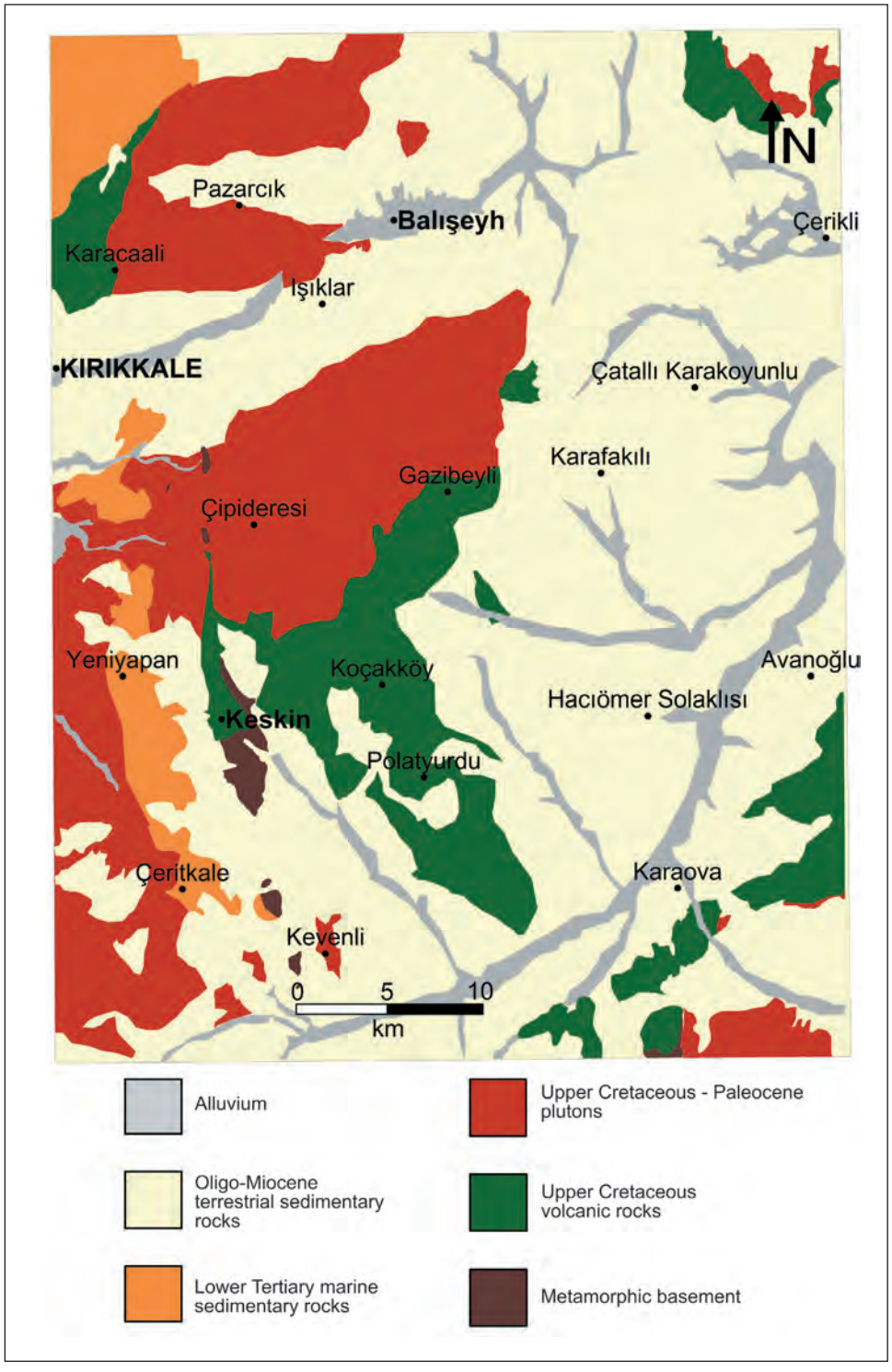

Figure 4- Geological map of 1/100000 scale Kýrþehir Ý31 sheet (modified after Dönmez et al. 2005).

by blue-colored + symbol define the inside of the source and the interval between 0° and -90° defines the outside of the source. The 0° contour shown with red dashed lines determines vertical structural contacts (Figure 5c and 6c).

Reduction-to-the-pole operation was carried out on the aeromagnetic data in order to eliminate dipolar effect. In the application, the magnetic tilt angle map proved to be more complicated compared to that of the gravity tilt angle and made the interpretation considerably difficult. For that reason, in order to eliminate the noise resulting from short wave lengths, 5-km upward continuation was applied to the reduced-to-the-pole map (Figure 6b).

In figure 6c, the anomaly is bordered by 0° contour which follows the settlements of Çerikli, Çatallý Karakoyunlu, Gazibeyli, Koçakköy, Polatyurdu, Kevenli, Hacýömer Solaklýsý and Avanoðlu. It is thought that the structure, which has high-amplitude magnetic anomaly and high susceptibility, was probably resulted from the volcanites underlying the thick terrestrial units (Figure 6b). It was observed that although Late Cretaceous aged volcanic rocks are present in the settlement area of Keskin, Koçakköy, and Polatyurdu on the geological map, magnetic anomaly amplitude was not high. The reason for that is the fact that the thicknesses of the volcanic rocks present here are low and the susceptibilities of the marbles within metamorphites belonging to Kýrþehir Massif and Early Tertiary aged limestones are low. However, on the gravity Bouguer map it is seen that this anomaly continues in the region which comprises Koçakköy, Polatyurdu and Keskin settlements. And the reason for that is the fact that the volcanites are thin and the density of the metamorphic rocks which are situated at the basement and belong to Kýrþehir Massif is higher than that of the volcanites. At the same time, the sporadic outcropping of the marbles and Early Tertiary aged limestones in the region gives rise to positive anomaly (Figure 4 and 5b).

On the other hand, the gravity Bouguer anomaly (Figure 5b) surrounded by Çatallý Karakoyunlu, Çipideresi, Yeniyapan, Kevenli and Karaova settlements is resulted from the fact that the density of the volcanic rocks is higher than that of the granites and terrestrial rocks. And the presence of magnetic anomaly in the same region corroborated the idea that terrestrial sediments are underlain by this volcanic unit.

It is thought that structural boundary differences on the maps of gravity and magnetic tilt angle are resulted from the reasons explained above (Figure 5c and 6c). It is observed that this large gravity and magnetic anomaly is not closed in the east of the sheet (Figure 5b and 6b). It was observed that there was continuation of the gravity Bouguer and magnetic anomalies seen on Ý31 map sheet in the E-W extension, on Ý32 and in part on Ý33 map sheets (Akýn and Çiftçi, 2010). For that reason, tilt angle work was applied also on Ý32 map sheet and it was seen that the anomaly extended up to Çiçekdað. Similarly, it is observed that the same lithological units outcrop at Çiçekdað when the geologic maps of the region are examined (MTA, 2002).

It was determined that the magnetic anomaly observed in small areas to the north of the settlements of Karacaali and Pazarcýk lying in the northwest of the field and also to the north of Çerikli settlement lying in the northeast of the field was also resulted from the volcanites (Figure 6b). In the same way, the gravity anomaly corroborates this (Figure 5b). The determined structural boundaries are observed on the tilt maps as well (Figure 5c and 6c). These structures were correlated with the volcanic rocks situated on the geologic map (Figure 4, 5a, 6a).

It is thought that the anomalies with low amplitude which are present to the south of the study area are resulted from the terrestrial unit with low density and low susceptibility and from the felsic granites (Figure 5b and 6b).

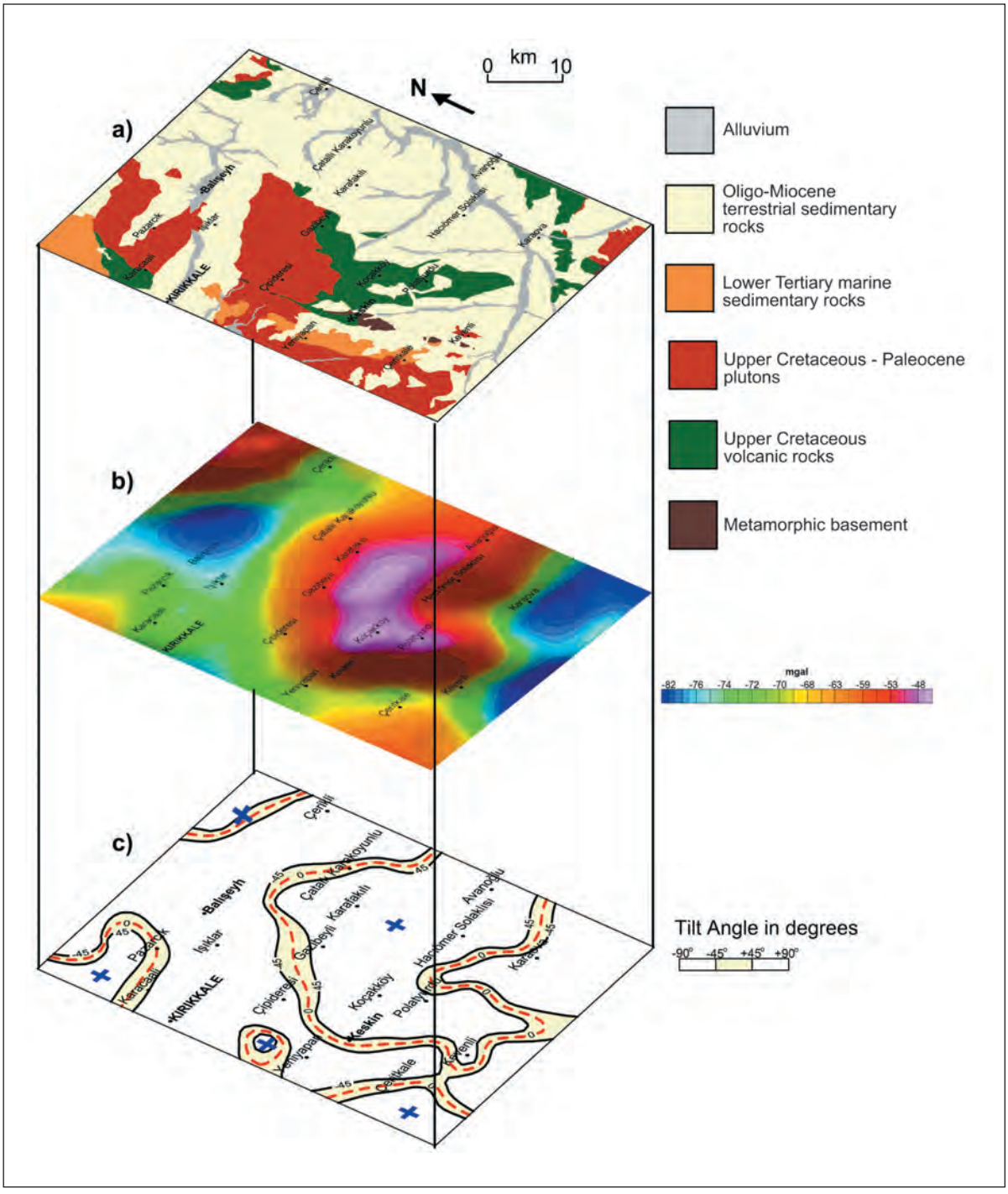

Figure 5- Comparison of study area; a) Geological map of Kýrþehir Ý31 sheet b) Gravity Bouguer map c) Gravity tilt angle map.

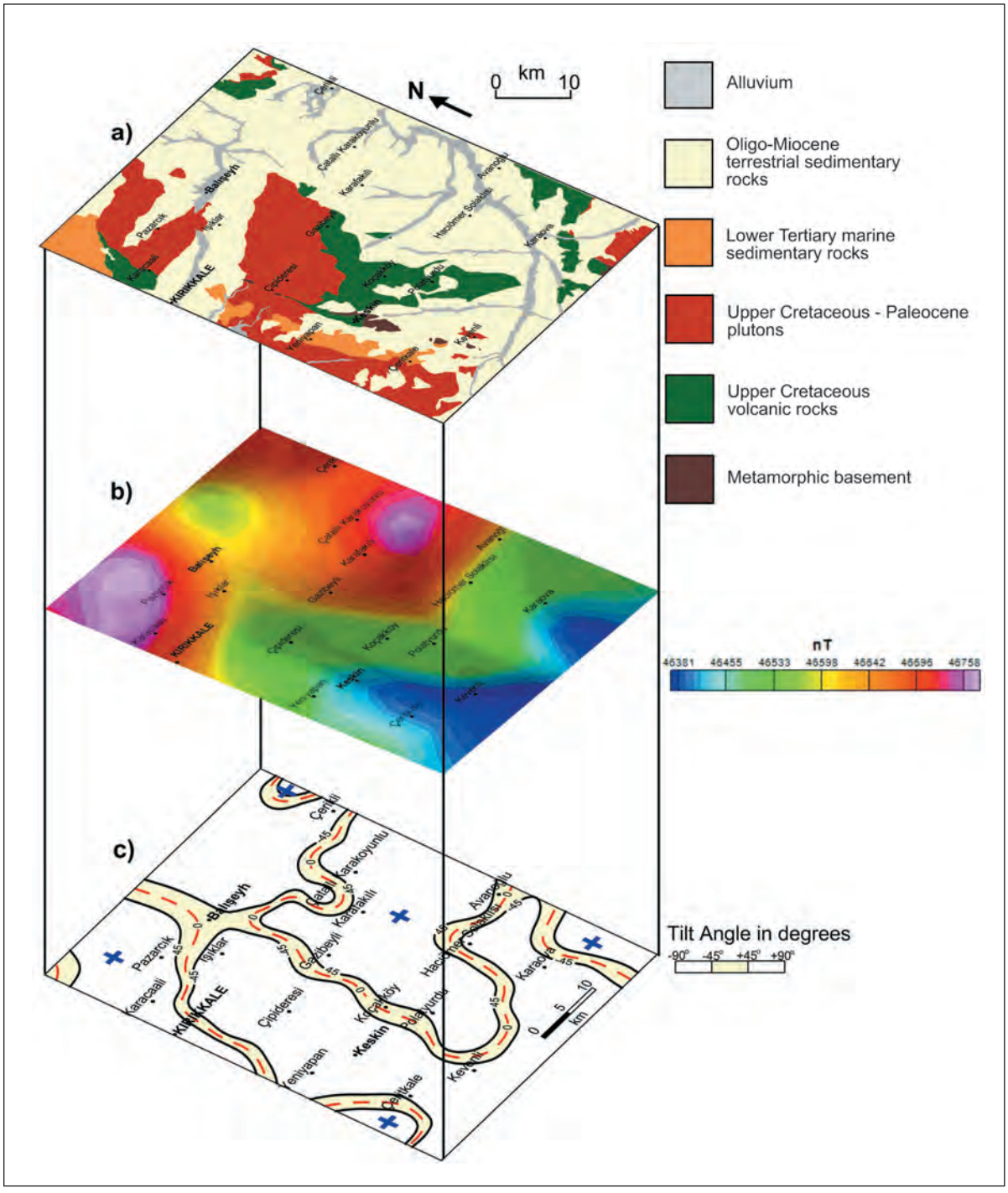

Figure 6- Comparison of study area; a) Geological map of Kýrþehir Ý31 sheet b) Aeromagnetic Anomaly map (Reduced-to-the-pole, then a 5-km upward continuation applied), c) Magnetic tilt angle map.

Tilt angle contour orientations situated to the west of the study area were affected by the tectonic developments (the lithological difference between the units belonging to Ýzmir - Ankara Zone and Kýrþehir Massif) which are present to the west of Ý31 sheet (Figure 5c and 6c).

The fact that half the difference between the ±45° contours does not show much variation on the gravity and magnetic tilt angle maps expresses that structure depth does not show much variation in itself, either. Upper depths were determined between 0.5 and 2.0 km approximately.

RESULTS

The 'Tilt Angle' method, which is a fast and practical method in detecting vertical contacts, was applied to the regional gravity and aeromagnetic data of 1: 100.000 scale Ý31 map sheet. Tilt angle maps which reveal the location of structural boundaries were obtained and they were correlated with the geology of the region.

By means of the work conducted here, information was obtained on the presence of Late Cretaceous aged volcanics buried under Tertiary aged sedimentary rocks in the field, their locations and average depths. Upper depths were determined between 0.5 and 2.0 km approximately.

This method brought a new point of view for the interpretation of geological problems and a practice practicability.

ACKNOWLEDGEMENTS

We express our thanks to the referees for their valuable critical reviews on this work. Thanks are also extended to Dr. Ahmet Üçer of General Directorate of Mineral Research and Exploration and Research Assistant M. Özgü Arýsoy of Ankara University for their contributions.

We feel great proud of knowing and working with our brother, Dr. Mehmet Duru, who has passed away soon before. He was a model engineer and had endless interest into all areas of Earth Sciences. We will always remember him with mercy and respect.

Manuscript received October 10, 2010

REFERENCES

Akýn, U. and Çiftçi, Y., 2010. Kýrýkkale-Kýrþehir-Nevþehir-Kayseri-Yozgat arasýndaki bölgenin ýsý akýsý ve radyoaktif ýsý üretimi araþtýrma raporu, Maden Tetkik ve Arama Genel Müdürlüðü, Report no. 11307, (unpublished) Ankara.

Ataman, G., 1972. Ankara´nýn güneydoðusundaki granitik/granodiyoritik kütlelerden Cefalýkdaðýn radyometrik yaþý hakkýnda ön çalýþma, Hacettepe Üniversitesi Fen ve Mühendislik Bilimleri Dergisi 2/1, 44-49.

Ayan, M., 1963. Contribution al etude petrographique et geologique de la region sidvec au Nord-Est de Kaman (Turquie), Maden Tetkik ve Arama Genel Müdürlüðü, Report no: 155, 332 s., (unpublished), Ankara.

Aydýn, A, 2000. Evaluating gravity and magnetic data by normalized full gradient. Azerbaijan International Geophysical Conference Book, Baku, p. 223.

_____, 2007. Interpretation of gravity anomalies with the normalized full gradient (NFG) method and an example. Pure and Applied Geophysics 164, 2329-2344.

_____, Sipahi, F., Karslý, H., Geliþli, K. and Kadirov, F., 1997. Interpretation of magnetic anomalies on covered fields using normalized full gradient method. International Geoscience Conference and Exhibition Book, Moscow, D3., 4 p.

Berezkin, V.M. and Buketov, A.P., 1965. Application of the harmonical analysis for the interpretation of gravity data, Applied Geophysics, 46, 161-166.

_____, Filatov, V.G. and Bulychev, E.V., 1994. Methodology of the aero-magnetic data interpretation

with the aim of direct detection of oil and gas deposits, Geofizika, Nr.5, 38 - 43.

Birgili, Þ., Yoldaþ, R. and Ünalan, G., 1975. Çankýrý-Çorum havzasýnýn jeolojisi ve petrol olanaklarý, Maden Tetkik ve Arama Genel Müdürlüðü, Report no: 5621 (unpublished), Ankara.

Blakely, R.J. and Simpson, R.W., 1986. Approximating edges of source bodies from magnetic or gravity anomalies, Geophysics Vol. 51, No.7, 1494-1498.

Cordell, L. and Grauch, V.J.S., 1982. Mapping basement magnetization zones from aeromagnetic data in the San Juan Basin; New Mexico: Presented at the 52nd Ann. Internat. Mtg., Sot. Explor. Geophys., Dallas; abstracts and biographies, 246-247.

_____ and _____, 1985. Mapping basement magnetization zones from aeromagnetic data in the San Juan basin, New Mexico. In: W.M. Hinze (Editor), The utility of regional gravity and magnetic maps. Society Exploration Geophysics, Tulsa, OK, pp. 181-197.

Dondurur, D., 2005. Depth estimates for slingram electromagnetic anomalies from dipping sheet-like bodies by the normalized full gradient method. Pure and Applied Geophysics 161, 2179- 2196.

Dönmez, M., Bilgin Z. R., Akçay, A. E., Kara, H., Yergök, A. F. and Esentürk, K., 2005. 1/100.000 ölçekli Türkiye jeoloji haritalarý, Kýrþehir Ý-31 paftasý, No:46, Maden Tetkik ve Arama Genel Müdürlüðü, Ankara.

Göncüoðlu, M.C., Dirik, K. and Kozlu, H., 1996. General charecteristics of Pre-Alpine and Alpine terranes in Turkey: Explanatory notes to the terrane map of Turkey. Annales Geologiques Des Pays, 37, 515-536, Atina.

Gunn, P.J., 1975. Linear transformations of gravity and magnetic fields, Geophysical Prospecting, 23, 300-312.

Hood, P.J. and Teskey, D.J, 1989. Aeromagnetic gra diometer program of the Geological Survey of Canada, Geophysics, 54, 1012-1022.

Kara, H., 1991. 1/100.000 ölçekli açýnsama nitelikli Türkiye jeoloji haritalarý serisi, Kýrþehir-G 18 paftasý, no: 37, Maden Tetkik ve Arama Genel Müdürlüðü, Ankara.

_____ and Dönmez, M., 1990. 1/100.000 ölçekli açýnsama nitelikli Türkiye jeoloji haritalarý serisi, Kýrþehir-G 17 paftasý, No: 34, Maden Tetkik ve Arama Genel Müdürlüðü, Ankara.

Karslý, H., 2001. The usage of normalized full gradient method in seismic data analysis and a comparison to complex envelope curves. PhD Thesis, Karadeniz Technical University, (unpublished), Trabzon.

Ketin, Ý, 1955. Yozgat bölgesinin jeolojisi ve Orta Anadolu masifinin tektonik durumu, Türkiye Jeoloji Kurultayý Bülteni, C. VI, Sayý 1, 1-40.

_____, 1963. 1/500.000 ölçekli Türkiye jeoloji haritasý, Kayseri paftasý ve açýklamasý, Maden Tetkik ve Arama Enstitüsü Yayýný, Ankara.

Miller, H.G. and Singh, V., 1994. Potential field tilt-a new concept for location of potential field sources. Journal of Applied Geophysics 32: 213-217.

Maden Tetkik ve Arama Genel Müdürlüðü, 2002. 1:500.000 ölçekli Kayseri Türkiye jeoloji haritalarý, Maden Tetkik ve Arama Genel Müdürlüðü, Ankara.

Nabighian, M.N., 1972. The analytic signal of two-dimensional magnetic bodies with polygonal cross section: its properties and us for automated anomaly interpretation. Geophysics 37, 507-517.

Norman, T., 1972. Ankara Yahþýhan bölgesinde Üst Kretase-Alt Tersiyer istifinin stratigrafisi, Türkiye Jeoloji Kurumu Kurultayý Bülteni, XV, 2, 180-276.

Oktay, F. Y., 1981. Savcýlý- Büyükoba (Kaman) çevresinde Orta Anadolu masifi tortul örtüsünün jeolojisi ve sedimantolojisi, Ýstanbul Teknik Üniversitesi Maden Fakültesi, Doçentlik tezi (unpublished), Ýstanbul.

Pasquare, G., 1968. Geology of Cenozoic volcanic area of Central Anatolia, attý Della Academia

Nazionella Des Lincei Memorie serie VII, Volume IX Roma.

Roest, W.R., Verhoef, J., and Pilkington, M., 1992. Magnetic interpretation using the analytic signal. Geophysics, 57, 116-125.

Salem, A., Williams, S., Fairhead, D., Ravat, D., and Smith, R., 2007. Tilt-depth method: A simple depth estimation method using first-order magnetic derivatives: The Leading Edge, December, 1502-1505.

_____, _____, _____, Smith, R., and Ravat, D., 2008. Interpretation of magnetic data tilt-angle derivatives. Geophysics, 73, L1-L10.

Seymen, Ý, 1982. Kaman dolayýnda Kýrþehir masifinin jeolojisi, Ýstanbul Teknik Üniversitesi Maden Fakültesi, Doçentlik tezi, 164 s. (unpublished), Ýstanbul.

Sýndýrgý, P., Pamukcu, O. and Özyalýn, S., 2008. Application of normalized full gradient method to self potential (SP) data. Pure and Applied Geophysics 165, 409-427.

Thompson, D.T.,1982. EULDHD: A new technique for making computer-assisted depth estimates from magnetic data: Geophysics, 47, 31-37.

Uygun, A., Yaþar, M., Çelik, E., Kayakýran, S., Erhan, C., Aygür, M., Ayok, F., Baþ, H. and Bilgiç, T., 1981. Tuzgölü havzasýprojesi, Maden Tetkik ve Arama Genel Müdürlüðü, Report No: 7188 (unpublished), Ankara.

Verduzco, B., Fairhead, J.D., Green, C.M., and MacKenzie, C., 2004. New insights into magnetic derivatives for structural mapping, The Leading Edge, 23, 116-119.

Mineral Res. Expl. Bull., 143, 13-35, 2011

THE TECTONOSTRATIGRAPHIC FEATURES OF THE BELEMEDÝK TECTONIC WINDOW AND ITS SURROUNDINGS

Ýsmet ALAN*, Þenol ÞAHÝN**, Alican KOP***, Bülent BAKIRHAN* and Nevzat BÖKE**

ABSTRACT.- The study area includes Belemedik and its vicinity located in the eastern part of Ecemiþ Fault Zone which constitutes the boundary between Central and Eastern Taurides.The area generally presents Belemedik sequence belonging to Aladað Unit, ophiolithic melange and ophiolithic rocks belonging to Bozkýr Unit and Tertiary sediments overlying all these units. Within Belemedik sequence, Late Devonian aged Küçükali, Carboniferous aged Belemedik, Early Permian aged Sarýoluk, Late Permian aged Kýzýlgeriþ and Yellice, Early-Middle Triassic aged Katarasý, Middle-Late Triassic aged Sarýyarma, Jurassic-Cretaceous aged Çamlýk and Yavça Formations were differentiated. In the previous studies on the vicinity of Belemedik, it was suggested that an incomplete Mesozoic series overlaying the Palaeozoic core and as a result of the erosion of this cover, a tectonic window was exposed. However, in this study, it was demonstrated that a complete Mesozoic series of Early Triassic-Late Cretaceous age overlaying the Palaeozoic rocks in the vicinity of Belemedik are presented and hence a tectonic window does not exist in the vicinity of Belemedik. In addition, it was determined that Belemedik Sequence displayed similar features with the rock associations of Aladað Unit in terms of lithological properties and the ages of the units it comprises. In the region, at the bottom of the Bozkýr Unit, which tectonically overlies the Belemedik Sequence, Late Senonian aged Kýzýlcadað Ophiolithic Melange and olistostrome are present. And, at the top of the Bozkýr Unit, Late Cretaceous aged Pozantý-Karsantý Ophiolithic Nappe is located. While the Pozantý-Ecemiþ Corridor formed by Ecemiþ Fault Zone is represented by Oligocene-Miocene aged units, the Adana Basin is represented by Paleocene-Late Miocene units.

Key words: Belemedik Sequence, Tectonostratigraphy, Aladað Unit, Pozantý, Taurides.

INTRODUCTION

The study area generally covers Ecemiþ Fault Zone which constitutes the boundary between Central and Eastern Taurides, and the area in the east of this zone (Figure 1). The major settlement units in the region are: Tekir Plateau (J2), Belemedik (H12), Eskikonacýk (C7), Keþli (S9), Kýralan (S18) and Karakýlýç (L19) villages (Figure 2). The study area has been studied by many researchers for various purposes until today. Paleozoic aged rock associations in the region were first introduced by Blumenthal (1947) under the name of 'Belemedik Tectonic Window'. In this study, the existence of an anticline has been shown, which Devonian and Permian aged units in the core and Mesozoic aged limestones in surrounding are situated. Üþenmez (1981) and Üþenmez et al. (1988) defined Late Devonian-Middle Cretaceous aged Belemedik-Köserelik and Late Cretaceous aged Akdað formations during their work in the vicinity of Belemedik. They asserted that Triassic and Jurassic were absent in the area and Belemedik-Köserelik formation was covered by Early- Middle Cretaceous aged marbles and dolomitic limestones. Gül et al. (1984) defined Aydos, Namrun, Belemedik, ophiolite and Niðde tectonic slices obducted on to the continental platform following the emplacement of ophiolitic mélange by a compressive tectonics at the end of Late Cretaceous. Their studies aimed to find out the tectonic and stratigraphic situations of the Bolkardaðý and Belemedik in the Taurides and to observe the exten-

* Maden Tetkik ve Arama Genel Müdürlüðü, Jeoloji Etütleri Dairesi, ANKARA
** Maden Tetkik ve Arama Genel Müdürlüðü, Adana Bölge Müdürlüðü, ADANA
*** Kahramanmaraþ Sütçü Ýmam Üniversitesi Müh. ve Mim. Fak. Jeoloji Müh. Bölümü, KAHRAMANMARAÞ (alican@ksu.edu.tr)

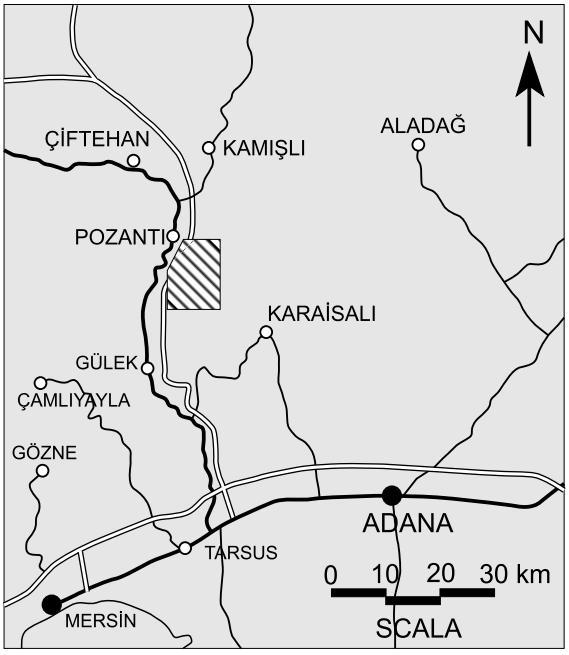

Figure 1- Location map of the study area.

sion of this units into the Adana basin. The researchers also stated also that Late Devonian aged units were conformably overlain by Carboniferous aged units, and Late Permian aged Köþkdere formation unconformably overlay these units in the Belemedik region. No findings related to Early Permian could be demonstrated in the study. Later, Flügel and Kahler (1988), who conducted researches in Palaeozoic aged units in the vicinity of Belemedik for biostratigraphic purposes, determined the presence of *Girvanella*-bearing Lower Permian in the region by examining Late Devonian-Permian facies.

The objective of this study was to determine the tectonostratigraphic features of Belemedik and its surroundings known as tectonic window, and to establish the position of the rock associations outcropping within the units defined by Özgül (1976) in the Taurides.

REGIONAL GEOLOGY

The study area in a regional scale covers Ecemiþ Fault Zone which constitutes the boundary between Central and Eastern Taurides, and the sector lying to the east of this zone. In this study, the rock associations outcropping in the region were assessed within the units defined in the Taurides by Özgül (1976). According to this, generally, while in the western sectors of Ecemiþ Fault Zone, Bolkar Mountain and Aladað Units (Özgül, 1976) and the rock associations constituting Namrun Tectonic Slice redefined by Alan et al. (2004*b*) are observed, in the area lying to the east of Ecemiþ Fault Zone, again Aladað Unit defined by Özgül (1976) and the rocks belonging to the Bozkýr Unit which tectonically overlies Aladað Unit are observed.

Middle Carboniferous-Late Cretaceous aged rocks, the outcrops of which are observed in the western sectors of Ecemiþ Fault Zone and that are not situated in the study area, constitute the basement in the region (Alan et al., 2004*a*).The Namrun Tectonic Slice comprising Carboniferous-Late Cretaceous aged rocks tectonically overlies Bolkar Mountain Unit (Alan et al., 2004*b*). To the north of Namrun and Aslanköy, the Namrun Tectonic Slice is tectonically overlain by the rocks belonging to the Aladað Unit. Bolkar Mountain Unit, Namrun Tectonic Slice and Aladað Unit face with the units belonging to the Bozkýr Unit and Oligocene-Miocene aged deposits along the corridor formed by Ecemiþ Fault Zone in the near west of Pozantý. At the base of the Bozkýr Unit, late Senonian aged Kýzýlcadað Ophiolithic Melange and Olistostrome are present. And, at the top of it, Late Cretaceous aged Pozantý-Karsantý Ophiolithic Nappe is located. In the area to the east of Ecemiþ Fault Corridor, Belemedik sequence comprising Late Devonian-Late Cretaceous units constitutes the basement, and further east, this basement is overlain with angular unconformity by the deposits of Adana Basin consisting of Paleocene-Late Miocene aged units (Figure 2, 3).

STRATIGRAPHY

In the study area covering Belemedik and its surroundings, in general, Belemedik Sequence,

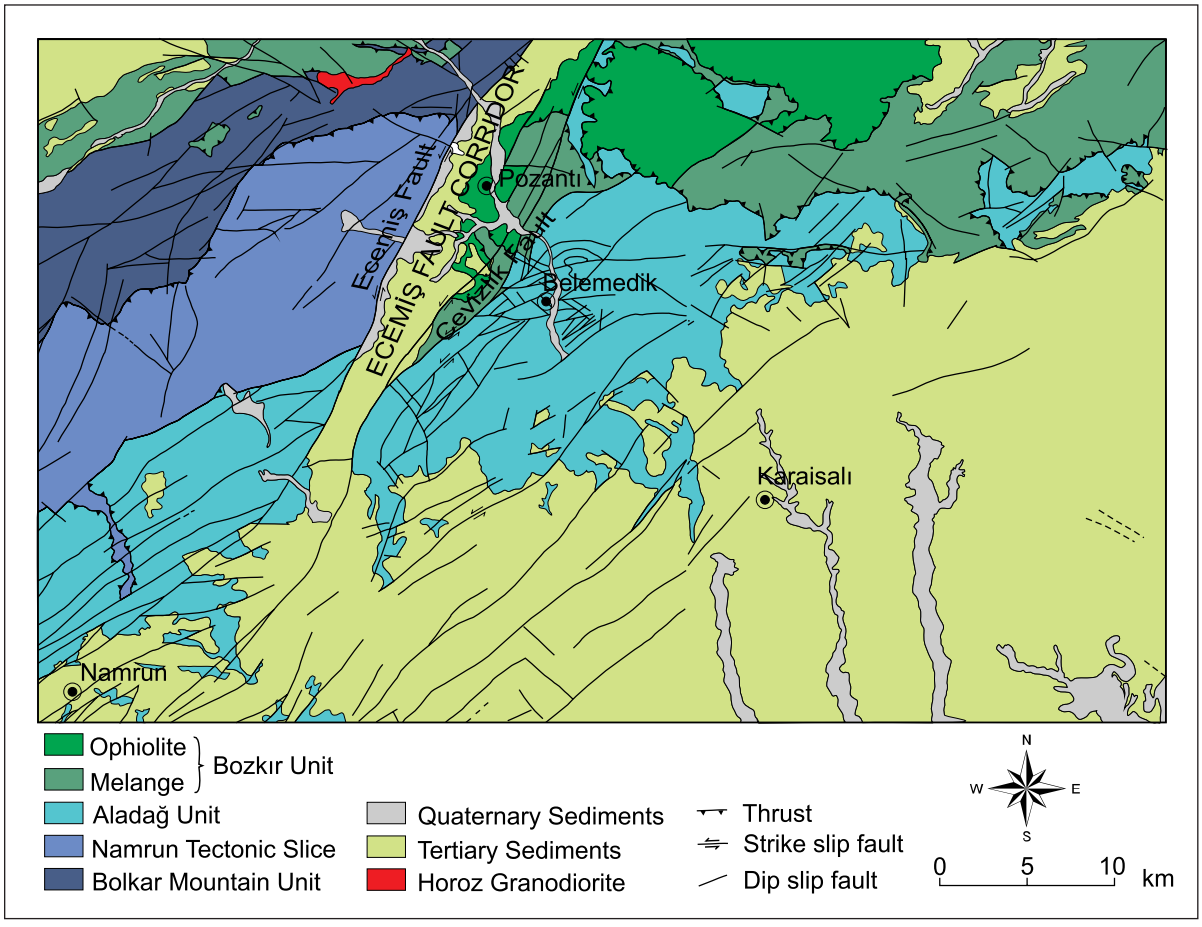

Figure 2- The settings of the units and tectonic slice defined in study area.

Ophiolithic melange and ophiolithic rocks belonging to the Bozkýr Unit, and Tertiary aged deposits overlying all these units are observed. Belemedik Sequence, which constitutes the basement in the study area, is tectonically overlain by the ophiolithic rocks belonging to the Bozkýr Unit along Ecemiþ Fault Zone, between Tekir Plateau (J2) and Pozantý. And, it is unconformably overlain Paleocene-Eocene aged Güzeller Formation to the southwest of the Gülek Strait (O1), by Oligo-Miocene aged Çukurbað Formation and Early Miocene aged Burç Formation between the Gülek Strait and Eskikonacýk village (B7). And, it was determined that, to the east of the Ecemiþ Fault Corridor, Belemedik Sequence is overlain by Paleocene-Miocene aged sediments deposited in Adana Basin. Considering that Belemedik Sequence is the equivalent of the Aladað Unit; the presence of Paleocene-Eocene aged units over the Aladað Unit was introduced for the first time in this study (Figure 4).

BELEMEDÝK SEQUENCE

Within the Belemedik Sequence, which outcrops over a large area in the study area; Late Devonian aged Gümüþali, Carboniferous aged Belemedik, Early Permian aged Sarýoluk, Late Permian aged Kýzýlgeriþ and Yellice, Early-

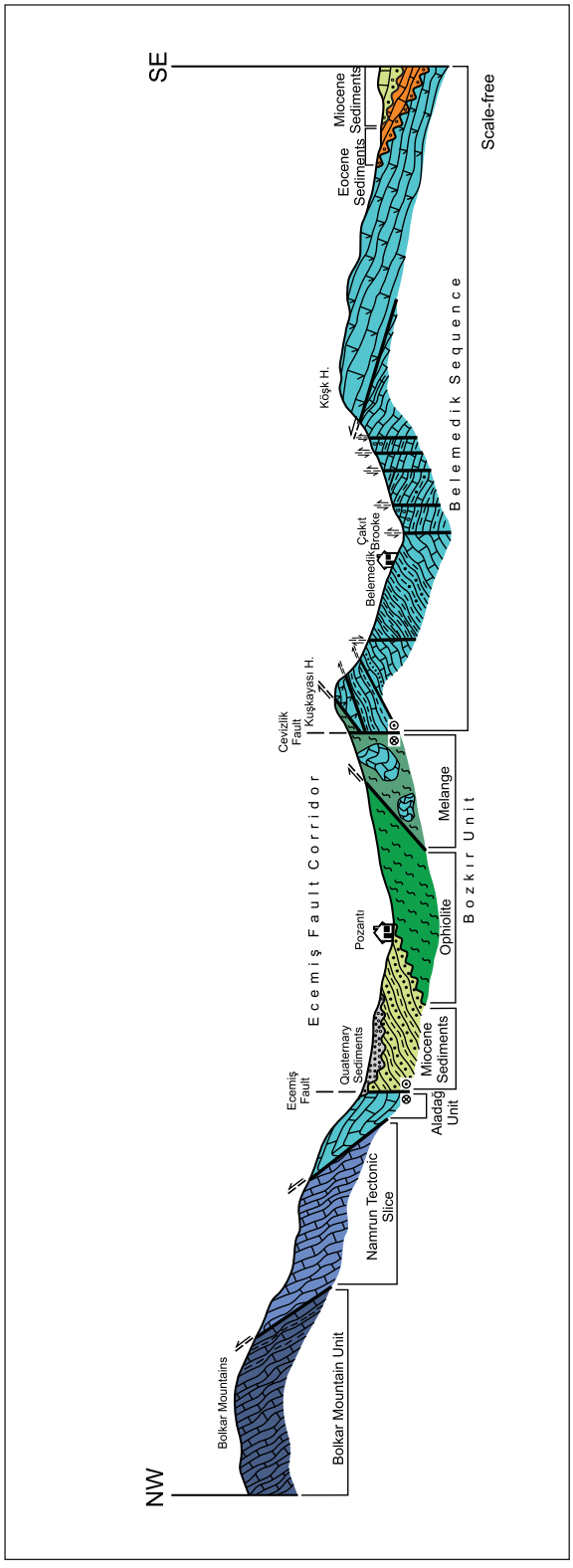

Figure 3- Geological cross-section showing the settings of the units and tectonic slices defined in the study area and its near vicinity.

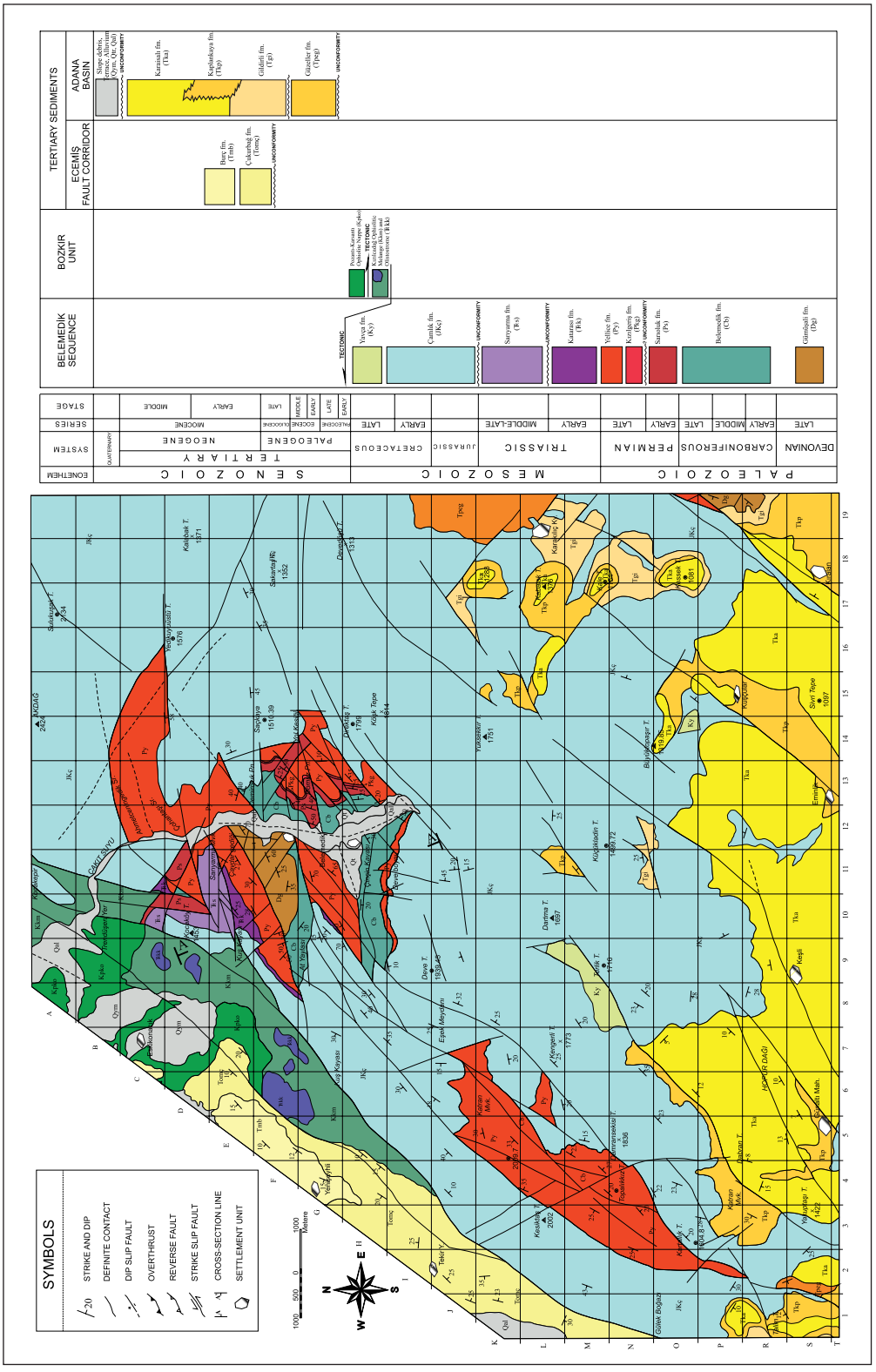

Figure 4- Geological map of the study area

Middle Triassic aged Kataraşý, Middle-Late Triassic aged Sarýyarma, Jurassic-Cretaceous aged Çamlýk and Late Cretaceous aged Yavça Formations were defined (Figure 5, 6). Since it comprises Early Permian aged rock association, in this study Belemedik Sequence was correlated with the rock associations defined as the Aladað Unit by Özgül (1976). However, since the name 'Belemedik' has long been used in the literature for the region and is well-known, in this study the name 'Belemedik Sequence' was adopted for the rock associations outcropping in Belemedik and its near vicinity and ranging in age from Late Devonian to Late Cretaceous.

Gümüþali formation (Dg)

Belemedik Sequence presents similar age and lithological characteristics as the Gümüþali formation determined for the first time by Demirtaþlý (1967) in the Geyikdaðý Unit. That's why, Late Devonian siltstone, shale, quartzite and limestone lithologies within Belemedik Sequence are introduced under the same name in this study as well.

In the study area, the unit is the best observed at a place 100 meters northwest of Belemedik village (Figure 4). (Both in the above mentioned place and in other areas, because of the outcrops of the unit take place in the close regions to Ecemiþ fault zone, presenting of adequate type section is prevented due to the related deformation). The outcrops of the Gümüþali formation in the vicinity of Feke outside the study area carry reference section feature for the unit.

Gümüþali formation is mainly represented by sandstone, dolomitic limestone, limestone, siltstone-quartzite and shale lithologies in the study area. At the base of the unit, the weathered surface of which is brownish-dark gray and the fresh fracture surface of which is yellowish-gray colored, thin-medium bedded, fine-medium grained, moderately sorted, hard-rugged, carbonate cemented and highly macrofossiliferous sandstones take place. On this level the alternation of dolomitic limestones of which the weathered surface is brownish-dark gray, fresh fracture surface blackish gray thin to thick bedded ,hard micritic and fractured with the calcide fillings and reefal limestone of which the weathered surface is bluish-dark gray, fresh surface is gray, medium to thick bedded, hard, micritic and with a high content of brachiopods and corals take place. The defined dolomitic limestone and the limestone horizons are in lenticular shape in the unit. After the limestone-dominant levels, the formation continues with levels which are siltstone-dominant and having limestone lenses in places. In the upper levels of the formation, the alternation of black colored shale; thin-medium bedded, beige-cream colored siltstone and quartzite is observed.

In the uppermost level of the unit, shales; the weathered surface of which is brownish-dark green, the fresh fracture surface of which is gray beige colored, and which are thin bedded, with splinter-like cracks and mica flakes; alternate with clayey limestones the weathered surface of which is gray, the fresh fracture surface of which is light gray, beige colored, and which are thin-medium bedded, moderately competent, highly jointed. After this level comes Carboniferous aged Belemedik formation.

In this study, the Gümüþali formation was given the age of Late Devonian based on its general lithological features, its macrofossil content of brachiopod and coral, and on the fact that Carboniferous aged Belemedik formation conformably overlies it and Flügel and Kahler (1988) obtained the age of Late Devonian in the vicinity of Belemedik.

Since Gümüþali formation is situated at the bottom of the Belemedik formation which constitutes the basement in the study area, the base of the Gümüþali formation cannot be observed. That's why; its real thickness could not be given.

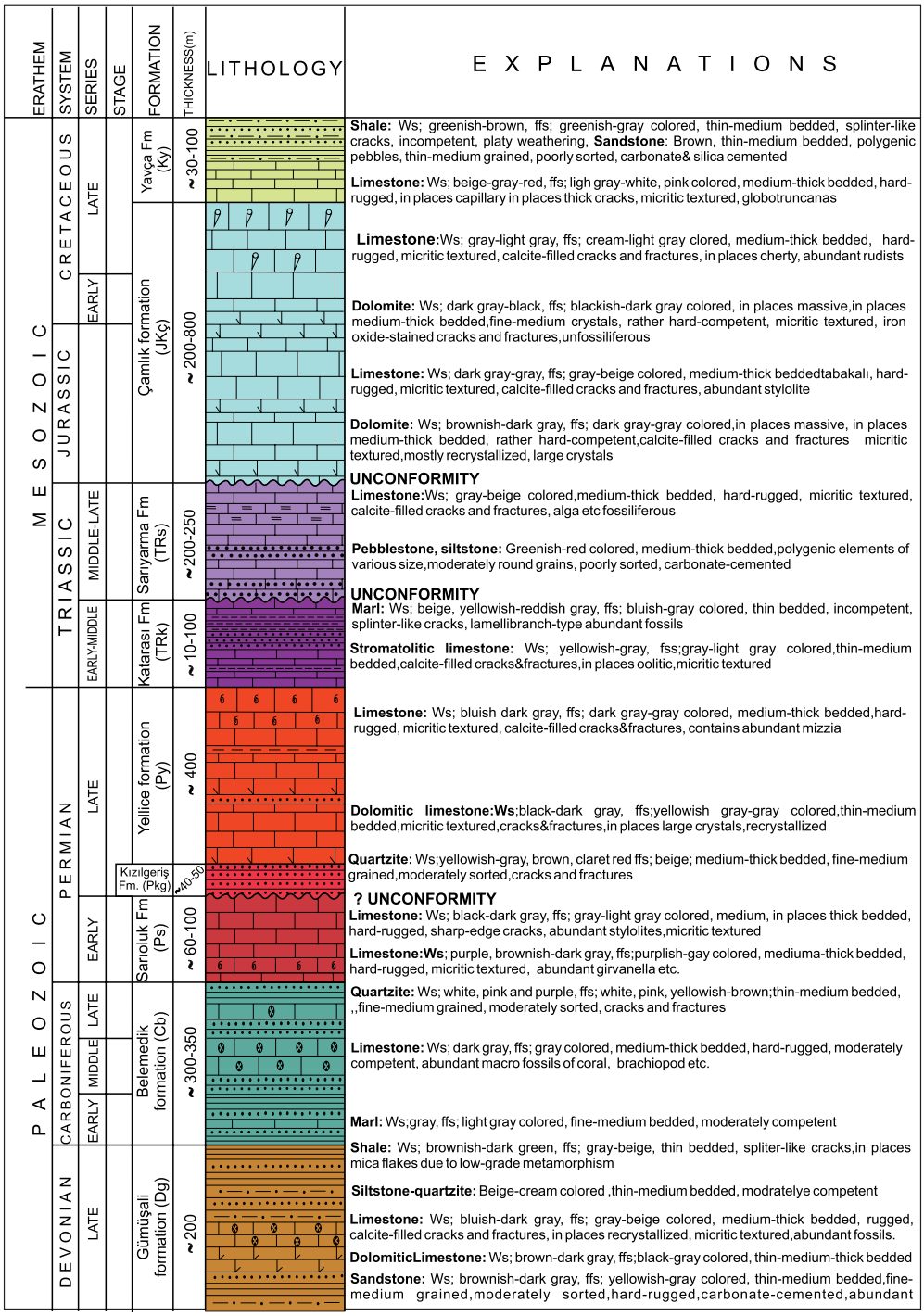

Figure 5- Generalized stratigraphic section of Belemedik Sequence (scale-free) (Ws: weathered surface; ffs: fresh fracture surface).

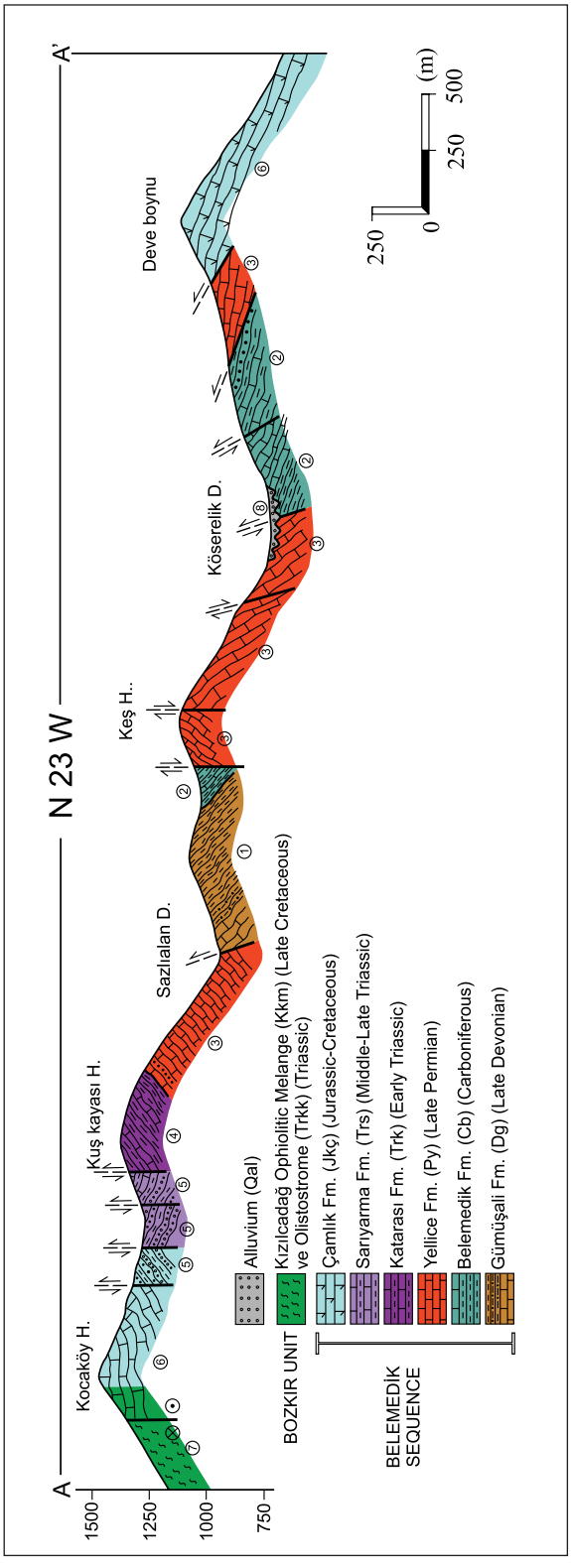

Figure 6- Geological cross-section of Belemedik Sequence

However, it can be said that the apparent thickness of the Gümüþali formation in the study area is approximately 200 meters.

Its lithology mainly composed of quartzite, siltstone, shale and lenticular limestones, its sedimentary structures and fossil content indicate that the Gümüþali formation may have deposited under conditions of shallow marine-coastal environment.

The Belemedik formation (Cb)

The Carboniferous aged rock association represented mainly by limestone, shale, marl and quartzite lithologies have been introduced under the name of Belemedik formation first time by Gül et al. (1984) and using of the same name was considered appropriate for similar lithologies in this study as well.

Due to many deformations developed during different periods, the different levels of the Belemedik formation are observed in different sections of the study area. For the bottom section of the unit Çýnçýn Kayasý Locality (H11), At Plateau (G9), for medium levels At Plateau (G9), Çýnçýn Kayasý (H11), Demiroluk spring (E13) and for the upper levels the surroundings of Demiroluk spring can be proposed as type section localities. In addition, At Plateau (G9), Çýnçýn Kayasý (H11) and Demiroluk spring (E13) localities are places where different lithologies belonging to the Belemedik formation can be observed and thus can be reference section areas for the unit (Figure 4).

The Belemedik formation generally represented by shale, sandstone, clayey limestone, quartzite and limestone lithologies, starts with the alternation of shale-siltstone-sandstone and limestone, conformable with the clastic levels of Late Devonian aged Gümüþali formation. Over the transition level are observed marls the weathered surface of which is gray, the fresh fracture surface of which is light gray colored, and which are fine-medium bedded, moderately competent. Within this level, by its soft topographical appearance and brown-dark brown color limestones are observed of which the weathered surface is gray, the fresh fracture surface is light gray colored, thin bedded, micritic textured, and is considerably rich in brachiopods, corals and crinoids. Overlying this level limestones take place of which the weathered surface is dark gray, the fresh fracture surface is gray colored, medium-thick bedded, hard-rugged, and contain solitary coral and brachiopod. Further up, thin bedded marls the weathered surface of which is brownish-gray, the fresh fracture surface of which is yellowish gray colored alternate with limestones the weathered surface of which is dark gray, the fresh fracture surface of which is gray colored, and which are thin-medium bedded, hard-rugged. In the uppermost levels of the formation is present an alternation of medium-thick bedded quartzites which display colors varying from white to purple; thin bedded, brownish-green colored shale and medium-thick bedded, gray-beige colored limestones.

Belemedik formation, which has a conformable contact with the underlying Gümüþali formation, is conformably overlain by the Sarýoluk formation. However, the cross-bedded sandstone levels observed at the uppermost section of the Belemedik formation in some places indicate that deposition environment became considerably shallower from time to time and thus, there may be some local unconformities in some sections of the contact between the Belemedik and the Sarýoluk formations.

The Belemedik formation was highly affected by the structural elements developed depending on the deformations that were active in the region during different periods and thus, its real thickness could not be determined. But its apparent thickness is around 300-350 meters.

As a result of the examinations performed on the samples collected from the outcrops of the

Belemedik Formation in different areas, the following fossil assemblages and ages were obtained. From the outcrops in the localities of Çýnçýn Kayasý (H11) and Domuz Spring (G13) *Koninckopora* ex. gr. *inflata* (Koninck), *Brunsia* sp., *Endothyra* sp., *Mediocris* sp., *Millerella* sp., *Kameana* sp., *Koninckopora* sp., *Eostaffella* spp. fossils and Early Carboniferous age; from the outcrops in the localities of At Plateau (G9) and Çýnçýn Kayasý (H11) *Archaediscus* sp., *Palaeotextularia* sp., *Eotuberitina* sp., *Bradyina* sp., *Earlandia* sp., *Brunsia* sp., *Forschia* sp., *Ozawainella* sp., *Schubertella* sp., *Beedeina* sp., *Climacammina* sp., *Ungdarella* sp., *Profusulinella* ex. gr. *rhomboides* (Lee and Chen) fossils and Middle Carboniferous age; from the outcrops in the locality to the east of Belemedik Village (H12) *Tetrataxis* sp., *Triticites* sp., gastropods, ostracods and echinite shell particles and Late Carboniferous age; in the locality of Demiroluk Spring (E13) *Palaeonubecularia uniserialis* Reitlinger, *Globivalvulina* sp., *Earlandia* sp., *Nodosinelloides* sp., *Pseudoepimastopora* sp., *Palaeonubecularia* sp. fossils were determined for the same time interval Accordingly the age of the unit named as the Belemedik formation in this study is Carboniferous.

According to its general lithological features and fossil content, Belemedik formation must have deposited in a marine environment which could become considerably shallower from time to time.

Sarýoluk formation (Ps)

The name Sarýoluk formation was used for the first time by Ayhan and Lengeranlý (1986) for rock types composed of *Girvanella*-bearing clayey limestones and limestones, the best outcrops of which were observed in the vicinity of Sarýoluk Plateau (M34) situated to the west of Baþyayla Corridor of Yahyalý (Kayseri) township outside the study area. The use of the same name was considered appropriate for similar lithologies observed in restricted areas, in this study as well. In the study area, the unit displays outcrops mainly at the east slopes of the Belemedik Valley and to the north of Topalýkkýz Hill (N4). In addition in the study area, the west of Yolkesiði Locality (F14) situated to the east of Belemedik Village and Domuz Spring Locality (G13) can be defined as reference section places for the formation (Figure 4).

Sarýoluk formation is represented by a lithology composed mainly of Girvanella-containing clayey limestones and limestones. At the base of the formation are situated limestones and large Girvanella-containing clayey limestones the weathered surface of which is purplish-brown and gray; the fresh fracture surface of which is purple-dark gray colored; and which are medium-thick bedded, solid, micritic textured, having calcite-filled cracks, with a total thickness reaching up to 40-50 meters. Overlying this unit is a *Pseudofusulina* Zone having a total thickness of 2-3 meters, the weathered surface of which is dark gray-black, the fresh fracture surface of which is grayish-black colored, and which is medium-thick bedded, hard-rugged, containing calcite-filled cracks and large fusulinids. This level grades into limestones the weathered surface of which is brownish-black, the fresh fracture surface of which is black colored, and which are thin-medium bedded and containing large amounts of crinoids and pseudoschwagerinids. The uppermost levels of Sarýoluk formation are composed of limestones the weathered surface of which is dark-gray, the fresh fracture surface of which is grayish-black colored, and which are medium-thick bedded, rugged and containing calcite-filled cracks.

Sarýoluk formation, which conformably overlies Carboniferous aged Belemedik formation is overlain by Late Permian-aged Kýzýlgeriþ Formation. In the study area, no field data was obtained to indicate that the contact between Sarýoluk and Kýzýlgeriþ formations is unconformable. However, the fact that Kýzýlgeriþ for-

mation, overlying Sarıyarma formation that ends with limestones at the top, is represented totally by quartzite lithology supports the opinion that the contact between these two units is unconformable.

In this study, it was determined that the thickness of Sarýoluk formation varied from 60 to 100 meters.

In the samples collected from the localities of Domuz Spring (G13) and Yolkesiði (F14) *Nankinella* sp., *Claracrusta catanoides* Homan, *Pseudofusulinoides* sp., *Zellia* sp., *Girvanella subparallela* Flügel and Flügel-Kahler, *Pseudofusulina* sp., *Eotuberitina* sp., *Pseudoepimastopora* sp., *Globivalvulina* sp., *Geinitzina* sp., *Tetrataxis* sp., *Palaeonubecularia* sp., *Hemigordius* sp., *Earlandia* sp. fossil assemblage was determined and Early Permian age was given to Sarýoluk formation.

The general rock type features and fossil content of Sarýoluk formation indicates that it may have deposited in a low-energy, shallow marine environment in which oxidation functions were effective due to becoming too shallow from time to time.

Kýzýlgeriþ formation (Pkg)

This unit, which was first defined as Kýzýlgeriþ member by Özgül (1997) during the study performed in the vicinity of Taþkent and Hadim, was upgraded to Formation rank and introduced as Kýzýlgeriþ formation in this study.

Kýzýlgeriþ formation, type section place of which is located to the southwest of Taþkent and Hadim region of Central Taurides outside the study area, exhibits outcrops having the quality of reference section in the vicinity of Domuz Spring Locality (G13) on the slopes of Belemedik valley in the study area (Figure 4).

The dominant lithology of Kýzýlgeriþ formation is composed of quartzites the weathered surface of which is yellowish-gray, brownish-claret red; the fresh fracture surface of which is beige colored and which are medium-thick bedded, hard-rugged, coarse grained. In some areas, in addition to the dominant quartzite lithology, shales are observed at the bottom sections of Kýzýlgeriþ formation.

The unit, which unconformably overlies Early Permian aged Sarýoluk formation at the bottom, is conformably overlain by Late Permian aged Yellice formation at the top.

Although the unit generally presents apparent thickness values varying between 40 and 50 meters, it was determined that it became thinner in the lateral direction and the apparent thickness could decrease down to 5-10 meters.

Kýzýlgeriþ formation does not contain any fossil findings due to its lithological composition composed of quartzites. Thus, taking into account its stratigraphic relation with the units underlying and overlying it and the ages of these units, Late Permian age was given to it.

When the lithofacies characteristics of Kýzýlgeriþ Formation are taken into account, it must have deposited in a beach environment of a high-energy sea where nourishment from the land is high.

Yellice formation (Py)

Mizzia-bearing limestones outcropping in the region of Taþkent and Hadim situated outside the study area were introduced for the first time by Özgül (1997) under the name of Yellice member. In this study, similar lithologies were redefined using the name Yellice formation. In the study area, the best outcrops of the unit are observed on the slope between Kuþkayasý (E9) and Çakýt Brook to the west of Belemedik Village. In addition, the west of Belemedik Village, Yolkesiði Locality (F14), Çavdar Gediði Locality (E11), Çohantaþý Ridge (D12) and Kat-

ran Locality (K6) are other areas where outcrops can be well observed and thus, they can be reference section areas (Figure4).

Yellice formation is generally represented by recrystallized dolomitic limestones, the weathered surface of which is black-dark gray, the fresh fracture surface of which yellowish-gray colored and which are thin-medium bedded, solid, having cracks and fractures and micritic textured; and *Mizzia*-bearing limestones the weathered surface of which is bluish dark gray, the fresh fracture surface of which is dark gray-gray colored and which are medium-thick bedded, hard-rugged, micritic textured. At the uppermost levels of the unit is observed a thick quartzitic horizon similar to Kýzýlgeriþ formation at the bottom of Yellice formation.

Since the bottom and top contacts of Yellice formation are tectonic in many sections of the study area, the real thickness of it could not be determined in this study. However, it can be said that the apparent thickness of the unit in the study area is around 400 meters.

In the samples collected from the outcrops of Yellice formation at Çavdar Gediði (E11) and Yolkesiði (F14) Localities, the fossil assemblage comprising *Ammodiscus* sp., *Agathammina* sp., *Bradyina* sp., *Chusenella* sp., *Climacammina* sp., *Dagmarita* sp., *Dagmarita chanakchiensis* Reitlinger, *Dunbarula* sp., *Eutuberitina* sp., *Frondina* sp., *Hemigordiopsis* sp., *Hemigordius* spp., *Hemigordius* sp., *Geinitzina* sp., *Globivalvulina* sp., *Geinitzina* spp., *Kamurana* sp., *Langella* sp., *Mizzia* sp., *Nankinella* sp., *Paradagmarita* sp., *Parafusulina* sp., *Paraglobivalvulina* sp., *Permocalculus* sp., *Pseudovermiporella* sp., *Pachyphloia* sp., *Pseudovidalina* sp., *Reichelina* sp., *Schubertella* sp., *Staffella* sp., *Tetrataxis* sp. and *Ungdarella* sp. was obtained. According to the defined fossil assemblage, the age of Late Permian was given to Yellice formation.

Yellice formation, the dominant lithology of which is composed of highly microfossiliferous and macrofossiliferous limestones must have deposited in a low-energy shelf environment.

Karasý formation (TRk)

The name Karasý formation was first used by Demirtaþlý (1967) for the rock association composed of stromatolitic limestone, sandy limestone, marl and mudstone alternation. The use of the same name was considered appropriate for similar lithologies in this study as well.

In the study area, the outcroppings of Karasý formation which can be places for type sections are observed to the east of Kuþkayasý Hill (E9) and in the vicinity of Çavdargediði Locality (E 11) (Figure 4).

Karasý formation starts at the base with stromatolitic limestones the weathered surface of which is gray-beige, fresh fracture surface is gray-light gray colored and which are thin-medium bedded, hard-rugged, having calcite-filled cracks and fractures and showing oolitic character in places. Overlying this level is a sandy limestone lithology which is brownish-gray colored, medium-thick bedded and hard-rugged. In the uppermost sections of Karasý formation are observed yellow-beige colored marls defined as mottled marls in the Taurides and claret red colored mudstone lithologies. Limestone levels which are observed in lenticular shape between marl layers are highly fossiliferous.

Karasý formation has a conformable contact with Yellice formation that it overlies. To the northeast of Kuþkayasý Hill (E9), Karasý formation is unconformably overlain by Middle-Late Triassic aged Saryyarma formation. And, to the east of Kuþkayasý Hill (E9), Karasý formation is overlain by Jurassic-Cretaceous aged Çamlýk formation. It was determined that Çamlýk formation moved on Karasý formation depending on the deformations which were active in the

region during different periods and thus, the contact between these two units lost its original position.

It can be said that the apparent thickness of the Katarasý formation in the study area varies between 10 and 100 meters.

In the samples compiled from the outcroppings of Katarasý Formation in the east of Kuþkayasý Hill (E9) and Çavdargediði (E11) locality; the fossil assemblage composed of *Spirorbis phlyctaena* (Brönnimann and Zaninetti), *Rectocornuspira kalhori* (Brönnimann, Zaninetti and Bozorgnia), *Cornuspira mahajeri* (Brönnimann, Zaninetti and Bozorgnia), *Glomospira facilis* Ho, *Glomospira* sp., *Earlandia* sp., *Ammodiscus* sp., *Calcitornella* sp., gastropods and lamellibranch shells was determined. Although the defined fossil assemblage gave the age Skythian (Induan), taking into account Middle Triassic age obtained by Ayhan and Lengeranlý (1986) from Diþdöken Formation which corresponds to Katarasý formation in the vicinity of Yahyalý, Katarasý formation was given the Early-Middle Triassic age.

Taking into account the general lithofacies characteristics and fossil content of Katarasý formation, it can be said that it deposited on a tidal flat, in a low-energy marine environment.

Sarýyarma formation (TRs)

The rock association composed mainly of pebblestone, siltstone, clayey limestone and limestone and the best outcroppings of which are observed at Sarýyarma Locality (E11) was introduced for the first time by Alan et al. (2004*a*) under the name of Sarýyarma Formation.

Sarýyarma formation, the type section place of which is situated on the west slope of Belemedik Valley to the south of Pozantý township of Adana province, exhibits outcrops having the character of reference section to the west of Kuþkayasý Hill (E9) in the study area (Figure 4).

At the base of Sarýyarma formation; between yellow-claret red colored, thin bedded marls lies a pebblestone level which is green-yellow-brown and red in color, middle-thick bedded, poorly sorted, ungraded, moderately rounded, with polygenic elements having dimensions varying from large blocks to silt. Within this level, Late Permian aged pebbles containing conspicuous *Mizzia* fossils. Overlying this defined level are limestones the weathered surface of which is gray-beige in color, and which are middle-thick bedded, hard-rugged, having calcite-filled cracks and fractures, containing fossil shell traces (alga, etc) and bituminous shale intercalations in places.

The contact between Sarýyarma formation and Early-Middle aged Katarasý formation, which is stratigraphically at the base of it, is faulted in the study area. However, Özgül (1997) stated that Çamiçi and Dikenli Members of Gevme formation, which is the equivalent of Sarýyarma formation in the region of Taþkent and Hadim, are unconformable over Skythian - Anisian aged units. That's why, it was accepted that Sarýyarma formation unconformably overlies Katarasý formation in the study area. And, Sarýyama formation is unconformably overlain by Jurassic-Cretaceous aged Çamlýk formation. However, It was determined that Çamlýk formation moved on Sarýyarma formation underlying it depending on the deformations in the region and thus, the contact between these two units lost its initial position as well.

Özgül (1997) stated that the total thickness of Çamiçi and Dikenli members corresponding to Sarýyarma formation in Taþkent and Hadim region is between 450 and 500 meters. As to the apparent thickness of Sarýyarma formation in the study area, it is around 200-250 meters.

No paleontological findings which can give an age to Sarýyarma formation were detected in the samples collected from the limestones within the formation. However, Erdoðan stated that with

regard to facies characteristics, the collected samples probably reflected a shallow marine environment belonging to Triassic-Jurassic period (Oral Com; Kemal Erdoðan, MTA). In addition to the fact that at the base of Sarýyarma formation lies Early Triassic aged Katarasý formation and at the top of Sarýyarma formation lies Jurassic-Triassic aged Çamlýk formation, Sarýyarma formation displays significant lithological similarities to Çamiçi and Dikenli members of Gevne formation defined by Özgül (1997) in Taþkent and Hadim region. Depending on these reasons, (?) Middle-Late Triassic age was given to the unit introduced as Sarýyarma formation in this study.

When its general lithological characteristics are taken into account, Sarýyarma formation must have deposited in a shallow marine environment where there was from time to time heavy material feeding from the land and tidal effect and lagoons were present in places.

Çamlýk formation (Jkç)

Çamlýk Limestone name was first used by Monod (1977) for Jurassic- Cretaceous aged limestones within Aladað Unit in the Middle Taurides to the west of Beyþehir. But, in this work, the use of the name Çamlýk formation was considered appropriate for lithologies of similar age.

The unit displays outcrops in a large area in the study area. Its best outcrops carrying reference section character are observed to the north of Belemedik Village (12), Akdað district (A14) to the north of Keþli (S9) and Kuþçular (P15) villages (Figure 4).

At the base of Çamlýk formation lie micritic textured dolomites the weathered surface of which is brownish dark gray, the fresh fracture surface of which is dark gray- gray colored, and which are medium-thick bedded, rather hard-rugged, having calcite-filled cracks and fractures, and large crystals. Overlying this level are micritic limestones the weathered surface of which is dark gray, the fresh fractured surface of which is gray-beige colored, and which are medium-thick bedded, hard-rugged, having abundant stylolites, containing alga etc fossils. Overlying these defined limestones are dolomites the weathered surface of which is dark gray-black, the fresh fractured surface of which is blackish-dark gray colored, and which are in places massive, in places medium-thick bedded, rather hard-rugged, micritic textured, having medium crystals, containing no fossils. In the uppermost sections of the unit are observed limestones the weathered surface of which is gray-light gray, the fresh fractured surface of which is cream-light gray colored, and which are medium-thick bedded, in places having nodular or banded chert, and with a rich content of rudists.

The initial contact of Çamlýk formation with Triassic aged units is unconformable at the base. It was determined that in some sections of the study area Çamlýk formation was conformably overlain by Late Triassic aged Yavça formation, and in some sections it was tectonically overlain by the melange and ophiolithic units without Yavça formation.

The real thickness of Çamlýk formation in the study area could not be determined. However, it can be said that the apparent thickness of the unit varies between 200 and 800 meters.

In the samples collected from the outcrops of Çamlýk formation to the north of Belemedik (H12) and Kuþçular (P15) Village the fossil assemblage composed of: *Mesoendothyra croatica* Gusic, *Cayeuxia piae* Frollo, *Valvulina lugeoni* Septfontaine, *Siphovalvulina* sp., *Nautiloculina* sp., *Thaumatoporella parvovesiculifera* (Raineri), *Praekurnubia crusei* Redmond, *Satorina apulensis* Fourcade and Chorowics, *Pfenderina trochoidea* Smout and Sudgen, *Salpingoporella selli* Cresconti, *Clodocoropsis*

mirabilis Felix, *Praechrysalidina infracretacea* Luperto and Sinni, *Debarina hahounerensis* Fourcade, Raoult and Vila, *Haplophragmoides joukowskyi* Charollais, Brönnimann and Zaninetti, *Orbitoides* cf. *tissoti* Schlumberger, *Globotruncana linneiana* (d'Orbigny), *Stoniosphaera sphaerica* (Kaufmann), *Discocylina schlumbergeri* Munier-Chalmas, *Moutcharmontia apenninica* (De Castro), *Haurania* sp., *Verneuilina* sp., Textulariidae*, Trocholina* sp., *Ophthalmidium* sp., *Pseudocyclammina* sp., Lageniidae, *Favreina* sp., *Chrysalinida* sp., *Pfenderina* sp., *Nezzazata* sp., *Bolivinopsis* sp., *Chrysalinida* sp., *Everticyclammina* sp., *Quinqueloculina* sp., *Involutina* sp., *Earlandia* sp., *Orbitolina* sp., Rotaliidae and *Siderolites* sp. was determined. Depending on the fact that the defined fossil assemblage represents the age range of Aalenian-Bajocian (Early-Middle Jurassic) and Maastrichtian (Late Cretaceous), Çamlýk Formation was given the age Jurassic-Cretaceous.

When its general lithofacies characteristics and fossil content are taken into account, it can be said that Çamlýk formation deposited in a shelf environment belonging to a shallow and calm sea where platform type carbonates deposited.

Yavça formation (Ky)

The rock association composed of mudstone-siltstone-sandstone alternation and limestone interbeds was introduced for the first time by Ýlker (1975) under the name of Yavça formation. The best outcrops of the unit that can be type section localities are observed in Yavça Village, situated 10 km east of Arslanköy Municipality of Mersin. North of Terlik Hill (M9), 1 km northwest of Kuþçular (P15) Village are areas where the outcrops of Yavça formation having the character of reference section are observed in the study area (Figure 4).

Yavça formation is generally composed of beige-claret red-brown-gray colored sandstone, mudstone and siltstone-shale alternation. Crinkly limestones lying at the base, the weathered surface of which is beige-gray, the fresh fracture surface of which is light gray-white-pink colored, and which are medium-thick bedded, hard-rugged, micritic textured, having calcite-filled fissures and globotruncanas; are overlain by brown, thin-medium bedded, polygenic pebbly, fine-medium grained, poorly sorted, carbonate and silica cemented sandstones and shales the weathered surface of which is greenish brown, the fresh fracture surface of which is greenish gray colored, and which are thin-medium bedded, incompetent, showing platy weathering and splinter-like fractures.

Yavça formation, which conformably overlies Jurassic-Cretaceous aged Çamlýk formation at the base, is tectonically overlain at the top by Kýzýlcadað Ophiolitic Melange and Olistostrome. It was determined that the limestones present within sandstone, siltstone and shale levels wedged out to form lenses in the lateral direction. The apparent thickness of Yavça formation in the study area varies between 50 and 100 meters.

The following nannofossil assemblage that gave the age of Campanian-Maastrichtian was defined from the samples taken from the clastic levels observed at Çetinlik Locality of Hamidiye Village located to the near north of the study area:

Arkhangelskiella cymbiformis Vekshina, *Chiastozygus amphipons* (Bramlette and Martini), *Ceratolithoides aculeus* (Stradner), *Biscutum constans* (Gorka), *Cretarhabdus crenulatus* (Bramlette and Martini), *Prediscosphaera cretacea* (Arkhangelsky), *Cribrosphaera ehrenbergi* (Arkhangelsky), *Watznaueria barnasea* (Black) Perch-Nielsen, *Microshabdulus decoratus* Deflandre, *Zeugrhabdotus embergeri* (Noel), *Micula decussata* Vekshina, *Calculites obscurus* (Deflandre), *Reinhardtites anthophorus* (Deflandre), *Glaukolithus diplo-*

grammus (Deflandre), *Lithraphidites quadratus* (Bramlette and Martini), *Micula concava* (Stradner) Verbeck, *Quadrum gothicum* (Deflandre).

In addition, the following foraminiferal fossil assemblage was obtained which gave the age of Late Cretaceous (Senonian-Maastrichtian) in the examinations performed on the rock samples taken from the limestone levels of the unit in the vicinity of Kuþçular (P15) Village:

Globotruncana linneiana (d'Orbigny), *Rosita fornicata* (Plummer), *Globotruncana bulloides* Vogler, *Marginotruncana pseudolinneiana* Pessagno, *Dicarinella concavata* (Brotzen), *Globotruncanita stuartiformis* (Dalbiez), *Stomiosphaera sphaerica* (Kaufmann), *Pithonella ovalis* (Kaufmann), Globigerinidae, Heterohelicidae, *Globotruncana* sp. *Siderolites* sp., *Ophthalmidium* sp., Anamolinidae, Rotaliidae. According to these fossil assemblages, the age of the Yavça Formation was accepted as Late Cretaceous.

Yavça formation, which presents a lithology composed of limestones at the base, and in the continuation of it, sandstone-mudstone intercalated with siltstone and shale alternation, must have deposited in an environment which extended from neritic to deep sea.

BOZKIR UNIT

Kýzýlcadað Ophiolitic Melange and Olistostrome (Kkm, TRkk)

The name 'Kýzýlcadað Ophiolitic Melange' was used for the first time by Poisson (1977) for the rock association observed in Western Taurides to the southwest of Korkuteli and composed of serpentinite, radiolarite, chert, limestone, cherty limestone, dunite and harzburgite. The use of the same name for similar lithologies was considered appropriate in this study as well.

Kýzýlcadað Ophiolitic Melange and Olistostrome exhibit outcrops in the northwest sections of the study area, at Kocakepir Hill (A11), to the northeast of Tekir Plateau (J2) and to the west of Kocaköy Hill (D10) (Figure 4).

The unit is mainly composed of dunite, harzburgite, serpentinite, radiolarite, limestone, cherty limestone and pillow lavas. Kýzýlcadað Ophiolitic Melange and Olistostrome, which tectonically overlie Yavça formation at the base, comprise dunite, harzburgite, serpentinite, radiolarite and different limestone blocks. At the base levels, brownish-green, in places red colored limestone blocks of various dimensions are conspicuous. And, at the uppermost levels of the unit are observed Triassic and Late Cretaceous aged limestones disseminated within dunite, harzburgite and limestones. Kýzýlcadað Ophiolitic Melange and Olistostrome tectonically overlie Jurassic-Cretaceous aged Çamlýk formation in the study area. And, it is overlain tectonically by Pozantý-Karsantý Ophiolite Nappe and unconformably by Tertiary aged sediments.

Pozantý-Karsantý Ophiolite Nappe (Kpko)

Ophiolite Nappe, which exhibits extensive outcrops between Pozantý and Aladað (Karsantý) and which is mainly composed of harzburgite, dunite, pyroxenite, gabbro and diabase dikes and metamorphic sole rocks, was introduced for the first time by Bingöl (1978) under the name of Pozantý-Karsantý Ophiolite. Tekeli (1980) and Tekeli et al. (1981) introduced a similar rock association under the name of Aladað Ophiolite Complex in the study they carried out in the region. In a different study carried out by Yetiþ et al. (1991) in the same region, similar rock association was given the name of Faraþa Ophiolite. And, in this study the use of the name 'Pozantý-Karsantý Ophiolite Nappe' was considered appropriate for similar lithologies observed in the vicinity of Eskikonacýk Village (C7) and Trendüþen Locality (B9). In the study area, widespread outcrops belonging to Pozantý-Karsantý Ophiolite Nappe can be observed to the east of Pozantý township (A-C 4-10) (Figure 4). The unit

is mainly composed of metamorphic sole rocks and harzburgite, dunite, pyroxenite, gabbro and diabase dikes. Metamorphic sole rocks are composed of green-blue-pink colored amphibolites and amphibolites, schists, calcschists and marbles that have undergone metamorphism in the greenschist facies.

In the study area, Pozantý-Karsantý Ophiolite tectonically overlies Kýzýlcadað Ophiolitic Melange and Olistostrome, and Jurassic-Cretaceous aged Çamlýk formation of Aladað Unit to the west of Belemedik Valley. And, the Ophiolite Nappe is unconformably overlain by Tertiary aged sediments. In this study, no assessment could be made directed to the thickness of the ophiolitic rocks. However, in the previous studies conducted in this area by Bingöl (1978) and Parlak (2002), it was stated that the total thickness of the ophiolite section varied between 8000 and 11000 meters.

TERTIARY SEDIMENTS

ECEMÝÞ FAULT ZONE

Çukurbað formation (Tomç)

The fluvial sediments composed of marls, mudstones and pebbly sandstones filling Ecemiþ Fault Corridor were introduced for the first time by Yetiþ (1978) under the name of Çukurbað formation. And, in this study the use of the same name was considered appropriate for similar lithologies. The type locality of the Çukurbað formation, outside the study area, is the vicinity of Çukurbað Village of Çamardý Township belonging to Niðde province. And, in the study area, all levels of the unit can be observed in an area between Pozantý Township and Tekir Plateau (J2) and Eskikonacýk Village (C7) (Figure 4).

Çukurbað formation is mainly composed of marls, mudstones and pebbly sandstones. At the base of the unit brown, green and claret red colored, medium-tick bedded, polygenic pebbly and pebbly sandstones are located. This level is overlain by green-gray colored, thin-medium bedded sandstones, siltstones and marls.

At the base, Çukurbað formation unconformably overlies Bolkar Mountain Unit, Namrun Tectonic Segment, Aladað Unit, Kýzýlcadað Ophiolitic Melange and Olistostrome and the units belonging to Pozantý-Karsantý Ophiolite. And, at the top the unit is transitive to Early Miocene aged Burç formation.

The apparent thickness of the unit varies in the study area between 300 and 350 meters. Because of the Çukurbað formation does not contain any paleontological findings the age estimation was made according to its stratigraphic position. The unit unconformably overlies Eocene age units in the Ulukýþla Basin and has a gradational contact with the overlying Miocene aged Burç formation. Accordingly, the age of the Çukurbað formation must be Oligocene-Early Miocene.

According to its general lithological properties Çukurbað formation must have deposited in a fluvial environment.

Burç formation (Tmb)

The lithology composed of coal-seamed marls, claystones and siltstones and the typical outcrops of which are observed in the vicinity of Burç Village, Çamardý township of Niðde province was introduced for the first time by Yetiþ (1978) under the name of Burç formation. And, in this study the use of the same name was considered appropriate for similar lithologies. In the study area, only in Yeniþeyhli (G4) district, to the south of Pozantý Township the outcrops of the formation are observed that can be reference section for the unit (Figure 4).

Burç formation which exhibits in general a morphological appearance with soft and flat

ridges, is mainly composed of marls, claystones, siltstones and coal seams. At the base sections of the unit green colored, thin-medium bedded and moderately competent marls, and in the upper sections an alternation of green and gray colored, thin bedded, weathered, coal-seamed claystone and siltstone take place. It was determined that in the unit there were coal seams the thickness of which varied between 50 cm and 1 m and which did not have lateral continuation; and gastropod and ostracoda type fossils.

At the base Çukurbað formation is transitive to Burç formation, and at the top, it is unconformably overlain by Quaternary aged terraces. The apparent thickness of the Burç formation in the study area is around 200-250 meters.

During this study no paleontological data was obtained to give an age to the Burç formation. However, during their studies Atabey et al. (1990) and Yetiþ (1978) determined the fossil assemblage that gave Miocene age from the samples they collected within the unit. That's why, in this study, the age of Burç formation was accepted as Early Miocene, taking into account its stratigraphic position.

Depending on its general lithological features and macrofossil content, the Burç formation must have deposited in a lacustrine - paludal environment.

ADANA BASIN

Güzeller formation (Tpeg)

Pebblestone, sandstone, clayey limestone and marl lithologies; the best outcrops of which are observed in the district of Güzeller (Çat) Village (N31), located to the south of Ayrancý township , Karaman Province outside the study area; were introduced for the first time by Demirtaþlý et al. (1973) under the name of Güzeller formation. And, in this study the use of the same name was considered appropriate for similar lithologies.

In the study area Güzeller formation exhibits outcrops mainly 3 km south of Gülek Strait (O1) and north of Karakýlýç Village (L19).

Güzeller formation is mainly composed of pebblestones, sandstones, limestones and marls. The unit starts at the base with red-pink and gray colored, medium-thick bedded polygenic pebbly pebblestones. It continues upwards with beige colored, thin-medium-thick bedded, highly fossiliferous limestones and clayey limestones. In the uppermost sections of the unit an alternation of beige-green colored, thin-medium bedded sandstone, marl and sparse limestone is observed. The pebblestone and limestone levels of the unit which is generally rich in fossils show lensing in lateral direction. The apparent thickness of the Güzeller formation in the study area varies between 500 and 550 meters.

In the study area, the Güzeller formation unconformably overlies the units belonging to the Aladað Unit, and it is unconformably overlain by Oligocene-Miocene aged Gildirli formation.

In the samples collected from the outcrops of the Güzeller formation north of Karakýlýç Village (L19) and 3 km south of the Gülek Strait (O1) the fossil assemblage comprising: *Distichopplax biserialis* (Dietrich), *Ranikothalia sindensis* (Davies), *Missippina binkhorsti* (Reuss), *Hottingerina anatolica* Sirel, *Elazýgella altýneri* Sirel, *Alveolina* (Glomalveolina) *primaeva* (Reichel), *Haymanella paleosenica* Sirel, *Nummulites* cf. *exilis* Douville, *Valvulina* sp., *Rotalia* sp., *Discocyclina* sp., *Miscellanea* sp., *Planorbulina* sp., *Belzungia* sp., *Vania anatolica* Sirel, *Caskinolina* (Caskinon) *rajkae* Hottinger and Drobne, *Smoutina* sp., *Crysalidina* sp., *Globorotalia* sp., *Nummulites* spp., *Assilina* sp., *Operculina* sp., *Sphaerogypsina*, *Cuvillerina* sp., *Miscellanea miscella* (d'Archiac ve Haime), *Distichoplax biserialis*, *Fabiania cassis* (Openheim), *Nummulites* gr. *laevigatus* (Bruguiere), *Assilina* gr. *exponens* (Sowerby), *Orbitolites* sp., *Opertorbitolites* sp., *Lockhartia* sp., *Asterigerina*

sp., *Alveolina* sp., *Heterostegina* sp., *Morozovella* sp., Discorbidae, Rotaliidae, Textulariidae, Miliolidae, Algae and bryozoa was obtained and accordingly the unit was given the age of Late Paleocene (Thanetian)- Middle Eocene (Lutetian).

Depending on its general lithological features and fossil content, the Güzeller formation must have deposited in an inner shelf environment where reefs could also form.

Gildirli formation (Tgi)

The lithologies, which outcrop in the vicinity of Gildirli Village north of Karaisalý, are composed of pebblestone, sandstone, siltstone and mudstone and were introduced for the first time by Schmidt (1961) under the name of Gildirli formation. And, in this study the use of the same name was considered appropriate for similar lithologies. Gildirli formation exhibits outcrops showing all levels, between Tekir Plateau (J2) and south of Gülek Strait (O1); in the old highway cuts between Gülek Township and Adana, north of Karaisalý, in the vicinity of Karakýlýç Village (L19), in the study area (Figure 4).

Gildirli formation is mainly composed of pebblestone, sandstone, siltstone and mudstones. The unit starts at the base with red-blackish-pink colored, thin-medium- in places thick bedded pebblestones. Overlying this level an alternation of pink-beige colored, thin-medium bedded, sandstone, siltstone and mudstones is obseved. Within the sandstones of this level, tabular and trough cross-beddings are observed.

At the base, the Gildirli formation unconformably overlies Aladað Unit, Bozkýr Unit and Paleocene-Eocene aged units, and at the top it has a contact with Kaplankaya formation, gradational in lateral and vertical directions. It was determined that the apparent thickness of the unit in the study area was around 350 meters.

As the Gildirli formation is of terrestrial character no fossil finding which can indicate an age was obtained; thus, estimation was made taking into account its stratigraphic position. At the base of the unit is present unconformably Paleocene-Middle Eocene aged Güzeller formation and at the top lies Early-Middle Miocene aged Kaplankaya formation, gradational in lateral and vertical directions. Accordingly, the age of the Gildirli formation must be Oligo-Miocene.

According to its general lithofacies and sedimentological properties, the Gildirli formation must have deposited in alluvial fan and braided river environment.

Kaplankaya formation (Tkp)

The rock association composed of pebbly sandstones, sandstones and limestones and the typical outcrops of which are observed at Kaplankaya Hill south of Karaisalý township of Adana, was introduced for the first time by Yetiþ and Demirkol (1986) under the name of Kaplankaya formation. And, in this study the use of the same name was considered appropriate for similar lithologies.

Outcrops of Kaplankaya formation having reference section quality can be observed in the vicinity of Hacýn Locality (P3), Günaltý Neighborhood (S5), Kuþçular Village (P15), Kýralan Village (S18) and Kabalak Hill (L17) in the study area (Figure 4).

Kaplankaya formation is mainly composed of limestones, pebbly sandstones and sandstones. At the base of it yellowish beige colored, thin-medium bedded pebbly sandstones are located. These pebbly sandstones are overlain by beige, in places reddish beige colored, thin-medium bedded, in places cross-bedded sandstones and limestones. The uppermost levels of the unit are composed of beige and light gray colored, thin-medium bedded clayey limestones.

Kaplankaya formation is gradational in lateral and vertical directions with Gildirli formation at the base and with Karaisalý at the top. The thickness of the Kaplankaya formation in the study area varies between 75 and 200 meters.

In the samples collected from the outcrops of the Kaplankaya formation in the vicinity of Kýralan (S18) and Keþli (S9) Villages, *Operculina* spp., *Heterostegina* sp., *Borelis* sp., *Amphistegina* sp., *Asterigerina* sp., *Elphidium* sp., *Gypsina* sp., *Globigerinoides* sp., *Globorotalia* sp., Textulariidae and Miliolidae fossil assemblage which gave the age of Early-Middle Miocene was determined. In addition, Yetiþ and Demirkol (1986) gave the age of Burdigalian-Langhian to the Kaplankaya formation in their study. When the above defined fossil assemblage and the results obtained in previous studies were evaluated, the age of the Kaplankaya formation must be Early-Middle Miocene.

According to its general lithological features and fossil content, Kaplankaya formation must have deposited in a beach and back-reef lagoonal environment.

Karaisalý formation (Tka)

Early-Middle Miocene aged limestones which outcrop in the vicinity of Karaisalý township of Adana province were introduced for the first time by Schmidt (1961) under the name of Karaisalý Limestone. However, in this study the use of the name 'Karaisalý formation' was considered appropriate. Karaisalý formation forms high hills and extending ridges in the west parts of the Adana Basin. Its major outcrops having reference section quality can be observed north of Hopur Mountain (R6), Keþli Village (S9), Eminlik Village (S13) and southeast of Kuþçular Village (P15) (Figure 4).

It was observed that at the base of the Karaisalý formation, which is mainly represented by reefal limestones, in places is situated a level composed of pinkish beige colored, massive-looking, ungraded, poorly sorted, carbonate-cemented pebblestones having a sand matrix and polygenic elements. Apart from the above defined pebblestones, the formation is composed of limestones which are gray and beige colored, medium-thick bedded, massive in places, hard-rugged, with calcite-filled cracks and fractures, and containing abundant hermatrypic organisms such as coral, algae, mollusk, bryozoa and echinoderm.

Karaisalý formation is at the base gradational with Gildirli and Kaplankaya formations in lateral and vertical directions. In some sections of the study area, Karaisalý formation overlies Paleozoic-Mesozoic aged basement units as angularly unconformable. Outside the study area, the formation is overlain by Cingöz and Güvenç formations as gradational in lateral and vertical directions. The apparent thickness of the Karaisalý formation in the study area varies between 5 and 500 meters.

In the samples collected from the outcrops of the Karaisalý formation in the vicinity of Hopur Mountain (R6) and Keþli Village (S9) the fossil assemblage composed of *Globorotalia* gr. *archeomenardii* Bolli, *Globorotalia obesa* Bolli, *Globigerinoides trilobus* (Reuss), *Globigerinoides immaturus* Leroy, *Orbulina* cf. *bilolobata* (d'Orbigny), *Borelis* cf. *melo* (Fichtel and Moll), *Globorotalia* cf. *archeomenardii* Bolli, *Borelis* cf. *curdica* (Reichel), *Globoquadrina* sp., *Globigerinoides* sp., *Praeorbulina* sp., *Rupertina* sp., *Borelis* sp., *Gypsina* sp., *Sphaerogypsina* sp., *Operculina* sp., *Dentritina* sp., *Miyosorites* sp., *Amphistegina* sp., *Peneroplis* sp., *Rotalia* sp., Miliolidae, alga, bryozoa and lamellibranch shell fragments and which gave the Early-Middle Miocene age. However, Kop (2003) stated that the age of the Karaisalý formation went from Middle Miocene up to Late Miocene in the region, by determining the fossil assemblage composed of *Borelis* cf. *melo* Fichtel and Moll, *Amphistegina* sp., *Archaias* sp., Victoriellidae, Soritidae, Calca-

rinidae, Alveolinidae in the samples he collected from the unit during his study in the near east of the study area.

According to its general lithological features and fossil content, Karaisalý formation must have deposited in a reef facies of a shallow and turbulent sea.

Slope Debris, Terrace and Alluvium (Qym, Qtr, Qal)

In the study area, the youngest deposition is represented by alluviums in the Pozantý Valley, terraces hanging on the slopes, and slope debris accumulated in various plains on valley slopes and especially within Ecemiþ Fault Zone. All of these three deposition types are generally from red to gray in color, thin-medium bedded, moderately cemented, carbonate-cemented and have sand matrix and polygenic elements.

RESULTS AND DISCUSSION

The results obtained in this study which covers Belemedik and its vicinity located in the eastern part of the Ecemiþ Fault Zone which constitutes the boundary between Central and Eastern Taurides, and the discussion about the findings obtained in this study and in the previous studies are presented below.

The rock association outcropping in the study area is grouped under the main headings of Belemedik Sequence, Bozkýr Unit and Tertiary Sediments.

The rocks in the Belemedik formation constitute the basement in the study area. Belemedik Sequence was introduced for the first time by Blumenthal (1947) under the name of Belemedik Tectonic Window and it was stated that the Devonian-Permian aged units were tectonically overlain by an incomplete Mesozoic rock association. In this study, it was determined that Belemedik formation was composed of Late Devonian-Late Cretaceous aged rock associations. In the study previously carried out by Gül et al. (1984) in the vicinity of Bolkar Mountains and Belemedik, it was stated that the sequence that they named 'Belemedik Tectonic Slice' contained rock associations of Late Devonian-Late Cretaceous age. However, the researchers asserted that within Belemedik Tectonic Slice, Early-Middle Carboniferous aged Belemedik formation was overlain by Late Permian aged Köþkdere formation with a contact that can be called as unconformity; and Early Triassic aged Diþdöken formation is overlain again with an unconformable contact by Middle Jurassic-Late Cretaceous Delikkaya formation; consequently, Late Carboniferous-Early Permian and Middle-Late Triassic-Early Jurassic aged units were absent in the region. The existence of Late Carboniferous-Early Permian aged rock formations within Palaeozoic aged units was determined for the first time in this study, apart from *Girvanella*-bearing Lower Permian stated by Flügel and Kahler (1988) who examined mainly Upper Devonian-Permian facies in their study. In addition, it was determined for the first time again in this study that Mesozoic aged units overlying the Palaeozoic sequence were not incomplete as asserted by Blumenthal (1947) and Gül et al. (1984) and it was composed of Early- Middle Triassic aged Kataraşý, Middle-Late Triassic aged Sarýyarma, Jurassic aged Çamlýk and Late Cretaceous aged Yavça formations respectively. Under the light of these findings, it was determined for the first time that the Belemedik Sequence, which contains in general Late Devonian-Late Cretaceous aged rocks and can be characterized by the presence of Early Permian aged rocks, could be thoroughly correlated with the Aladað Unit, which one of the units defined by Özgül (1976) in Taurides.

The fact that the Belemedik Sequence, located farthest west of the Eastern Taurides and bordered by Ecemiþ Fault Zone similar to the Eastern Taurides, was described as a window without stating its setting within Tauride Units

until today, and caused difficulties in explaining the transition of the units defined by Özgül (1976) between the Central and Eastern Taurides. Depending on the correlation made in this study, it was determined what kind of extension the rock associations, defined as units in the Taurides, present between Eastern and Central Taurides separated by the Ecemiþ Fault. The determination of the position of the Belemedik Sequence within The Tauride Units will make significant contributions to the grouping of the other rock associations overlying and underlying this sequence and their correlation with the units defined in the Taurides at the same time.

It was determined in the study area that the Belemedik Sequence was tectonically overlain by the rocks belonging to the Bozkýr Unit, and the Tertiary aged rocks which unconformably covered the rocks of both Belemedik Sequence and The Bozkýr Unit.

It was determined that owing to numerous deformation cycles the region underwent, the contact between Palaeozoic and Mesozoic aged rocks in the Belemedik region lost its initial position and Mesozoic aged rocks moved on Palaeozoic aged rocks. Consequently, it can be said that the units at the base of the Mesozoic sequence were subjected to tectonic erosion in some parts of the study area.

Late Paleocene (Thanetian) - Midde Eocene (Lutetian) Güzeller formation which unconformably overlies the units belonging to the Aladað Unit in the study area was defined in Adana Basin for the first time in this study.

ACKNOWLEDGEMENT

This article involves part of the works carried out within the scope of the project titled 'Geodynamic Evolution of the Central Taurides' conducted by the Department of Geological Researches of the General Directorate of Mineral Research and Exploration (MTA) and covered Ereðli (Konya), Ulukýþla (Niðde), Karsantý (Adana) and Namrun (Ýçel) district. We would like to express our thanks to Necati Turhan for his support and contribution to the realization of the study and to MTA paleontologists Kemal Erdoðan, Birkan Alan, Associate Prof. Dr. Cengiz Okuyucu, B. Özdeyiþ Çakýrsoy and Ayþegül Aydýn for the descriptions of the samples collected in the field.

Manuscript received January 12, 2010

REFERENCES

Alan, Ý., Þahin, Þ., Kop, A., Bakýrhan, B. and Böke, N., 2004*a*, Belemedik Ýstifi'nin jeolojik özellikleri ve Toroslarda tanýmlanan birlikler içerisindeki konumu, 57. Türkiye Jeoloji Kurultayý, 08-12 Mart, Bildiri özleri, s. 269, Ankara.

_____, Kop, A., Keskin, H., Altun, Ý. and Balcý, V., 2004*b*, Namrun ve kuzeyindeki metamorfik istifin Toroslarda tanýmlanan birlikler içerisindeki yeri. 57. Türkiye Jeoloji Kurultayý, 08-12 Mart, Bildiri özleri, s. 273, Ankara.

Atabey, E., Göncüoðlu, M.C. and Turhan, N., 1990, 1/100 000 ölçekli açýnsama nitelikli Türkiye jeoloji haritalarý, Kozan-J19 paftasý, Maden Tetkik ve Arama Yayýnlarý, Ankara.

Ayhan, A. and Lengeranlý, Y., 1986, Yahyalý-Demirkazýk (Aladaðlar yöresi) arasýnýn tektono-stratigrafik özellikleri. Jeoloji Mühendisliði Dergisi, 27, 31-45, Ankara.

Blumenthal, M.M., 1947, Belemedik Paleozoyik penceresi ve bunun Mesozoik kalker çerçevesi: Maden Tetkik ve Arama Enstitüsü Yayýnlarý Seri D, 3, 1-97, Ankara.

Bingöl, A.F., 1978, Petrologie du Masif Ophiolitique de Pozantý-Karsantý (Taurus Cilicien, Turquie): Etude de la Orientale. These 3'e Cycle, Universite Strasbourg.

Demirtaþlý, E., 1967, Pýnarbaþý-Sarýz-Maðara Civarýnýn Jeolojisi Raporu: Maden Tetkik ve Arama Rapor no: 4384, 39 s., (unpublished), Ankara.

_____, Bilgin, A. Z., Erenler, F., Iþýklar, S., Sanlý, D. Y., Selim, M. and Turhan, N., 1973, Bolkar-

daðlarýnýn Jeolojisi. Cumhuriyeti'in 50. Yýlý Yer bilimleri Kongresi, Maden Tetkik ve Arama Özel Yayýn, 42-57s. Ankara.

Flügel and Kahler, 1988, Faziell-stratigraphische Entwicklung im Paläozoikum von Belemedik ("Bagdad-bahn-Profil"), Südanatolien (mit Beiträgen von Buggisch, W. and Flügel, H.W.).- Facies, 18, 123-168, Pls. 12-21, 8 Figs., 2 Tabs., Erlangen.

Gül, M.A., Çuhadar, Ö., Öztaþ, Y., Alkan, H. and Efeçýnar, T., 1984, Bolkardaðý-Belemedik yöresinin jeolojisi ve petrol olanaklarý. TPAO Raporu, No: 1972, 159 s., (unpublished), Ankara

ÝIker, S., 1975, Adana baseni kuzeybatýsýnýn jeolojisi ve petrol olanaklarý: TPAO Arama Arþiv No: 973, 63s. (unpublished), Ankara.

Kop, A., 2003, Gökçeköy - Kýþlak - Menkez - Akdam (D-KD Aladað, Adana) Dolayýnýn Tektono-Stratigrafisi ve Yapýsal Evrimi, Çukurova Üniversitesi Fen Bilimleri Enstitüsü, Doktora Tezi, 311 s., (unpublished), Adana.

Monod, O., 1977, Recherches Geologiques Mineralogique Dans le Taurus Occidental au Sud de Beyþehir (Turquie): These d'etat, l'Univ. de Paris Sud, Center d'Orsay, sr. A, 896, 571 s.

Özgül, N., 1976, Toroslarýn Bazý Temel Jeoloji Özellikleri. Türkiye Jeoloji Kurumu Bülteni 19, 5-78, Ankara.

_____, 1997, Bozkýr-Hadim-Taþkent (Orta Toroslarýn kuzey kesimi) dolayýnda yeralan Tektono-stratigrafik birliklerin stratigrafisi. Maden Tetkik ve Arama Dergisi, 119, 113-174, Ankara.

Parlak, O., Höck, V. and Delaloye, M., 2002, The suprasubduction Pozantý-Karsantý ophiolite, southern Turkey: evindence for highpressure crystal fractionation of ultramafic cumulates Lithos, 65: 205-24.

Poisson, A., 1977, Recherches geologiques dans les Taurides occidentales (Turquie): Thesis Üniversite Paris Sud, Orsay France, 796.

Schmidt, G.C., 1961, Stratigraphic Nomenclature for the Adana Region Petroleum District 7. Petroleum Administration Bull. 6, 47-63, Ankara.

Tekeli, O., 1980, Toroslarda Aladaðlarýn yapýsal evrimi. Türkiye Jeoloji Kurumu Bülteni, 23, 11-14.

_____, Aksay, A., Ertan-Evren, Ý., Iþýk, A. and Ürgün, M. B., 1981, Toros ofiyolit projeleri, Aladað projesi. Maden Tetkik ve Arama Raporu No. 6976, 32 s., (unpublished), Ankara.

Üþenmez, Þ., 1981, Belemedik ve çevresinin jeolojisi: S.Ü.F.F. Yer bilimleri Dergisi, seri A, l, 67-80.

_____, Friedman, G.M. and Kopaska - Merkel, D.C., 1988, Fabric and composition of dolostones and dedolomites from near karapinar (Adana, Southern Turkey), Carbonates and Evaporites, 2/2,101-108.

Yetiþ, C., 1978, Çamardý (Niðde ili) yakýn ve uzak dolayýnýn jeoloji incelemesi ve Ecemiþ Yarýlým kuþaðýnýn Maden Boðazý - Kamýþlý arasýndaki özellikleri. Ýstanbul Üniversitesi Fen Fakültesi, Doktora Tezi, 164 s. (unpublished).

_____ and Demirkol, C., 1986, Adana baseninin batý kesiminin detay jeolojisi etüdü Maden Tetkik ve Arama Raporu No:8037, 187 s., (unpublished), Ankara.

_____, _____, Lagap, H. and Ünlügenç, Ü., 1991, 1/100.000 ölçekli Kozan K 20 paftasýnýn açýnsama nitelikli raporu. Maden Tetkik ve Arama Rapor No: 36, (unpublished) Ankara.

Mineral Res. Expl. Bull., 143, 37-52, 2011

SOME STRUCTURAL CHARACTERISTICS OF AZMAR ANTICLINE - NE IRAQ

Ibrahim Saad I. AL-JUMAILY* and Hadeer Ghazi M. ADEEB**

ABSTRACT.- The purpose of this study is to elucidate the structural style of Azmar structure, a major anticlinorium within the imbricate partition of Zagros fold-thrust belt in northeastern Iraq. Structural analysis of this anticlinorium demonstrated that it consists of four main NNW-SSE trending anticlines. They are imbricated SW ward through NE dipping reverse faults merge to a deep seated detachment. Furthermore, analysis of minor folds on hinge and limbs of the main Azmar anticline revealed the versatile style of such minor folds and their opposing vergencies. These features emphasize the role of faulting in development of the major fold and the minor folds. This interpretation has been supported by hinge angularity, as well as by association of hinge and limb disrupting reverse slip mesofaults with those minor folds. Therefore a progressive fault related folding is proposed for Azmar structure in this work.

Key words: Azmar Anticline, tectonic, thrus belt, Iraq

INTRODUCTION

Tectonically, the study area belongs to the Zagros orogenic belt. The Zagros belt developed along the oblique collisional suture zone between the NE Arabian margin and Eurasia. It is linked toward the northwest to the Bitlis suture zone, which separates the Arabian and Anatolian plates. To the southeast, the convergence movement is still accommodated by the northward oceanic subduction beneath the Makran accretionary prism (Alavi, 2004) (Figure 1).

Azmar anticlinorium is situated within the Zagros Imbricate Zone. To the northeast this zone is sutured with Sanandaj-Sirjan Zone along the Main Zagros Reverse Fault. To the southwest inside Iraq, the imbricate zone is bounded by Zagros Foreland High Folds Zone through High Zagros Reverse Fault. Further to the southwest, the Zagros Mountain Front Fault represents the boundary between the later mentioned zone and the Zagros Foreland Low Folds Zone (Ibrahim, 2009) (Figure 2).

Azmar anticlinorium consists of a number of anticlines on either sides of its main hinge (Figures 3 and 4). Their hinges follow the trend of the main hinge (i.e NNW-SSE). All are asymmetrical to the SW, the SW limb of the main Azmar fold is overturned. Furthermore, their flanks are dissected by longitudinal reverse slip and transversal strike slip faults. The reverse slip faults verged towards both SW and NE directions. The strike slip faults are dextral and senistral, oblique and transverse to the trend of the anticlinorium respectively (Al-Hakary, in press) (Figure 3).

The older rocks exposed in the core of the main Azmar anticline belong to Balambo Formation of Valanginian-Turonian age. It consists of alternating layers of yellowish grey marl, shale and marly limestone. This formation is overlain by well bedded fine grained limestone with chert bands of Kometan Formation of Late Turonian-Early Campanian age. Shiranish Formation of Campanian-Maastrichtian age overlies Kometan Formation and consists of alternating layers of bluish marl and marly limestone. Tangero Forma-

* Musul Üniversitesi, Fen Koleji, Jeoloji Bölümü, IRAK
** Musul Üniversitesi, Baraj ve Su Kaynaklarý Araþtýrma Merkezi, IRAK

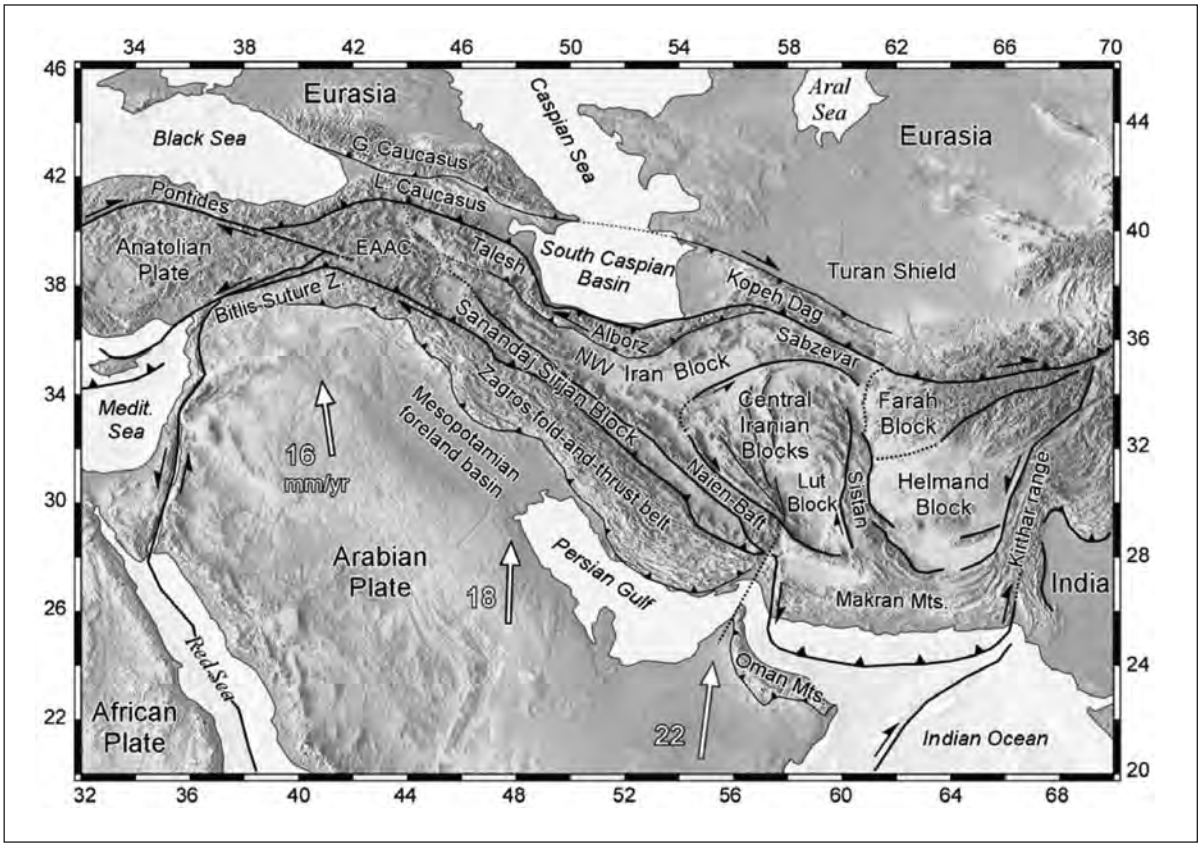

Figure 1- Plate tectonic context of the Arabian-Eurasian collision zone. Velocities of movement of Arabia with respect to Eurasia, in mm/yr, are from Sella et al., 2002. EAAC = East Anatolian Accretionary Complex (Alavi, 2004).

tion of Late Campanian-Maastrichtian age consists of clastic layers (sandstone, shale, marl, and sandy limestone) overlies the Shiranish Formation (Figures 3 and 4).

The main goal of the present work is to clarify the fold style of Azmar structure together with its minor constituents. In order to know whether this structure has been formed by passive folding or through fault propagation folding. Further more, to decipher the fold style of this structure in view of plate tectonic configuration of northern Iraq.

METHOD OF STUDY

Field data for present investigation were gathered throughout a traverse along road cuts across Azmar Mountain (Figure 3). They include attitude measurements of bedding planes, field descriptions and interpretations aided by sketches and field photographs. The collected data were analyzed later in the office with the aid of stereographic projection manually and computationally as well. Georient software (GEORIENT 9.2) was used to prepare pi- diagrams of folds.

Any structural analysis of folds whatever their size scale, accomplished by designating the following characteristic elements of fold style: (1) shape of the fold in a profile plane which classified as parallel, similar … etc., (2) the interlimb angle in profile plane, (3) cylindericity of the fold in three dimensions, and (4) the presence and

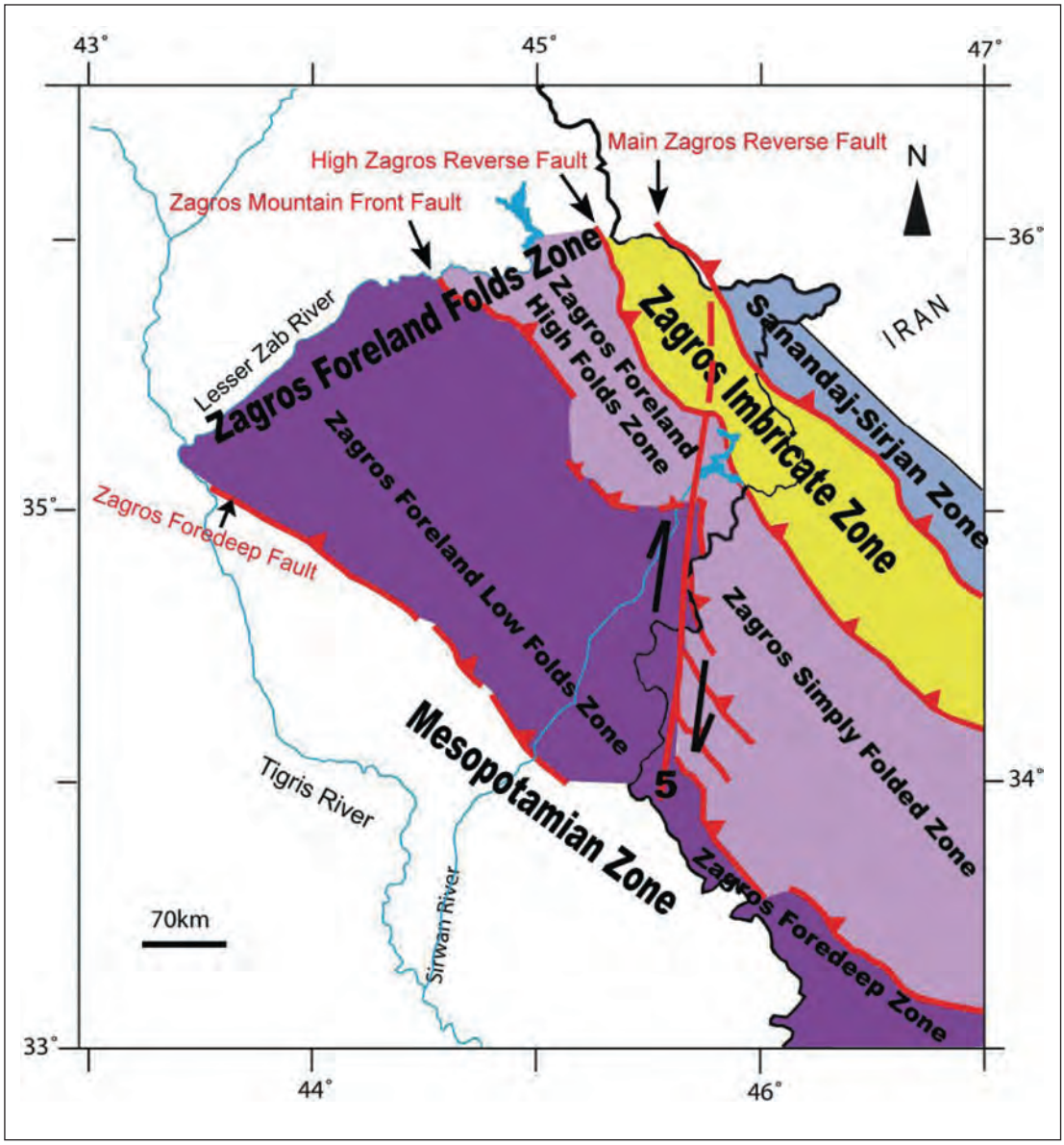

Figure 2- Main morphotectonic zones in the study area (NW segment of the Zagros Fold-Thrust Belt) and their continuations in Iran. The deep major basement faults which separate the main morphotectonic zones are drawn in red lines. The Khanaqin Fault (5) which is a dextral strike-slip has been considered as a boundary between the northwestern segment (Iraq Zagros part) and the southeastern segment (Iranian Zagros part) (Ibrahim, 2009).

type of associated axial plane foliation and/or lineation which is generally a characteristic feature in metamorphic domains (Van der Pluijm and Marshak, 1997).

The fourth parameter discarded in the present investigation because the study area consists exclusively of sedimentary successions and lacks any kind of foliations. The fold profile shape

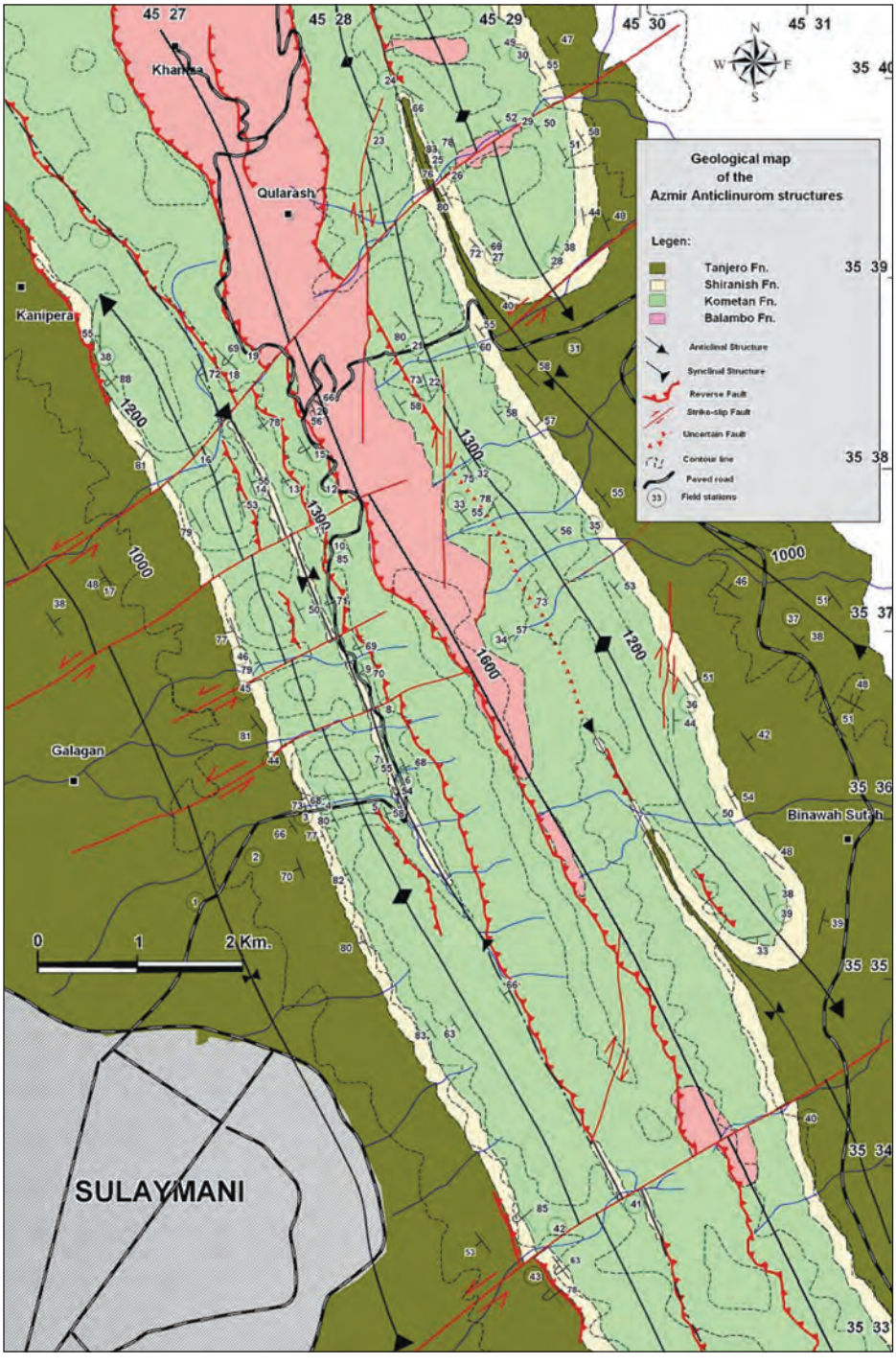

Figure 3- Geological map of Azmar anticlinorium (Al-Hakary, in press).

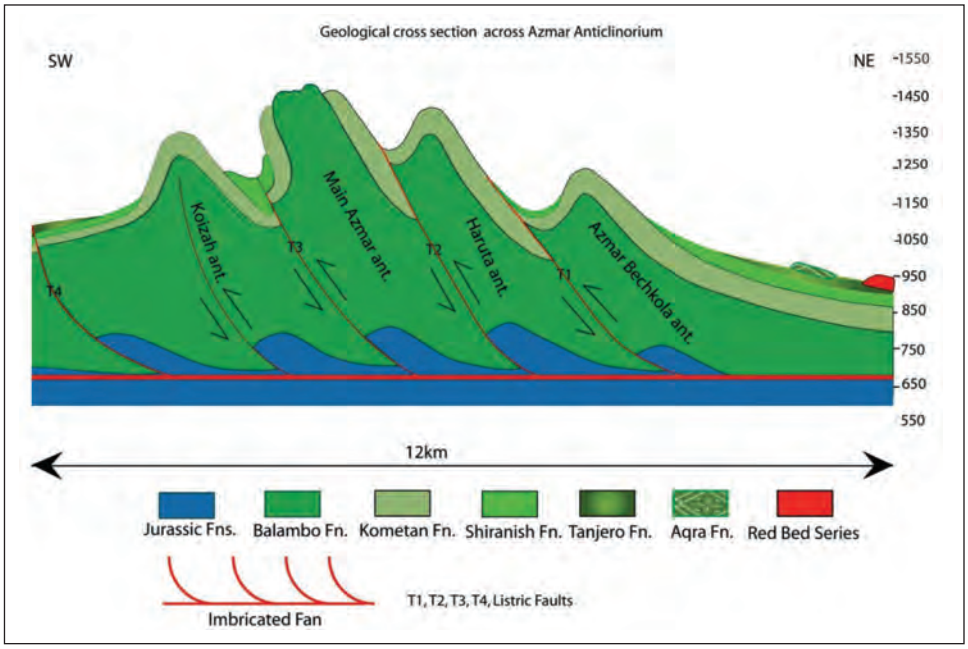

Figure 4- Geological cross section of the studied traverse in Azmar anticlinorium (Al-Hakary, in press).

examined by field photographs which clearly demonstrate the nature of curvature and bending of strata around hinge zones of folds.

Stereographic representations as pi-diagrams of bedding poles both synoptically and individually aided to detect attitudes and geometry of various fold elements. The output of this step was used to classify the main fold as well as its minor constituents. The pi-diagrams were critical also for checking the cylindericity of these folds.

FOLD ANALYSIS

Azmar anticlinorium consists of four imbricated anticlines (Figures 3 and 4). The main folds as well as their minor ones developed in a multibeds system of alternating competent (limestone, marly limestone, dolomitic limestone) and incompetent (marl, shale) beds of Balambo, Kometan and Shiranish formations. The shapes of folds are well manifested in the competent beds, and they all appear as parallel folds class 1B of Ramsay. Whereas their shapes in the intervening incompetent beds approach classes such as 1C and 2 (similar fold) of Ramsay (Ramsay and Huber, 1987).

The main anticlines of this anticlinorium structure are named from NE toward SW: Azmar Bechkola, Haruta, Main Azmar and Koizah. All are doubly plunging, trending in NNW-SSE direction and imbricating towards SW through NE dipping imbricated fan faults (T1,T2,T3 and T4) which submerge into a deep seated detachment (Figures 3 and 4). They characterized with somewhat narrow and subangular hinge zones. Their SW limbs are steeply dipping and occasionally overturned towards NE as in Azmar main anticline, whereas the NE limbs are less steep. Accordingly their axial planes are NE dipping and verging towards SW (i.e foreland verging) (Figure 5). The range of interlimb angles 58-65º for these main anticlines refers to their closed class (Table 1; Fleuty, 1964). Furthermore the scattering of S-poles moderately around the Pi-

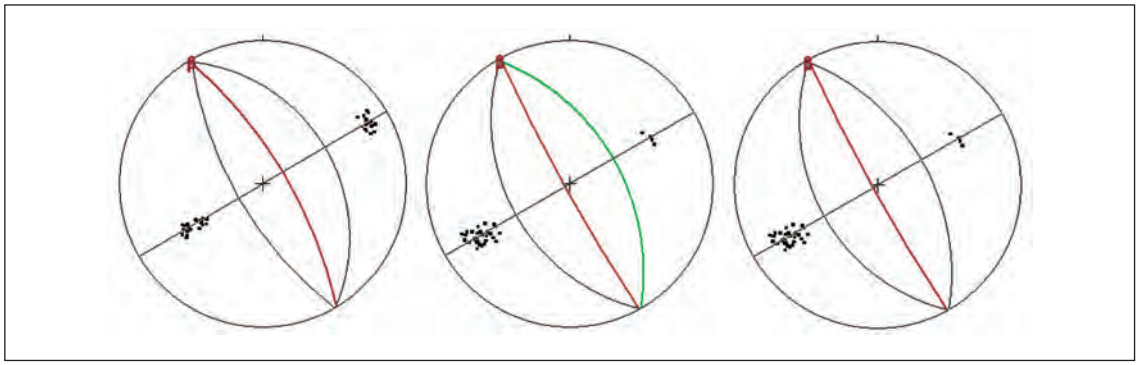

Figure 5- PI diagrams of Azmar anticlinorium (a: Azmar Bechkola, b: Main Azmar, c: Koizah anticlines). Red great circles refer to axial planes of these folds. Green great circle refers to normal NE limb and overturned SW limb of the same fold which represents at the same time the axial plane between these specific limbs.

Table 1- The geometrical parameters of Azmar anticlinorium.

Folds		Folds axis	Axial plane	Interlimb angle	Vergency	Fluety classification (1964)	
						Based on interlimb angle	Based on dip of axial plane and plunge angle
Main Folds (A)	Azmar Bechkola	330/01	149/ 77	58	SW	Closed	Steeply dipping-subhorizontal
	Main Azmar	330/01	331/87	65	NE	Closed	Upright-subhorizontal
	Koizah	329/03	150/83	60	SW	Closed	Upright- subhorizontal

planes refers to semicylindrical character of these folds (Ramsay and Huber, 1987).

MINOR FOLDS

They are of outcrop scale and may have been developed on limbs and hinge zones of larger (major) folds. The major folds containing minor ones are termed anticlinoria or synclinoria, and their presence implies to genetic relationship with the enclosing major folds, even though they vary in shape and position in the larger structure. However, the orientations of these small folds resemble approximately with each other, and at the same time approximate their enclosing major folds orientations. Therefore, the small folds are sometimes called parasitic folds, because they are closely related to a larger structure (Van der Pluijm and Marshak, 1997; Ragan, 1986).

The geometric relationship between parasitic folds and the regional structure gives a powerful concept in structural analysis, known as Pumpelly's rule (Twiss and Moores, 2007). This concept states that the orientation of small (high order) structures is representative of the orientation of regional (low-order) structures. Thus the orientations of hinge line and axial surface of a small (minor) fold predict these elements for a regional fold. But field testing of this concept has proven to be remarkably robust in regional analysis.

There is a train of minor (high-order) folds in the hinge zone (Figure 6) and NE limb (Figure 7), and in the SW limb (Figure 8), of the main Azmar anticline (Figure 3). They have been developed through a stack of Balambo Formation made up

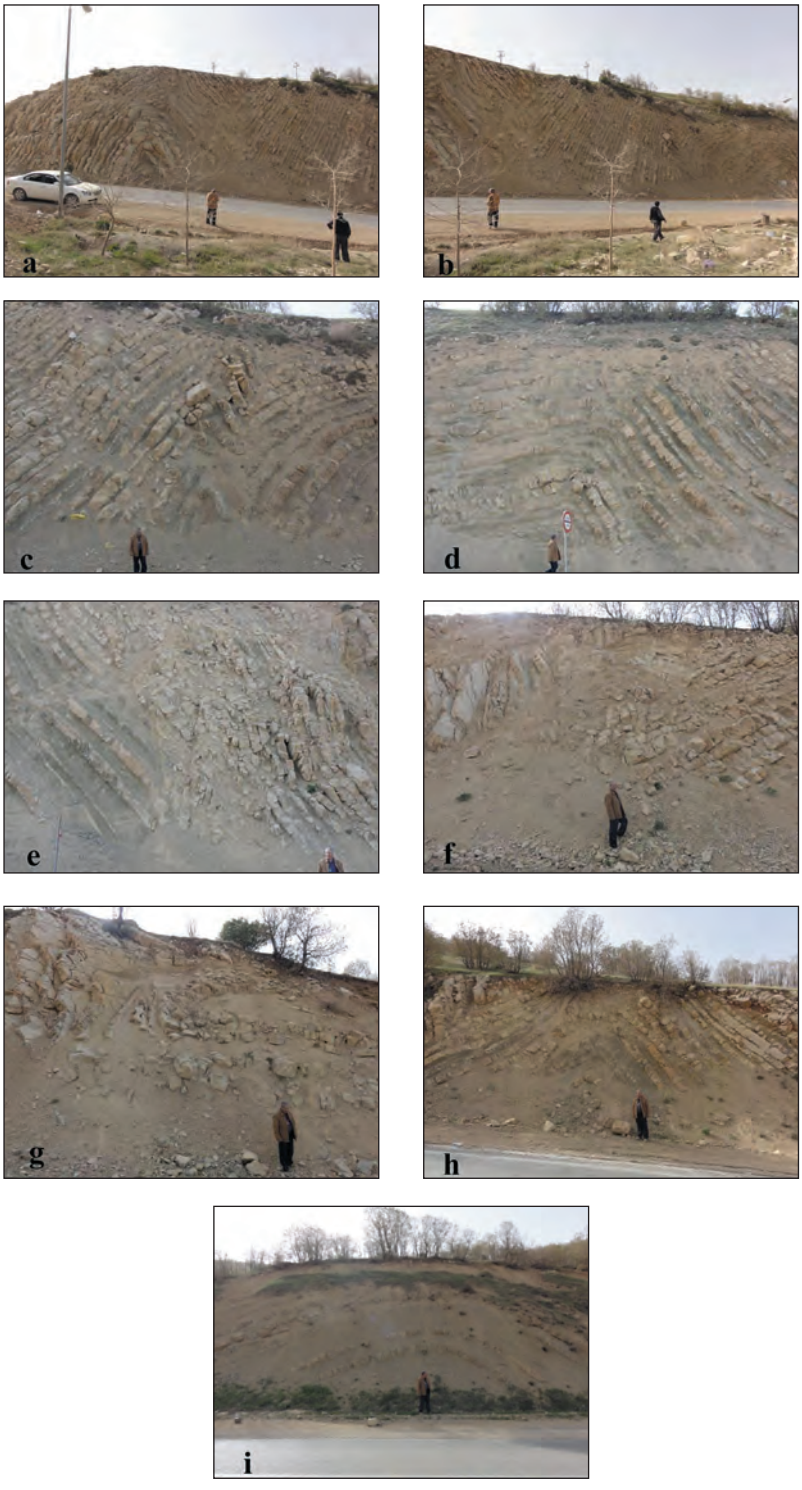

Figure 6- Train of varied style congruent minor folds in Balambo Formation at the hinge of main Azmar anticline. (a,b,c,d,e,f) are tight with angular hinges; g is recumbent; h and i are open with rounded hinges; e is disrupted with a reverse fault.

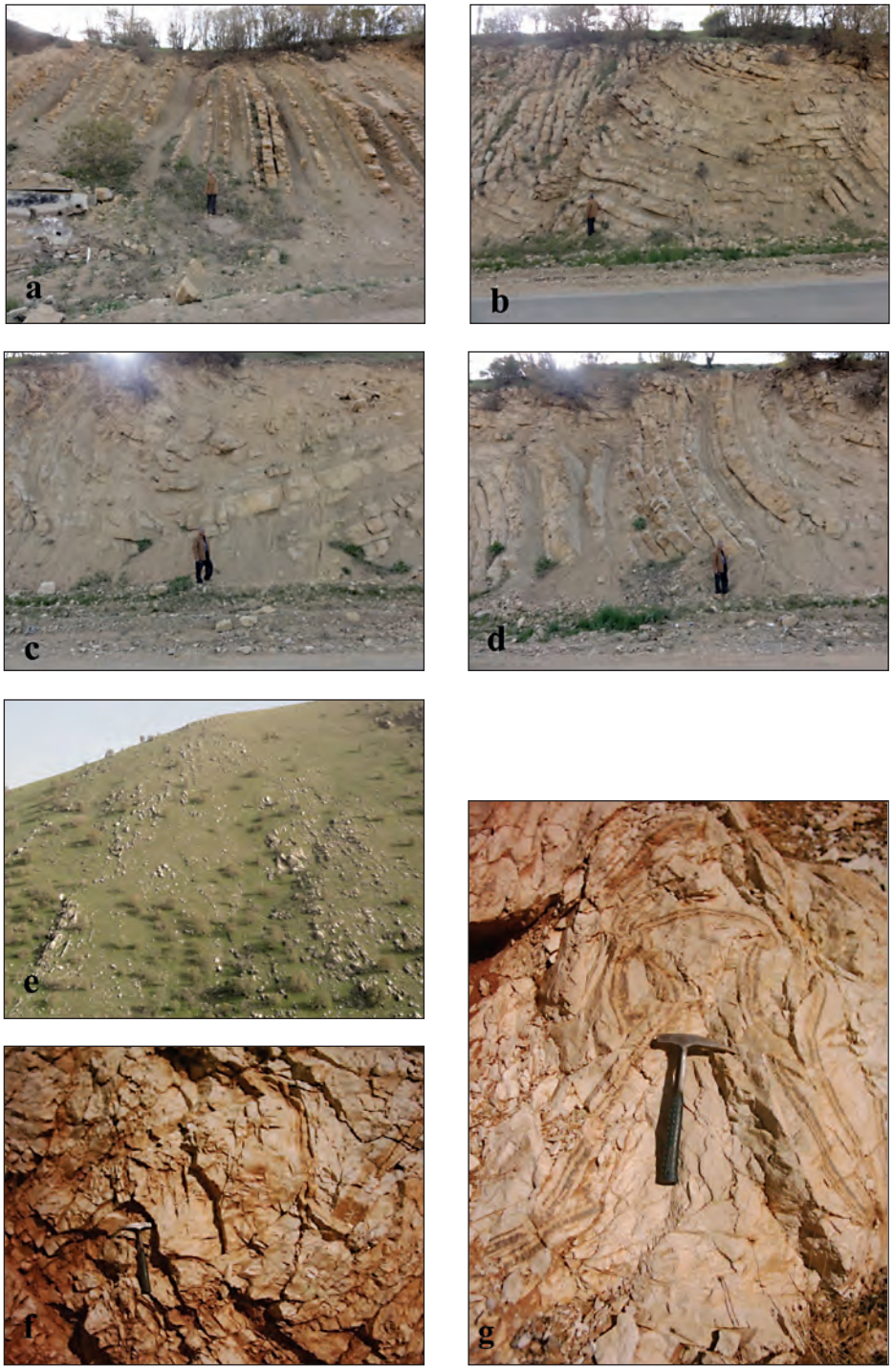

Figure 7- Varied style congruent minor folds at NE limb of main Azmar anticline. (a, b, c, d) in Balambo Formation; (e, f, g) in Kometan Formation. a is isoclinal; b , d and e are with angular hinges, the synclinal hinge of b is disrupted with a reverse fault; c is with rounded hinge; f and g are chert band minor folds; g is fan shaped.

Figure 8- Train of varied style congruent minor folds at SW limb of main Azmar anticline. (a and b) in Balambo Formation; a is a recumbent; b is a monoclonal minor fold separated from the recumbent one by a probable reverse fault dipping SW ward. (c and d) in Kometan Formation; c is recumbent; d is a recumbent minor fold sandwiched between an upper and a lower reverse faults dipping NE ward.

of alternating dolomite, limestone and marl, and the Kometan Formation thin limestone beds. The common characteristic feature of most of these minor folds is the angularity of their hinge zones and the general conformity of their axial trends (NW-SE) with the axial trend of their enclosing main Azmar anticline. The association of reverse faults with angular hinges and limbs of these minor folds (Figures 6e, 7b, 8b,8d) is powerful indication for the fault related type of these minor folds. This is a characteristic phenomenon of folding in the imbricated zone. The competency contrast between thin stiffer chert bands and the fine grained relatively thicker limestone beds of the Kometan Formation is distinctly obvious within the parallel fold style of limestone beds. Thus, the stack of limestone beds with chert bands gives up a disharmonic character for minor folds in this formation on both limbs of the main Azmar anticline (Figure 7f). Occasionally some chert bands give rise fan-shaped folds particularly in the NE limb of the main fold (Figure 7g). However the style of minor folds within the main fold varies through concurved (Figures 6h,i; 7c), chevron (Figures 6a,b,c,d,f,e; 7b,d,e), isoclinal (Figure 7a), recumbent (Figures 6g; 8a,c,d), disharmonic (Figure 7f), fan shaped (Figure 7g) and monoclinal (Figure 8b).

However, as evident from the representative Pi-diagrams of (27) minor folds (Figures 9,10 and 11) and (Table 2), there exist remarkable dis-

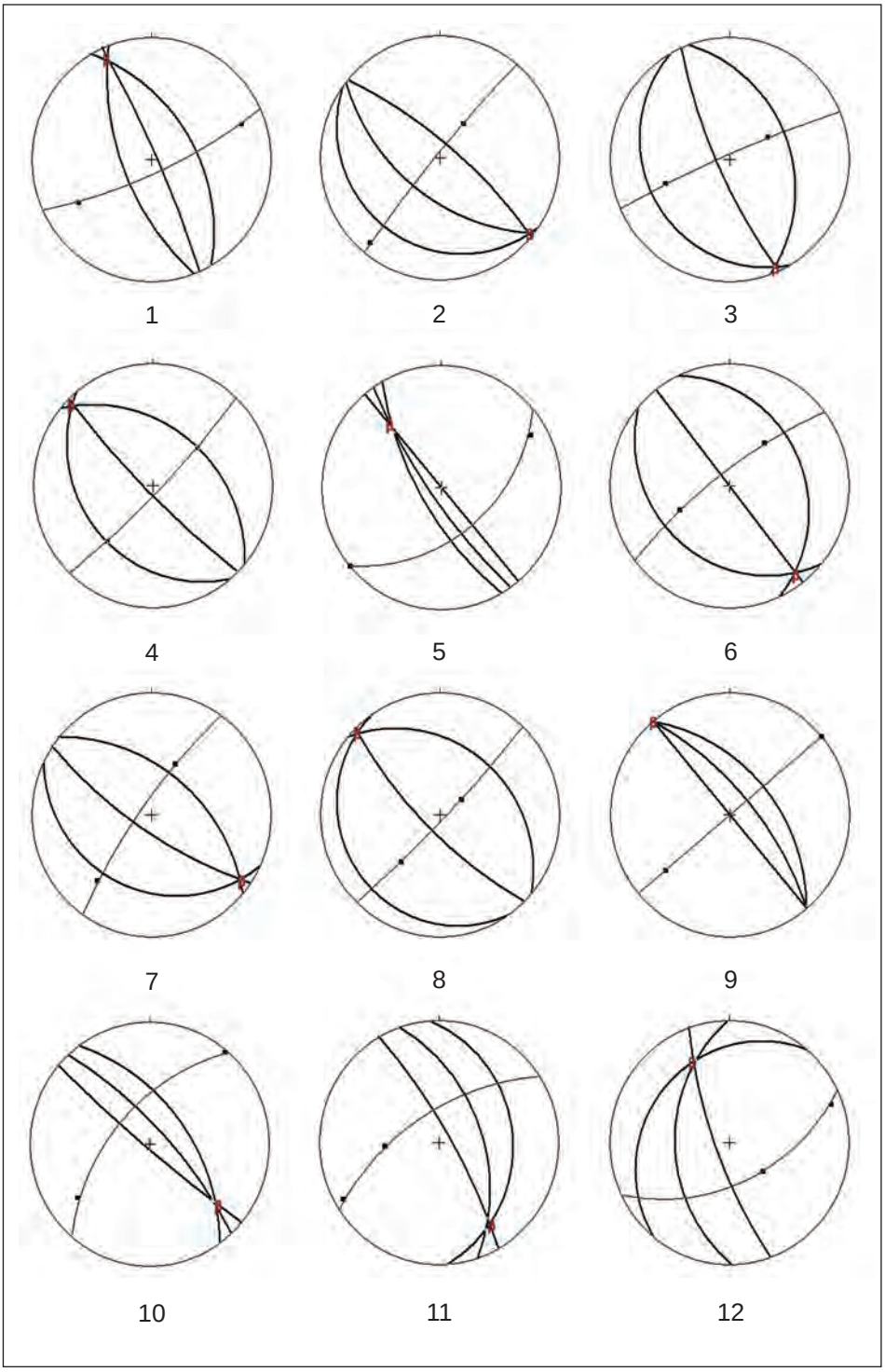

Figure 9- Stereographic representations (Pi-diagrams) of minor folds in main Azmar anticline. β: fold axis, ▪: poles to bedding.

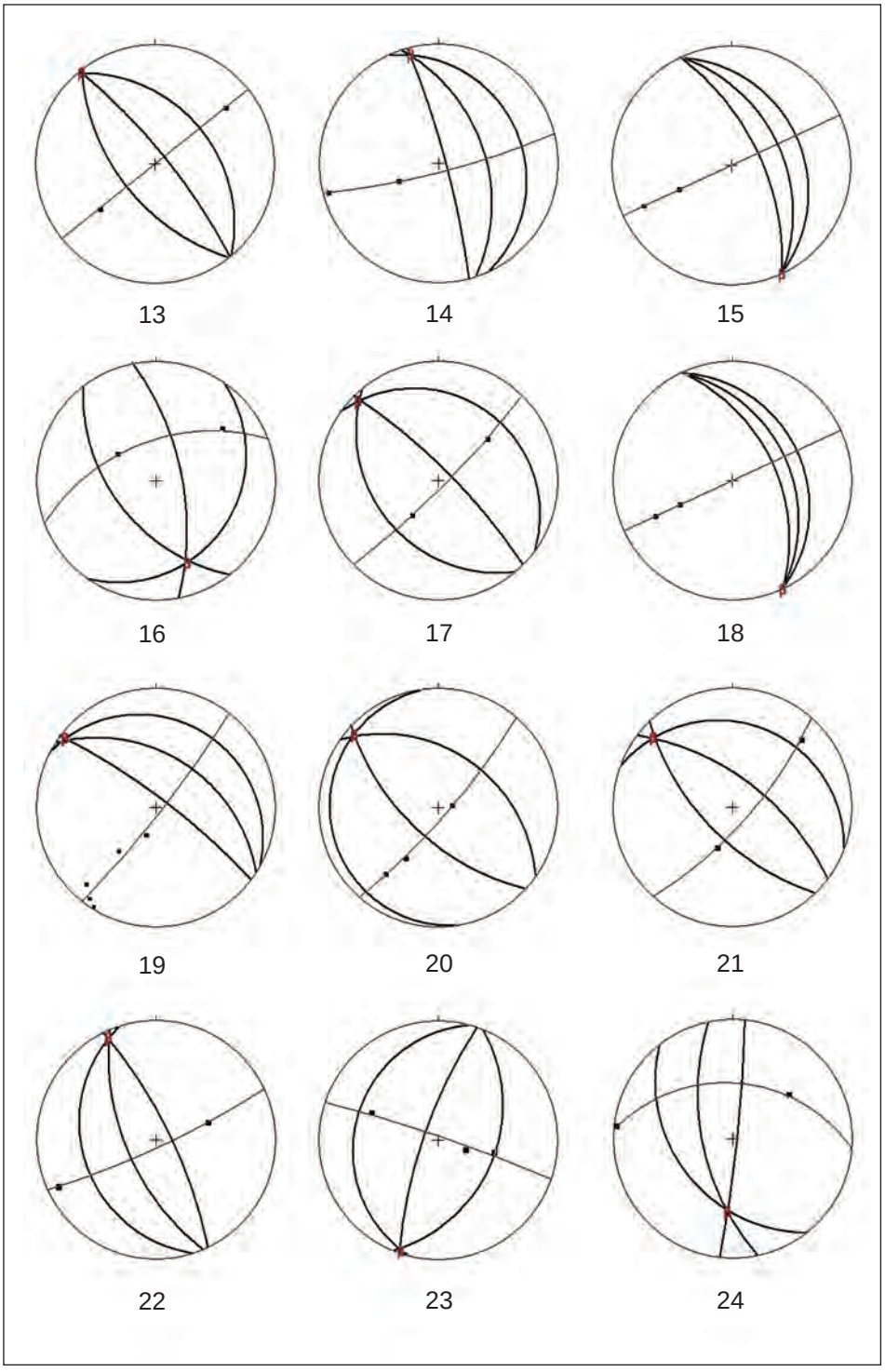

Figure 9- Continued

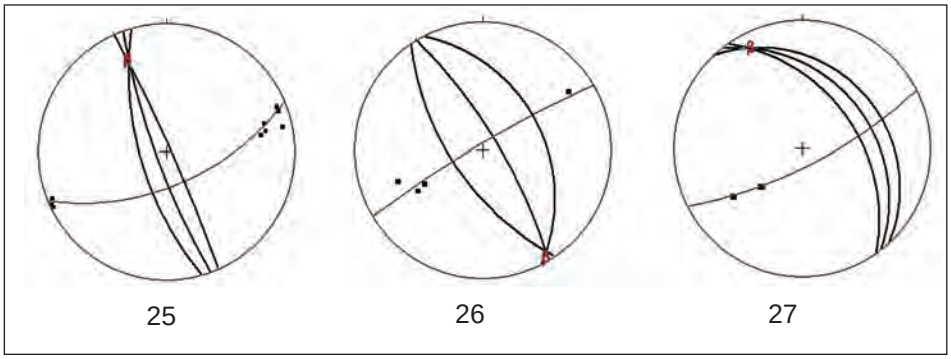

Figure 9- Continued

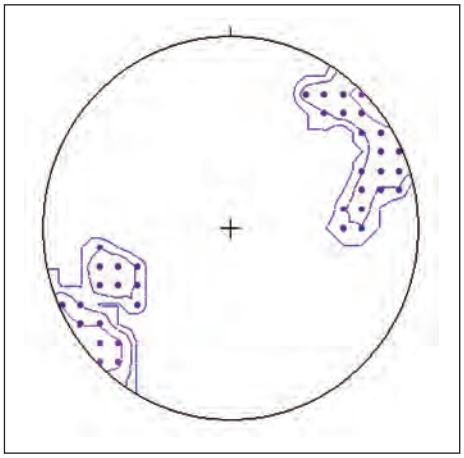

Figure 10- Gridded contour diagram of axial planes poles of 27 minor folds at Azmar main anticline.

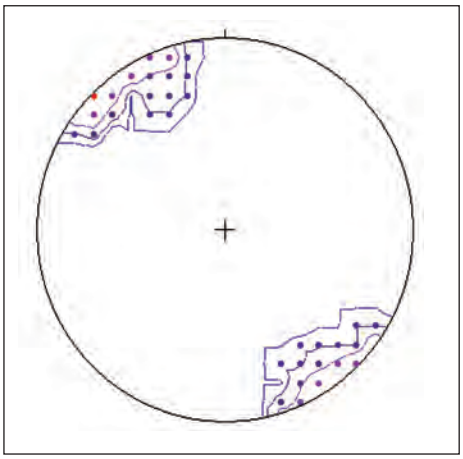

Figure 11- Gridded contour diagram of fold axes of 27 minor folds at Azmar main anticline.

Table 2- The geometrical parameters of minor folds in the main Azmar anticline.

Minor fold no.	Location in main Azmar anticline	Fold axis attitudes Plunge / Trend	Axial plane attitudes Dip / Dip direction	Interlimb angle	Fluety classification (1964)	
					Based on interlimb angle	Based on axial plane dip
1	NE	10/336	86/066	50	Close	Upright - subhorizontal
2	NE	02/130	64/218	72	Open	Steeply dipping - subhorizontal
3	NE	04/157	81/246	102	Open	Upright - subhorizontal
4	SW	05/314	85/225	90	Open	Upright - subhorizontal
5	SW	33/320	82/235	17	Tight	Upright - moderately plunge
6	SW	10/143	90/052	106	Open	Upright - subhorizontal
7	hinge	08/125	79/214	84	Open	Steeply dipping - subhorizontal
8	hinge	04/314	79/225	120	Gentle	Steeply dipping - subhorizontal
9	NE	00/320	75/050	31	Close	Steeply dipping - subhorizontal
10	SW	25/131	79/047	32	Close	Steeply dipping - gently plunge
11	SW	21/147	60/071	49	Close	Moderately dipping-gently plunge
12	NE	28/335	52/269	67	Close	Moderately dipping-gently plunge
13	NE	02/321	82/051	65	Close	Upright - subhorizontal
14	NE	06/346	58/072	56	Close	Moderately dipping-subhorizontal
15	SW	00/335	55/065	30	Close	Moderately dipping-subhorizontal
16	NE	27/159	72/079	106	Open	Steeply dipping - gently plunge
17	NE	05/315	82/045	105	Open	Upright - subhorizontal
18	SW	00/335	50/065	20	Tight	Moderately dipping-subhorizontal
19	NE	04/308	54/035	57	Close	Moderately dipping-subhorizontal
20	NE	07/311	69/223	122	Gentle	Steeply dipping - subhorizontal
21	NE	12/312	70/037	83	Open	Steeply dipping - gently plunge
22	NE	05/335	69/247	62	Close	Steeply dipping - subhorizontal
23	NE	02/199	80/289	100	Open	Upright - subhorizontal
24	NE	39/184	69/258	58	Close	Steeply dipping-moderate plunge
25	NE	22/337	83/250	22	Tight	Upright - gently plunge
26	SW	04/149	80/059	59	Close	Upright - subhorizontal
27	SW	11/333	45/052	20	Tight	Moderately dipping-gently plunge

crepancies in many respects among these minor folds and between them and the main Azmar anticline as well. The range of axial attitudes of these minor folds falls into three groups. A group (2,4-11,13,17,19-21) with axes trending generally in NW-SE direction. Another group with axes trending generally NNW-SSE in accordance with the trend of the main Azmar anticline, these are namely (1,3,12,14-16,18,22, 25,27). Yet there is a third group of two minor folds with somewhat discordant fold axes with regard to the first two groups, these are (23 and 24) trending in NNE-SSW direction, both of them are lying in the NE limb of the main Azmar anticline. Furthermore, these three groups are also differentiated somewhat in trends of their axial surfaces (Table 2). Accordingly, they are sorted in ENE, NE hinterland and SW foreland vergencies. Thus they are diversely verging with respect to hinge of the main Azmar anticline. This phenomenon contradicts with a normal vergency of minor folds on both flanks of a main fold, that is the minor folds on both limbs verge toward each other and towards the hinge zone of the

main fold (Van der Pluijm and Marshak, 1997; Ramsay and Huber, 1987; Hobbs et al., 1976; Suppe, 1985).

Furthermore the interlimb angles of these minor folds vary largely, thus, they fall into tight (5,18,25,27), open (2,3,4,6,7,16,17,21,23), closed (1,9-15,19,22,24,26) and gentle (8,20) according to Fleuty (1964), (Table, 2).

BOUDINAGE STRUCTURES

They are sausage-shaped lenses of relatively rigid (competent) beds embedded in a more ductile matrix in a rock that has undergone bed parallel stretching. In three dimension, they are long tabular bodies separated by boudin necks, that can be regarded as linear objects (Van der Pluijm and Marshak, 1997 ; Suppe, 1985).

It is observed in the present investigation that the thin chert bands embedded in relatively thicker limestone beds of the Kometan Formation were segmented into boudin like fragments (Figure 12). Thus it is obvious that the process by which this chert boudinage has been formed resembles to the mechanism just cited above. That is by bed parallel stretching on the NE limb of the main Azmar anticline. Such stretching in NE-SW direction might have been dominated during the relaxation episode that succeeded folding (i.e. during the uplifting stage of the major fold). This extension (stretching) direction accords with the step like minor normal faults in the same limb of the main fold (Figure 13), and with the bedding parallel stylolite seams with their peaks pointing vertically upward (Figure 14). Another form of chert boudine is also noted on the same NE limb of Azmar anticline. But the chert band in this case has not been segmented into pieces, rather it has a necked fashion (Figure 15). However, it is also the product of bed-parallel stretching in NE-SW direction.

In the subvertical part of SW limb of the main Azmar anticline, there are also boudinage structures, that have been developed within competent limestone beds of the Kometan Formation (Figure 16). Boudinage formation here is attributed to the tightening compressive direction which become sub perpendicular to the bedding at this limb. Thus secondary bed-parallel stretching of limestone beds occurred leading to the development of such boudinage structures.

TECTONIC INTERPRETATION

The structural architecture of Azmar anticlinorium indicates that it has been developed through progressive folding with contribution of hinterland dipping reverse faults. Such these faults might merge with a deep seated detachment related to the collision of Arabian-Iranian plates led to Zagros Orogeny. Thus, it is postulated that the main regional compressive stress responsible for development of such structures was directed NE-SW. (Talebian and Jackson, 2002; Alavi, 2004; Agard et al. 2005).

The progressive folding is also manifested by versatile styles of minor folds disposition on main Azmar anticline. The differentiation of three groups of minor folds according to their orientations (Table 2, Figure 9), and their diverse vergency relative to hinge zone of the main Azmar anticline, besides their variance in interlimb angles, all indicate that these minor folds were developed progressively in accordance with the major fold development. They might have been developed during the tightening stage of the major fold and their modification continued contemporaneously with it. Moreover, the form of the major Azmar anticlinorium as well as the angular hinges of its various minor folds (chevron folds) refer to fault related folding scheme for this major structure.

However, the progressive folding was finally terminated by bed-parallel stretching oriented normally to the trend of Azmar anticlinorium. This stretching might be attributed to final uplift of the

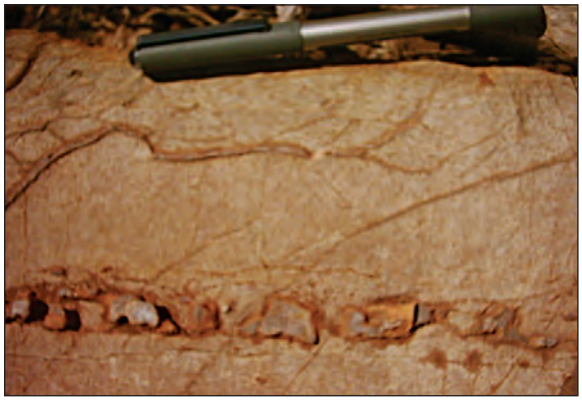

Figure 12- Segmented boudin structures through limestone bed of the Kometan formation at NE limb of the main Azmar anticline.

Figure 13- A series of step-like minor normal faults in the limestone beds of the Kometan formation at NE limb of the main Azmar anticline.

Figure 14- Bedding parallel stylolite seam in the Kometan formation at NE limb of the main Azmar anticline.

Figure 15- Necked boudin of a chert band in the Kometan formation at NE limb of the main Azmar anticline.

Figure 16- Boudin limestone beds in Kometan formation at the subvertical part of SW limb of the main Azmar anticline.

whole structure and manifested by normal faulting (in NE limb), bedding parallel stylolite seams and boudin formation in chert bands and limestone beds in both limbs of the main fold.

CONCLUSIONS

Fold characterization study of Azmar anticlinorium NE Iraq has revealed the followings.

1. Azmar anticline is a major NNW-SSE trending anticlinorium involving four main SW verged anticlines (Azmar Bechkola, Haruta, Main Azmar and Koizah), and imbricated to each other through NE dipping imbricate fan faults which submerge into a deep seated detachment.

2. The both limbs and hinge zone of the main Azmar anticline bear minor folds of various size (wavelength and amplitude), and style (curved hinge, angular hinge, chevron, isoclinal, recumbent) and associated with reverse faults disrupting their hinges or limbs. Minor folds on the either limbs verge differently relative to the hinge zone of the main fold, and they fall into three categories according to strike of their respective axial surfaces.

3. The shape of Azmar anticlinorium together with the angular hinges of most minor folds refer to fault related folding of the anticlinorium.

4. Disharmonic folds were displayed in thin chret bands embedded in relatively thicker limestone beds of the Kometan Formation at the NE limb of the main Azmar fold. Some of them display distinct forms such as fan folds.

5. Chert bands in the NE limb of the main Azmar anticline have been segmented into boudined pieces due to the bed parallel stretching that accompanied final stage of folding (uplifting). Whereas boudined thin limestone beds within marl matrix in the vertical part of the SW limb of the main fold reflect compression subnormal to the subvertical beds during the tightening stage of earlier formed fold.

Manuscript received, October 28, 2010

REFERENCES

Agard, P., Omrani, J., Jolivet, J. and Mouthereau, F., 2005. Convergence history across Zagros (Iran): constraints from collisional and earlier deformation: International Journal of Earth Sciences, 94, 401-419.

Alavi, M., 2004. Regional stratigraphy of the Zagros fold-thrust belt of Iran and its proforeland evolution: American Journal of Science, 304, 1-20.

Al-Hakary ,S., H. Geometrical analysis and structural evolution of a selected area from NE Zagros Fold Thrust Belt and their tectonic implications, Northeast Iraq region, NE Iraq. Ph. D. Thesis, Sulaimani University in press.

Fluety, M.J., 1964. The description of folds: Geological Association Proceeding, 75/ 4, 461-492.

Hobbs, B.,E. Means, W.D. and Williams, P.F., 1976. An outline of structural geology: John Wiley and Sons, New York, 571 p.

Ibrahim, A.O., 2009. Tectonic style and evolution of the NW segment of the Zagros fold- thrust belt, Sulaimani governorate, Northeast Iraq region, NE Iraq: Unpublished Ph. D Thesis, Sulaimani University.

Ragan, D.M., 1986. Structural geology; an introduction to geometrical techniques: John Wiley and Sons, Inc., 196 p.

Ramsay, J.G. and Huber, M.I., 1987. Folds and fractures: The techniques of modern structural geology: 2, Academic Press, New York, 700 p.

Suppe, J., 1985. Principles of structural geology: Prentice-Hall, Inc., New Jersey, 537 p.

Talebian, M. and Jackson, J., 2002. Offset on the main recent fault of NW Iran and implications for the late Cenozoic tectonics of the Arabia-Eurasia collision zone: Geophysical Journal International, 150, 422-439.

Twiss, R.J. and Moores, E.M., 2007. Structural geology: W.H. Freeman and Company, 41 Madison Avenue, New York, 736 p.

Van der Pluijm, B.A. and Marshak, S., 1997. Earth structure: An introduction to structural geology and tectonics: WCB/McGraw-Hill, USA, 495 p.

Mineral Res. Expl. Bull., 143, 53-73, 2011

HEAT FLOW OF THE KIRÞEHÝR MASSIF AND GEOLOGICAL SOURCES OF THE RADIOGENIC HEAT PRODUCTION

Uður AKIN* and Yahya ÇÝFTÇÝ**

ABSTRACT.- It is not often easy to distinguish the components of the mantle originated heat flow and radiogenic heat generation from each other. Surface heat flow is composed of two components. The first is the radiogenic heat source and the second is the heat flow originated from the upper mantle and the lower crust. In this study, heat flow and the radiogenic heat production of the Kýrþehir Massif and its geological sources were investigated. Curie point depths were calculated from aeromagnetic data. Geothermal gradient values were formed by considering the medium as homogenous and isotropic. The heat flow of the region was calculated using the heat transfer values of rock samples collected from field and it was determined that this value had ranged between 53 mWm^{-2} and 108 mWm^{-2}. Besides the radiogenic heat production of the study area has been calculated from the radiogenic heat production map of the region prepared by previously gathered airborne spectral gamma-ray data. As a result of the evaluation of heat flow and heat production maps together, it was calculated that 60-92% of the average heat flow values of the region are mantle and 8-38% are radiogenic sourced. The radiogenic heat production in the study area, generally showed high anomaly values in young granitoids as predicted.

Keywords: Kýrþehir Massif, heat flow, radiogenic heat production, Curie depth.

INTRODUCTION

The heat on Earth's crust is formed by the constitution of mantle sourced heat and the heat derived by the degradation of radiogenic elements. The radiogenic sourced heat is formed by isotopes with short and long half lives on the Earth's crust. While radiogenic isotopes with short half life, (^{26}Al, ^{26}Cl and ^{60}Fe) were effective in producing the heat in the former stages of the Earth, isotopes with long half life (^{235}U, ^{238}U, ^{232}Th and ^{40}K) were effective in heat energies produced starting from the earlier stages of the Earth until today (Göktürkler, 2002).

According to Birch (1947), the radiogenic heat production on the upper part of the earth crust is associated with the distribution of thermal energy which radioactive elements had formed and with great tectonic processes. Turcotte and Schubert (1982) asserted that the radiogenic heat production is an important factor in the thermal structure of the continental crust. It was also explained in different studies that heat changes due to crustal processes such as metamorphism, magmatism and deformations are important in heat production (Bea et al, 2003; Andreoli et al, 2006, Sandiford and McLaren, 2006). Besides, Jaupart and Mareschal (2003) associated the studies of radiogenic heat production at surface with the heat flow at depths of the earth crust.

It will be useful firstly to introduce the regional geology and regional tectonic elements in order radiogenic heat production and other elements to be correctly interpreted in the study area.

REGIONAL GEOLOGY

The study area covers a significant portion of the Kýrþehir Massif which takes place in the

* MTA Genel Müdürlüðü, Jeofizik Etütleri Dairesi Baþkanlýðý, 06800 - Balgat-Ankara / Türkiye, akin@mta.gov.tr
** MTA Genel Müdürlüðü, Maden Etüt ve Arama Dairesi Baþkanlýðý, 06800 - Balgat-Ankara / Türkiye

middle part of the Anatolian Plate (Figure 1). This massif defines the area which is bounded by the North Anatolian Fault Zone (NAFZ) at the north and the East Anatolian Fault Zone (EAFZ) at the east. In the area, several transform faults take place developed being associated with the main Neotectonic structures stated above (Figure 2). In the crustal thickness map of Turkey which has been produced by using the gravity data, the Kýrþehir Massif has been cut by two profiles. The first and the second profiles are in north-south and east west directions, respectively. The crustal thickness of the Kýrþehir Massif was calculated ranging in between 35 - 40 km along both profiles (Arslan et al., 2010).

In this study, the 1/500.000 scale Kayseri sheet which had been published by MTA (General Directorate of Mineral Research and Exploration) (2002) was used as the geological base map. This map was re-prepared by being simplified depending on the purpose of the study and units were presented according to their origins (Figure 3). The basement of the study area is generally composed of Cambrian-Ordovician aged metamorphic schists, Precambrian / Palaeozoic aged gneiss, schist, amphibolite and similar metamorphic rocks and of Permian aged marbles (Figure 3). In the region, plutonic activities in various composites have been formed in Upper Cretaceous - Eocene period and these are generally represented by the Upper Cretaceous - Paleocene aged granitoids and syenites. The Upper Cretaceous - Paleocene aged volcanites have taken their recent positions in the region as the last stage products of this magmatic province. Ophiolitic complex associated with the forming of the Ýzmir - Ankara - Erzincan Suture zone and various products of it have emplaced in the region within the same period (Figure 3).

STRATIGRAPHY

Metamorphic rocks take place at the basement of the study area (Figure 3). Opholitic groups have tectonically overlaid these basement rocks. Magmatic intrusive rocks and their volcanic associates have taken place within the region by cutting the basement rocks and the ophiolitic groups. All these metamorphic and magmatic series have been covered by volcano-sedimentary and sedimentary series starting from Eocene with volcanics and then continued with clastics (Figure 4).

In compliance with the purpose of the study, rock assemblages within this area were briefly introduced below.

Metamorphic basement rocks

Metamorphic rocks consisting of the basement of the study area are represented by several formations having various mineralogical compositions. Cambrian - Ordovician aged rocks outcrop in NE of the study area and NW parts of Nevþehir. The oldest unit distinguished at the Palaeozoic basement was named as Gümüþler formation by Göncüoðlu (1977) (Figure 4). This formation mainly bearing of lithologies such as gneiss, sillimanite bearing gneiss, marble, calcschist, amphibolite schist, micaschist which extensively crop out in the east and northeast (Figure 3).

Gümüþler formation at the basement is conformably overlain by Kaleboynu formation (Göncüoðlu, 1981) which consists of lithologies such as gneiss with biotite and garnet, amphibole schist, marble and muscovite schist and is Precambrian - Palaeozoic in age. This formation constitutes the main lithologies cropping out in the study area and was divided into three units. These are, from bottom to top, Sarýkavak Unit (gneiss with biotite, marble and amphibole schist), Marble unit (marble and calcschist) and Muscovite schist unit (quartz, muscovite schist, calc schist and marble).

The deposit on the uppermost layer of the metamorphic basement rocks was named as Bozçaldað formation (Seymen, 1981*a*). It gene-

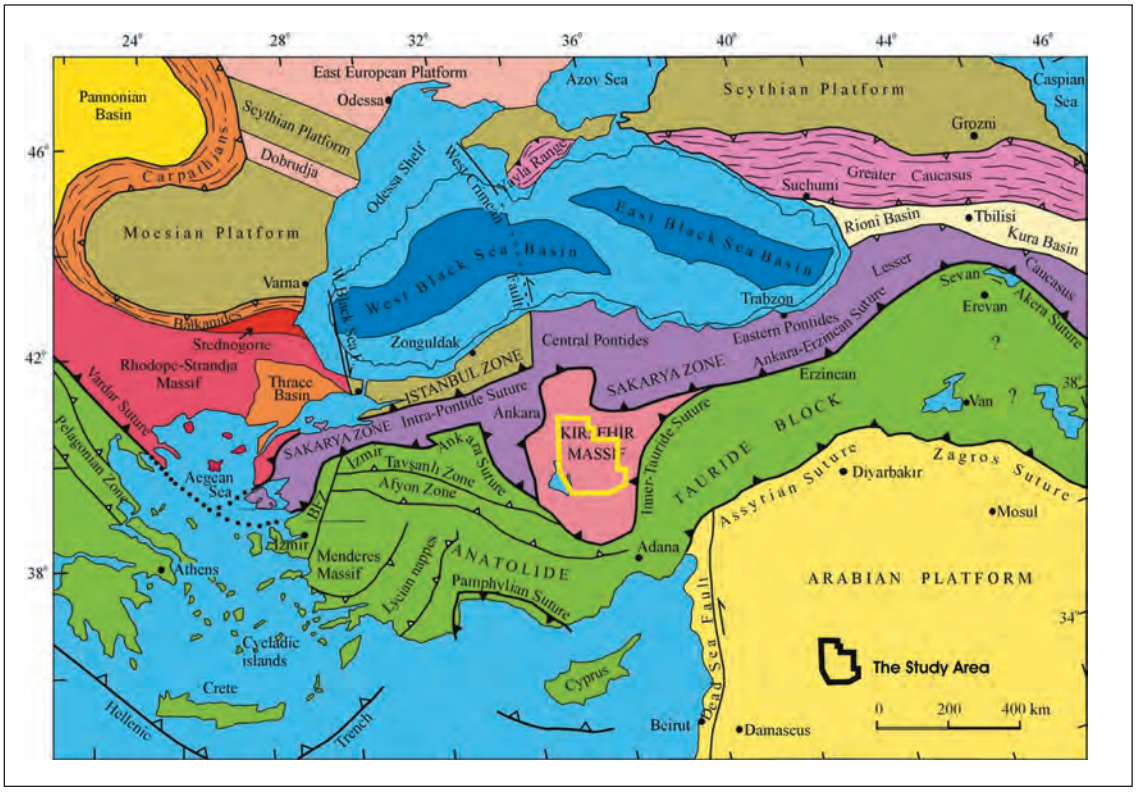

Figure 1- The overall tectonic view of the study area (area drawn in yellow line) (modified from Okay and Tüysüz, 1999).

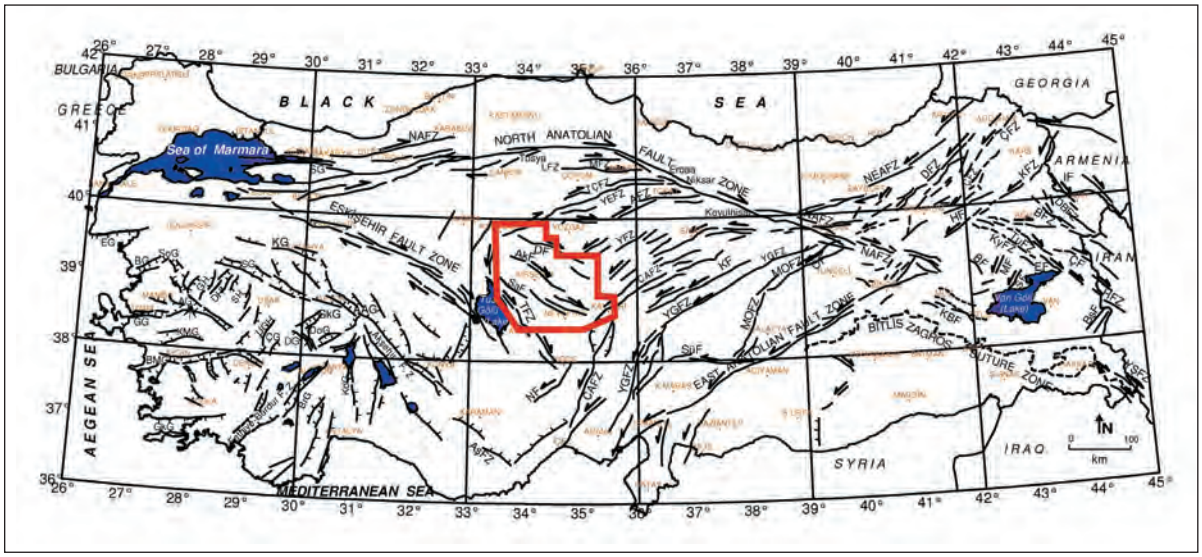

Figure 2- Neotectonic discontinuities of Turkey prepared by Bozkurt (2001) by combining the maps of Bozkurt, 2000; Yýlmaz et al, 2000; Seyitoðlu 1997; Þaroðlu et al, 1992; Koçyiðit, 2000; Koçyiðit et al, 2000; Bingöl, 1989; Koçyiðit and Erol, 2001; Bozkurt and Koçyiðit, 1996 and Dirik and Göncüoðlu, 1996). Area drawn in red shows the location of the study area (modified from Akýn and Çiftçi, 2011).

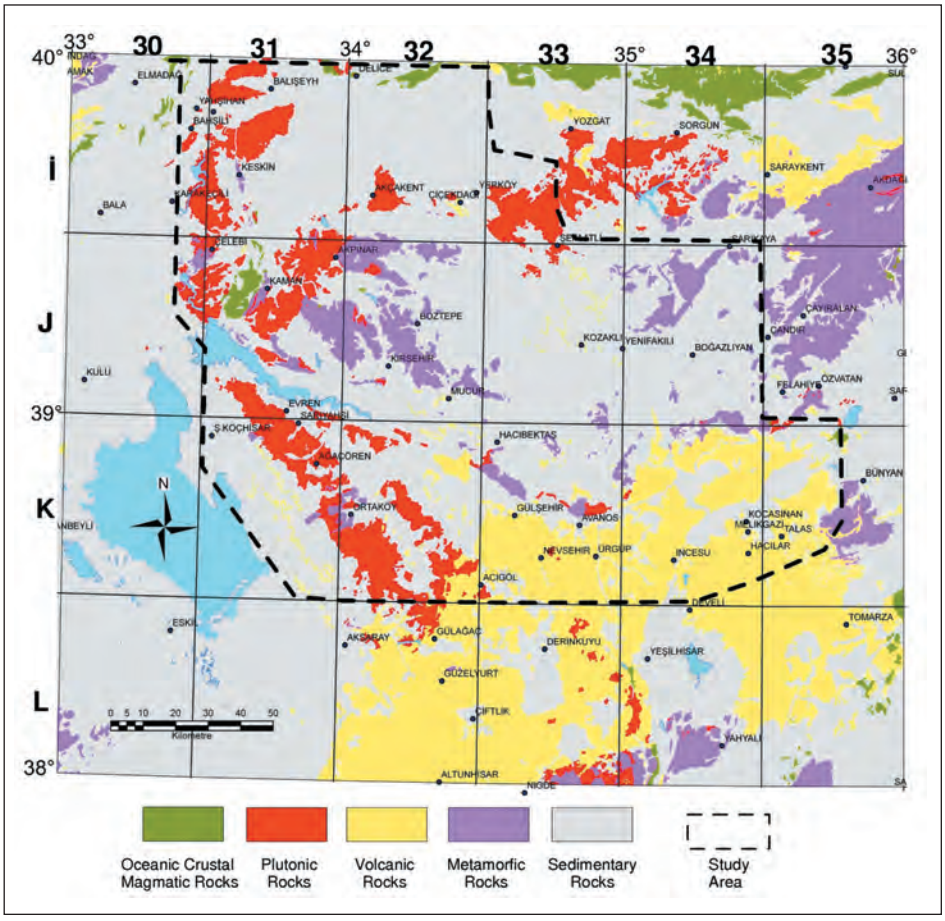

Figure 3- Geological map of the study area (simplified from 1/500 000 scale Kayseri Sheet, MTA, 2002).

rally consists of marble and is Permian in age. This formation was distinguished as Aþýgediði formation by Göncüoðlu (1977) and as Bozçaldað marbles by Kara (1977).

This formation shows extension in middle and northeastern parts of the study area. Significant skarn zones were formed sporadically in places where it was cut by magmatic rocks in NW of Kýrþehir (Kara, 1977).

Ophiolitic complex

Two different ophiolitic series crop out in NW and NE of the study area. Ophiolites cropping out in north of Yozgat are known as ophiolites of Ýzmir - Ankara - Erzincan Zone. Ophiolites remaining within portion of the study area of this zone were nomenclatured as Artova Ophiolitic Complex (Özcan et al., 1980) and mainly consist of undistinguished slices and blocks of basic, ultrabasic, volcanic, metamorphic and of sedimentary rocks (Figure 3 and 4).

However, ophiolitic series dispersing at NW of the study area was nomenclatured as Çiçekdað formation (Kara and Dönmez, 1990) and is generally in a view of volcano sedimentary group. This formation is also equivalent to groups

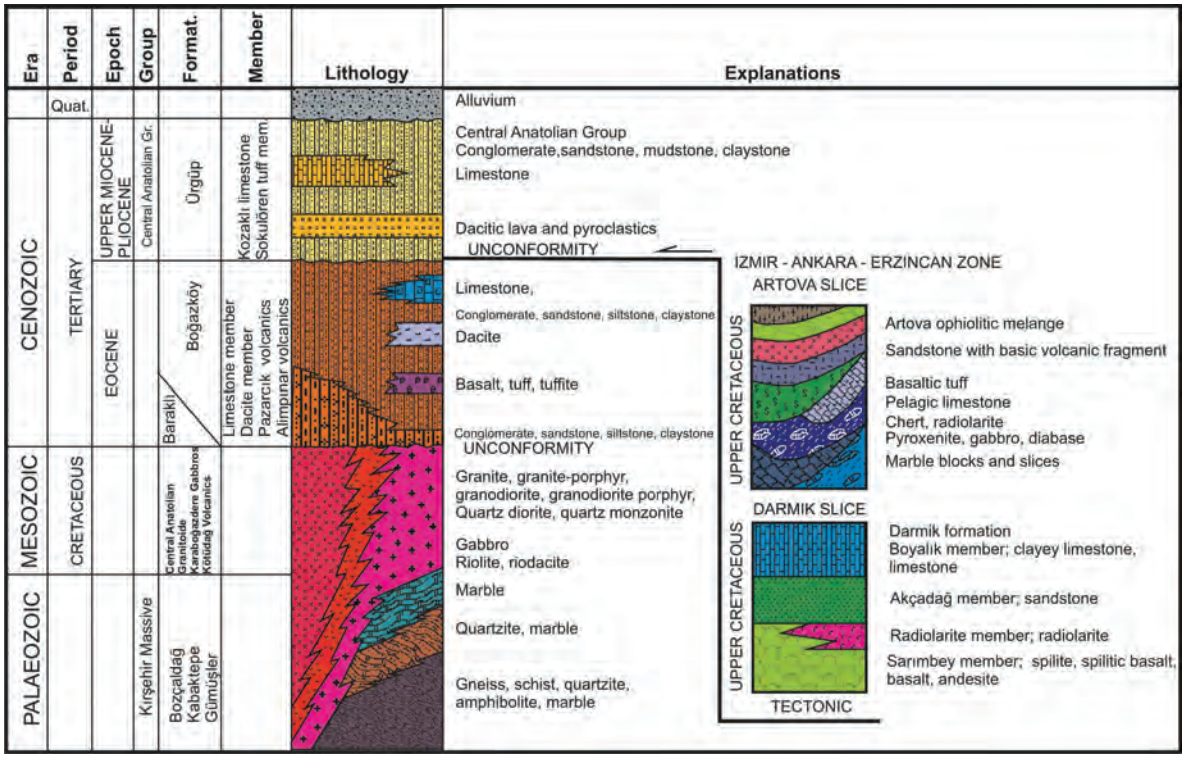

Figure 4- Generalized tectono - stratigraphic columnar section of the study area (simplified from Akçay et al., 2008).

defined as serpentine and radiolarites (Baykal, 1943), as Upper Cretaceous submarine volcanic series / ophiolitic series (Ketin, 1955, 1963), as Ankara melange (Bailey, McCallien, 1950), as Yahþihan formation (Norman, 1972), as Ankara Complex (Seymen, 1982) and as Kasýmaða formation (Bilgin et al., 1982) (Figure 3 and 4). Black - dark green gabbro and micro gabbros observed within the basement of this formation were defined as Karaboðazdere gabbro unit by Bilgin et al. (1986). This unit is the equivalent of basic intrusives (Ketin, 1955; Ayan, 1963), Karakaya Ultramafics (Seymen, 1982) and Ortaköy granitoid (Atabey et al., 1987) (Figure 4).

The Central Anatolian granitoids

Granitoids exposing in the study area were discussed under this subsection, although their compositions and time of emplacements are different (Dönmez et al., 2005*a*). Granitoids belonging to this group have been investigated under various names such as Baranadað massif (Ayan, 1963), Cefalýkdaðý granodiorite (Ataman, 1972), Karacadað pluton (Norman, 1972), Üçkapýlý granodiorite (Göncüoðlu, 1977), Baranadað pluton (Seymen, 1982), Ortaköy granitoid (Atabey et al., 1987) in previous studies.

The Central Anatolian granitoids, starting from the NW of the study area extend as an assemblage approximately in N - S trend around Kýrýkkale, as an assemblage in NE - SW trend around Yozgat and as an assemblage trending in NW - SE at the east of Tuz Lake. Besides, another assemblage is observed between Kýrþehir and Kýrýkkale (around Kaman) trending in NE - SW (Figure 3) too.

These units were mapped as assemblages of four compositional groups emplaced in different time intervals in the 1: 500 000 scale geological map of Turkey. All Late Cretaceous - Paleocene aged granitoids will be introduced under two categories in compliance with the regional approach of this study (Figure 3).

Granitoids.- Granitoids outcropping to the east of Aksaray in the study area were nomenclatured as Ortaköy granitoid (Atabey, 1989). The same granitoids were defined as Ekecikdað granitoids by Türeli et al. (1993). While this granitoid includes both mafic and felsic units, the members of deep and shallow emplacements are accommodated in it as well. Mainly; gabbro, banded gabbro, diorite, tonalite, granite, granodiorite, porphyry diorite, monzonite, syenite, monzodiorite, leucogranite and porphyry granite units were distinguished (Atabey, 1989). This rock assemblage is equivalent of Baranadað pluton (Seymen, 1981) in literature. The intrusion and cooling age of this pluton was given as 54 ma by Ayan (1963), 74 ma by Ataman (1972) and as 95 ma by Göncüoðlu (1982, 1986). However; the age of this pluton is Paleocene according to Seymen (1981*b*).

Granitoids exposing to the east and southeast of Kýrýkkale cut Bozçaldað and Santonian aged Çiçekdað Formations of the Kýrþehir Massif with a hot contact (Dönmez et al., 2005*b*).

Granitoidic group at south of Yozgat is composed of shallow seated pluton and stocks of various stages and phases and vein rocks which developed in their outer zones (Akçay et al., 2007).

Syenites.- Magmatic rocks spreading towards northern parts of 1/100.000 scale Kýrþehir J31 and J32 sheets and successively associating with Central Anatolian granitoids were nomenclatured as Buzlukdað syenite in the region (Kara and Dönmez, 1990). This assemblage is equivalent of Buzlukdað pluton and was defined by Seymen (1982).

Syenites which crop out generally between Çelebiuþaðý and Himmetuþaðý settlements to the NE of Ýzmir 33 sheet is composed of micro syenite, trachyte, quartz syenite, quartz micro syenite, quartz trachyte and alkali syenite type of lithologies.

These rocks are transitional with the Central Anatolian granitoids (Dönmez et al., 2005*b*). However, it was stated that while granitoids are cut by phonolites, syenites are cut by porphyry granodiorites respectively (Kara and Dönmez, 1990).

Volcanic series

A volcanic series crops out in E- W direction along the southern boundary of Ýzmir - Ankara - Erzincan Zone towards northern parts of the study area (Figure 3). This Late Cretaceous aged volcanic series cropping out in the region was defined as Darmik formation and is characterized by agglomerate, tuff, sandstone, pelagic limestone, basaltic andesitic pillow lava, radiolarite, and are cut by andesitic, basaltic and porphyry dikes (Akçay et al., 2008) (Figure 4).

Lithological assemblages contemporaneous with the deposit between Kýrþehir and Kýrýkkale mentioned above was named as Kötüdað volcanite (Seymen, 1982) and mainly consist of vein and surface rocks composed of rhyolite, rhyodacite, dacite and latite. These are the last stage volcanic deposits of the Central Anatolian granitoids and were generally developed around the outer zones of these granitoids.

Sedimentary deposits

Although clastic and carbonaceous deposits widely spreading in the study area have been mapped in details with different purposes and several deposits have been distinguished, all these terrigenous and lacustrine deposits in this study will be presented under the name of "Central Anatolian Group" (Akçay et al., 2008).

Middle Miocene - Pliocene aged continental deposits which show a wide distribution in the Central Anatolian Region were formed by reddish brown, none or less markedly bedded conglomerate, sandstone, mudstone, gypsum, anhydrite and by intercalations of limestone and ignimbrite. These groups were collected under the name of "Central Anatolian Group" and mapped by Akçay et al., (2008) (Figure 3, 4). It was stated in this study that, this deposit was equivalent of a part of the Kýzýlýrmak formation defined by Birgili et al. (1975). The lower contact of the deposit shown in figure 4 is unconformable. Sokulören Tuff unit (Akçay et al., 2008) which is composed of dacitic lava and pyroclastics takes place in the lower sections of the sequence namely the Ürgüp formation (Pasquare, 1968) which is generally composed of conglomerate, sandstone, mudstone and claystone intercalations. However, at mid sections of the sequence, Kozaklý limestone unit takes place (Kara and Dönmez, 1990) which shows laterally transitional contact relationships with the surrounding units (Figure 4). Since the radiometric age taken from the oldest ignimbrites exposing around Ürgüp is 11.2 ± 2.5 ma (Temel, 1992), the age of this deposit is accepted as Late Miocene (Akçay et al., 2008).

All deposits in the study area are covered by Quaternary clastic deposits with an angular unconformity.

HEAT FLOW

PREVIOUS STUDIES AND OUTLINE

Surface heat flow is the heat value transferred from a unit area at a unit time from depths of the ground to outer side and its unit is mWm^2. Heat flow studies in Turkey have been made in regional scale or as overall Turkey so far (Ericson, 1970; Jongsma, 1974; Fytikas, 1980; Tezcan and Turgay, 1989; Ýlkýþýk, 1992 and 1995; Yemen, 1999; Göktürkler et al., 2003; Bal, 2004; Akýn and Duru, 2006; Akýn et al., 2006; Karlý et al., 2006). In these investigations, it was stated that heat flow values were observed that these had reached high values in corrections made due to rapid sedimentation although these were low in Mediterranean and Black Sea (Ericson, 1970). Heat flow studies are also available in Aegean Sea (Jongsma, 1974). According to the heat flow estimations in Aegean Sea, three high heat flow regions were determined extending along tectonic structures. The first is the region with high heat flow reaching out Bodrum Karaada vicinity through Astipalia, Kavaro islands along Palegonia - Parnos Zone which is located in inner part of Hellenic island arc (Figure 1) and it presents values exceeding 120 mW/m^2 sporadically. The second is the region exceeding 100 mW/m^2 located in Central Aegean, on the western end of the Ýzmir - Ankara zone (Figure 1). The last region is the high heat flow anomaly belt observed along Macedonia, northern Aegean islands and shores of Biga and Gelibolu peninsula (Fytikas, 1980).

Tezcan and Turgay (1989) prepared heat distribution map for 1000 m. depth selecting the average heat transmission coefficient as λ=2.1 (W/m°C) for overall Turkey. Ýlkýþýk (1992, 1995) has carried out heat flow studies of Turkey by silica heat method. The investigator has performed regional heat flow studies in west Anatolia using silica geothermometer in thermal sources and proposed average heat flow values as 107±45 mW/m^2.

Yemen (1999), assessed the heat flow distribution values of Aegean Region using geothermal gradient values in wells. However, Göktürkler et al. (2003) modelled crustal temperatures in the west Anatolia by two dimensional profiles and measured the heat distribution of grabens which are full of sediments in the upper crust and in lower parts of the crust. Bal (2004) carried out a study towards the determination of heat flow values by using aeromagnetic data of Aydýn and Ýzmir vicinities and the investigation of the heat flow distribution. One of the two studies in which heat flow map of Turkey had been prepared by

Akýn and Duru (2006) and the other belongs to Karlý et al. (2006). Akýn and Duru (2006) carried out their investigations using Curie point depths calculated from aeromagnetic data, however, Karlý et al. (2006) performed their studies measuring geothermal gradient in shallow deep cold water wells.

DATABASE AND METHOD

MTA started to carry out aeromagnetic studies in 1978 in order to explore underground resources and ended in 1989. During 11 years period, the regional aeromagnetic map of Turkey has been generated performing 460 000 km flight above 2 000 feet from ground. Flight lines have been selected as 1 - 5 km intervals. IGRF 1985 magnetic correction has been applied in estimations. Within this period, total of 813 639 km^2 has been surveyed as sea, lake and land. In accordance with boundary conventions, boundaries of Syria, Iran and Iraq have been approached not more than 5 km and 15 km distance have been preserved with the former Soviet Union, Greece and Bulgarian boundaries.

Magnetic anomaly map which was prepared by aeromagnetic data of the study area and its vicinity is shown in figure 5. When looking at this map, it is seen that the highest magnetic anomaly values are formed along Akçakent - Yerköy - Çiçekdað line, towards the east of Keskin. A weak magnetic anomaly belt directing in SW - NE could also be defined in the same Figure along the Nevþehir - Keskin line. Anomaly belts on this map were discussed in detail in studies of Akýn and Çiftçi (2010).

By using the database shown above, the Curie point depth map was obtained (Akýn and Çiftçi, 2010). Geosoft Oasis package software was used in producing maps. Curie point is the depth at which the magnetite mineral loses its magnetic property under the temperature of 580°C and gains paramagnetic property. Window in 128 x 128 km dimensions was used at Curie point measurement. Windows were positioned as shifting 32 km side by side towards east and two dimensional power spectrum of each window was calculated. Then values obtained were assigned to midpoint of the window. In doing so, the Curie point depth map was obtained applying the method which Tanaka et al. (1999) had revealed who developed the spectral analysis technique which Spector and Grant ((1970) and Okubo et al. (1985) had applied (Figure 6). Curie points in the study area were calculated as 11 km at the shallowest point and 15 km at the deepest point. The effective anomaly in figure 6 is in E - W direction and represents shallow depths. Curie depths of the northern part of the study area seem approximately 2 km shallower compared to southern part.

Surface heat flow is affected from astenosphere and lithosphere. Regional heat flow values obtained from surface provide significant contributions in assessing the geological structure of the region. In this study, geothermal gradient data was obtained using Curie point depth values in Figure 6. However; heat transmission coefficients of 32 rocks representing the study area were calculated by Karlý et al. (2006) in laboratory using QTM (Quick Thermal Measurement) device. These values were then used in calculating the heat flow (K). The heat flow map of the region was produced using the formula given in equation 1 (Figure 7).

$$q = K\,(\partial T/\partial z) \qquad (1)$$

where;

K: thermal conductivity,

q: surface heat flow,

$(\partial T/\partial z)$: vertical heat gradient.

Heat transfer coefficients of rocks in the region (as average value) were estimated as 2.5 W/m°C for plutonic rocks, 2.75 W/m°C for meta-

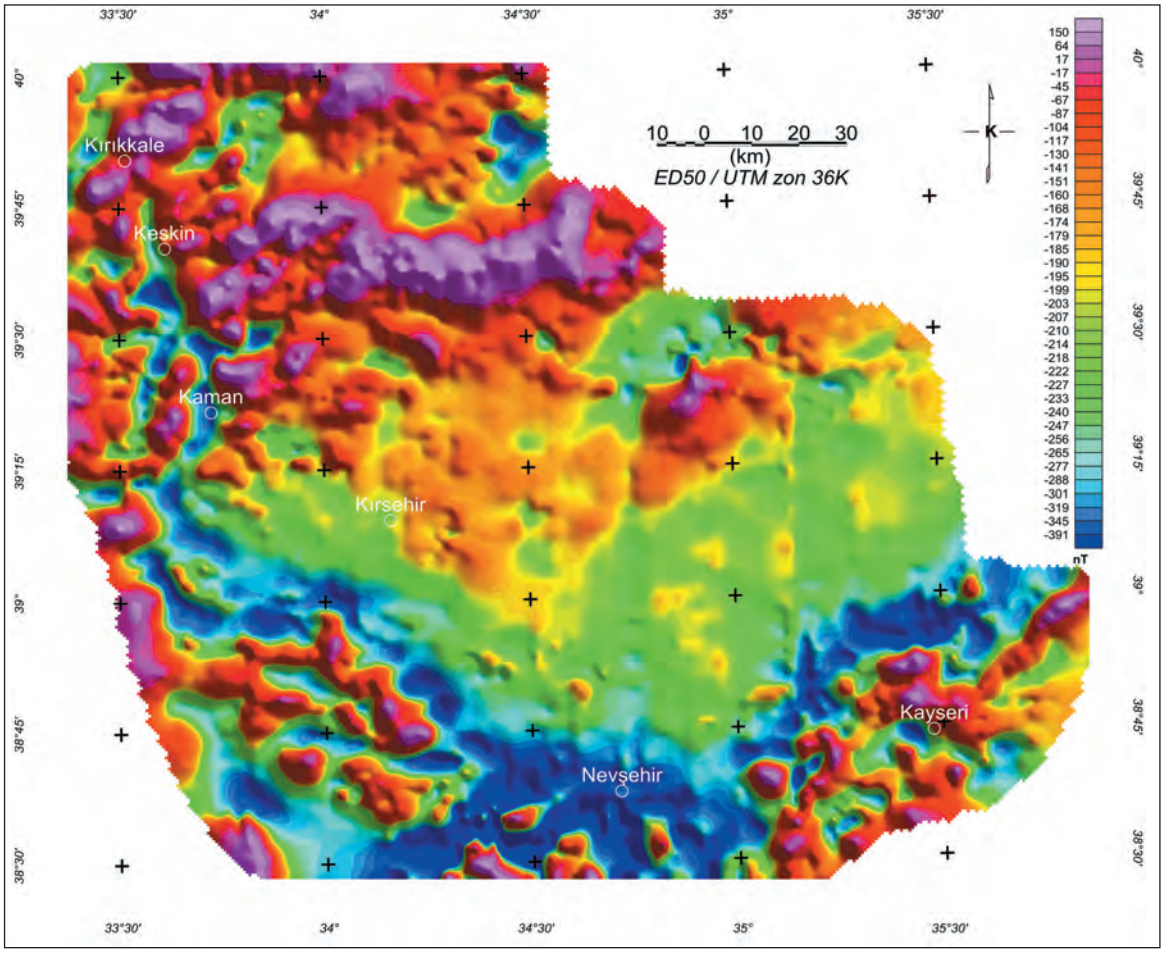

Figure 5- Aeromagnetic anomaly map of Kýrþehir vicinity.

morphic rocks, 1.87 W/m°C for volcanic rocks and as 2.06 W/m°C for sedimentary rocks.

When looking at the heat flow map of the region, it was seen that heat flow values vary in between 50 mW/m^2 and 110 mW/m^2 (Figure 7). The average heat flow of the region was estimated as 72 mWm^2. This value is again compatible with the average heat flow value of the 1/500.000 scaled Kayseri sheet on the heat flow map of Turkey which was produced by using aeromagnetic data (Akýn and Duru, 2006). The anomaly possessing the high heat flow on heat flow map (Figure 7) is approximately in north - south direction. However; the region that have low heat flow was located at northwest of Kayseri and southwest of Nevþehir.

RADIOACTIVE HEAT PRODUCTION

THEORY AND LITERATURE

"Radiogenic heat" forms as a result of the natural decay of radioactive elements such as uranium, thorium and potassium on Earth's crust. As a result of the decay of radioactive elements, α and β particles release, and electromagnetic wave propagation occurs. As a result of both the absorption of electromagnetic waves by other atom in medium and the collision of other atoms

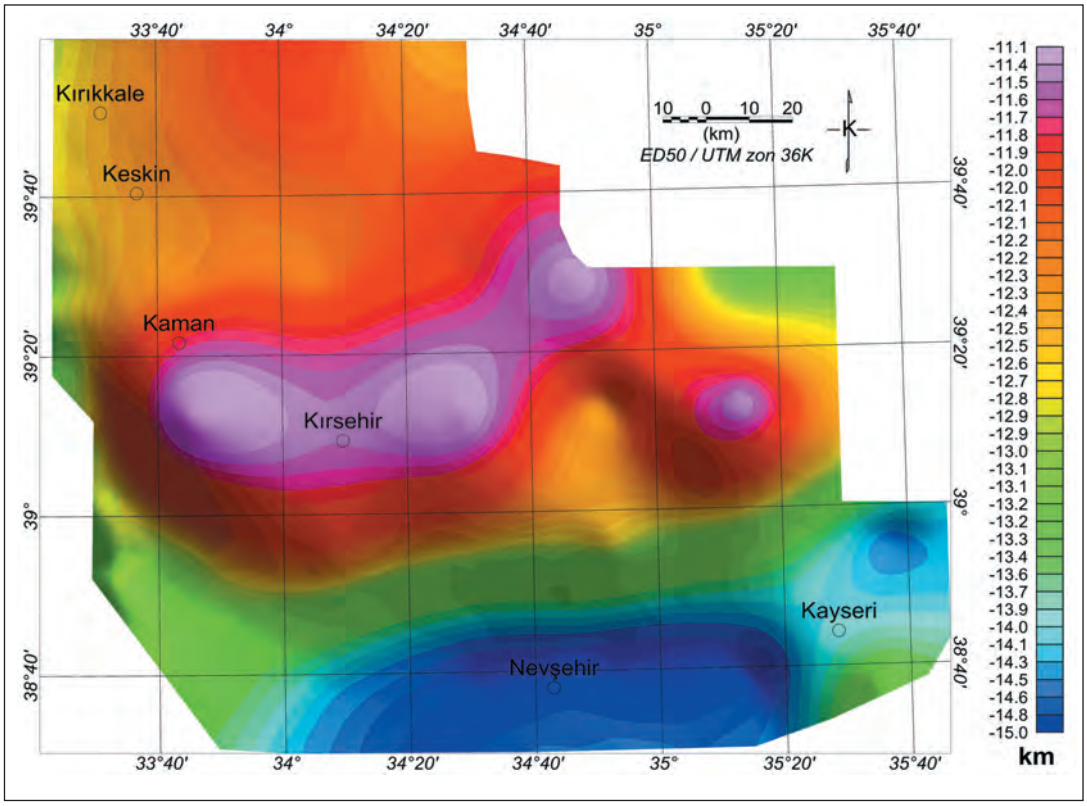

Figure 6- Curie point depth map of the study area (from Akýn and Çiftçi, 2010).

with α and β particles, an increasing occurs in the kinetic energy of these atoms. Thus, the average kinetic energy of the medium, that is; the temperature increases (Göktürkler, 2002). The energy released from the radiogenic heat on the upper crust and this energy is added to the heat flow of the lithosphere and causes the rising of the heat flow value. Radiogenic heat originating from crust forms the 50 - 70% of the total heat generally radiated from the uppermost portion of the continental basement (Rudnick and Fountain, 1995; Waples, 2001). According to Mc. Lennan and Taylor (1996), the radiogenic heat value of the earth crust remains between 21 mW/m² and 34 mW/m².

DATABASE AND METHOD

The database of this study is the radioactive data collected from the aerial gamma ray spectrometer research which was conducted in Kayseri - Kýrþehir - Yozgat and around Nevþehir in years 1987- 1988. In that research a total area of 25 000 km² has been surveyed. The survey has been carried out by Cessna 402B type aircraft belonging to the General Directorate of Mineral Research and Exploration (MTA) using 33.5 liter in volume crystal spectrometer. Instrumental support of the project was supplied by International Atomic Energy Agency (IAEA). This research has provided data to the project of the Central Anatolian uranium survey (Aydýn, 1990).

Radiogenic heat production on crust is denoted by symbol A and its unit is µW/m³. Rybach empirical formula was used in calculating the radiogenic heat production (Rybach and Buntebarth, 1982). It is necessary to know the uranium, thorium and potassium concentrations

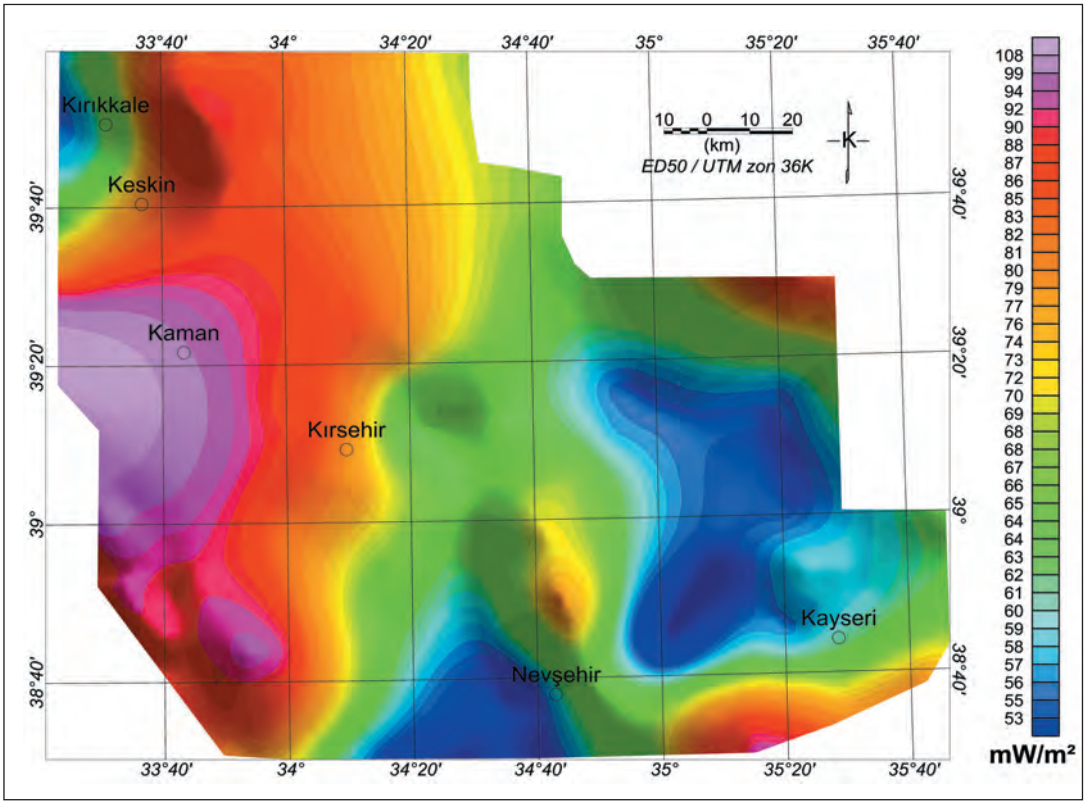

Figure 7- The heat flow map of the study area.

and density values of rocks in the equation given below.

$$A(\mu W/m^3) = 0.1325\ \rho\ (0.718\ C_U + 0.193\ C_{Th} + 0.262\ C_K) \quad (2)$$

where;

C_U: Uranium concentration (in ppm),

C_{Th}: Thorium concentration (in ppm),

C_K: Potassium concentration (in wt %)

ρ: density (g/cm^3).

Density values (ρ) of rocks in this study were taken as a constant but apparent densities were obtained for each cell from Bouguer gravity map. Apparent density values range in between 2.27 g/cm^3 and 2.64 g/cm^3. Later on, equation (2) was used to obtain the radiogenic heat production map (Figure 8). Radiogenic heat value shows variation between 0.62 µW/m^3 and 5.68 µW/m^3.

THE RELATIONSHIP BETWEEN THE HEAT FLOW AND RADIOACTIVE HEAT PRODUCTION

There is a linear relationship between the heat flow and the radiogenic heat production (Birch et al., 1968).

$$q = q_o + Ab \quad (3)$$

where;

q : surface heat flow,
q_o : reduced heat flow,
A : radiogenic heat flow,
b : slope of the line.

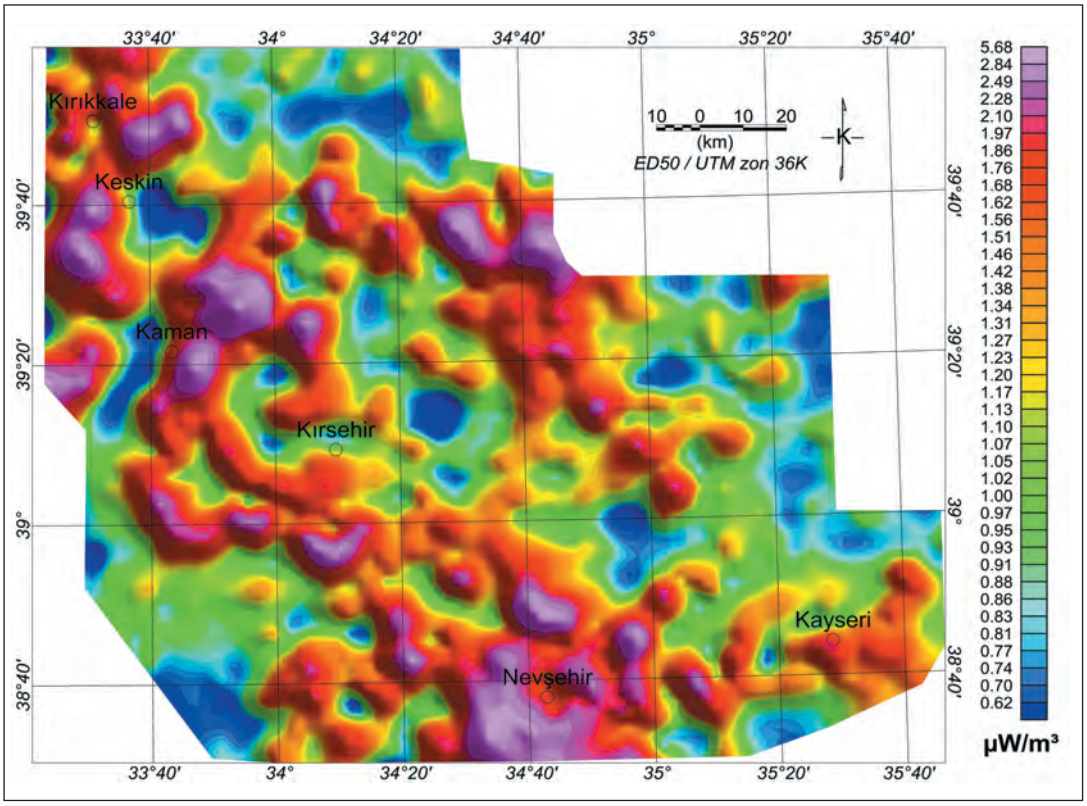

Figure 8- Heat production map of the study area originated from U, Th and K radiogenic elements.

b is the characteristic depth at which the radiogenic heat flow equals zero and q_o is the mantle source heat flow at which the radiogenic heat production on crust equals zero. This value is represented by the equation (4) which was produced by using equation (3) (Blackwell, 1971).

$$q_o = q - Ab \quad (4)$$

The ratio among heat amounts revealed by the mantle source heat flow and the radiogenic source heat production were calculated and its graph was formed (as percentage) (Figure 9).

The relationship coefficient in this graph is low as data scattering is randomly distributed. Therefore; b value was accepted as 10 km instead of 8.27 and the percentage amount map was obtained from the mantle source heat flow in figure 10.

Mantle source heat flow has shown variations between minimum 60% and maximum 92% in the study area (Figure 10). Thus; the heat flow amount originating from the decay of radiogenic elements (U, Th and K) in this area is between minimum 8% and maximum 40%. The region where the mantle source heat flow is the lowest in percentage are areas where Quaternary aged pyroclastic and basalts spread out in and around Nevþehir (Figure 3, 4 and 10). The heat flow of the region of which its coordinates are 33°40' - 34°30' in longitude and to the north of 39°40' in latitude is mantle source as in percentage of 85 - 92%. This anomaly most probably occurs due to magmatic rocks originating from the ocean

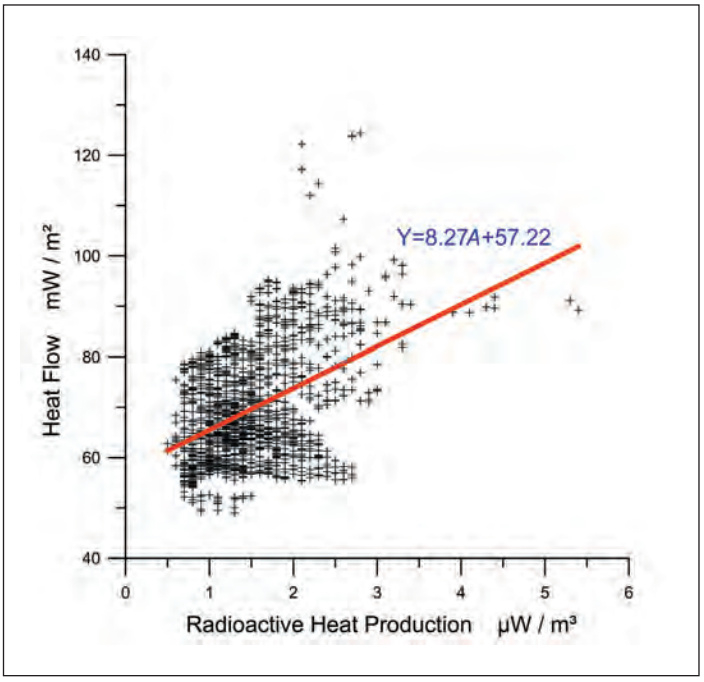

Figure 9- The relationship between the heat flow and the radioactive heat production.

bottom which is considered that it continues beneath the sedimentary rocks in the region and shows small outcrops sporadically (Akýn et al, 2011). Thus; it is known that q_o parameter (reduced mantle source heat flow) in Birch - Lachrenburg Equation has high values in active regions in terms of tectonism and magmatism. With this respect, findings might give significant clues related to the tectono-magmatic activity in the region. The region where q_o component is high (north of Kaman) is equivalent to the area where alkali syenites occur which its formation is considered due to the contemporary tensional tectonic regime. When aforesaid data were totally assessed, we consider that high q_o component in the related region might indicate a magmatic mass which its cooling process still continues.

DISCUSSION

The heat flow and radiogenic heat production reveals thermal behavior types of areas. Generally data group obtained from well logs are used in such studies. However, in this study, grid data were fully used in estimations in order to reveal the heat regime of the Kýrþehir massif located in Central Anatolia. The reason is that all data were not present at the same observation points. In order to ease calculations in data analyses in the study area, field data were used converting them into grid data. It can be said that grid intervals of aeromagnetic, aerial spectral gamma ray and on land regional gravity data were compatible with the purpose of this study and consisted of sufficiently small intervals and frequent data.

The density value in equation (2) used in calculating the radiogenic heat flow was obtained from apparent densities coming from Bouguer gravity map. Instead of using only one average density value for the whole area, density values for each grid areas were formed to increase analysis sensitivity in lateral sense. In doing so,

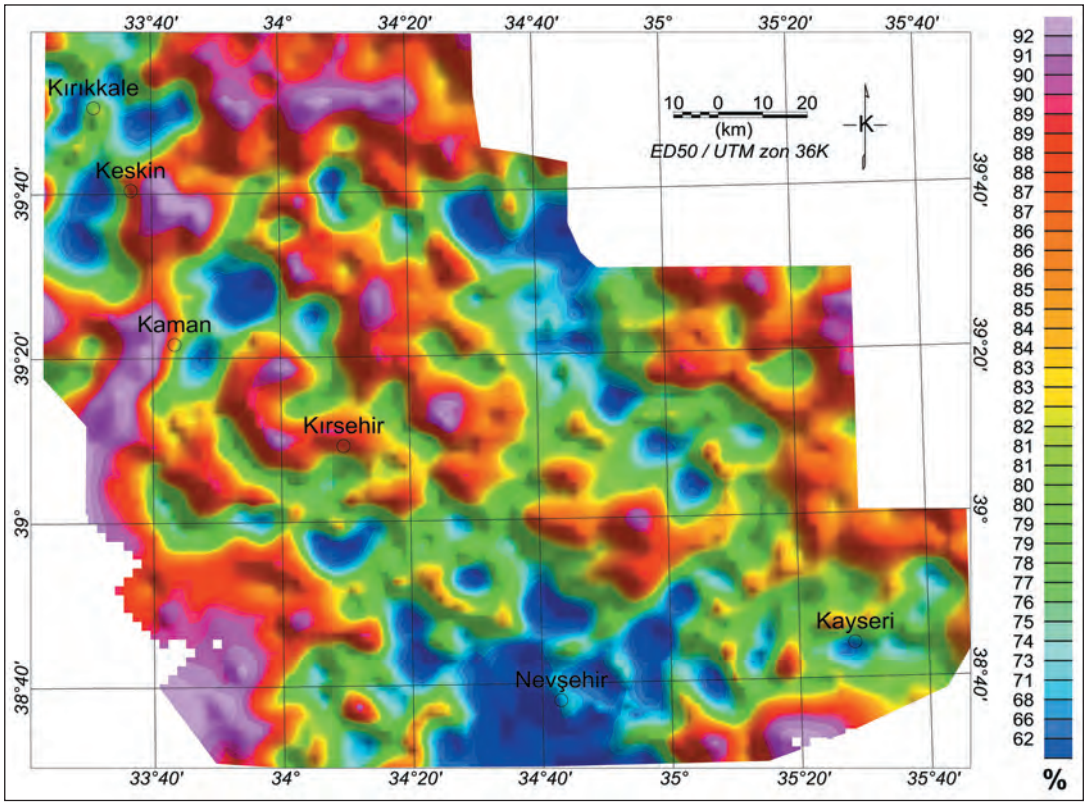

Figure 10- The percentage amount of the mantle source heat flow of the study area.

rock assemblages were represented in more detail.

Rock heat transfer in equation (1) which was used for obtaining the heat flow map or the grid file in which thermal conductivity coefficient had been used was generated by 32 data. Undoubtedly; more field data will give better results.

As also seen in figure 11a which shows the relationship between rock assemblages and the heat flow, high standard deviation values indicate that margin of error in calculations is high. In the study, the b coefficient in which the radiogenic layer depth has been used in equation (4) were calculated as 8.27 km using the linear equation Y=8.27A + 57.22 (Figure 9). Nevertheless; as data scattering in this graph is excessive, 10 km depth value which is much accepted in world literatures was assigned as b coefficient and was used in calculations. The mantle source heat flow in map produced by using this value (Figure 10) was estimated as 60% in minimum and 92% in maximum.

Bar graphs in figure 11 were produced using 311 data from volcanic rocks, 415 data from sedimentary rocks, 194 data from plutonic rocks and 111 data from metamorphic rocks which were located in the study area. Numerical values given in parentheses in each bar, state the standard deviation values of average values belonging to that rock group.

Standard deviation values of heat flow data in figure 11a were high and values showed variations in between 7.2 and 8.7. It was seen that the magnitudes of heat flow bars among rock groups

in this diagram did not show much variation. Only plutonic rocks showed the most variation in the heat flow.

Radiogenic heat production in plutonic rocks in figure 11b is over the average 2 μW/m². Whereas; the average radiogenic heat productions in metamorphic and sedimentary rocks are rather low.

Figures 11c, 11d and 11e show average ratios of uranium, potassium and thorium elements, respectively. Although standard deviation values in these graphs remained in small intervals, this value remained relatively higher for Th. While uranium value gets the highest value in volcanites (Figure 11c), plutonites get the highest values in graphs of potassium (figure 11d) and thorium (figure 11e). The highest value representing of uranium in volcanites as shown in Figure 11c should be specialized to the study area. Howewer, volcanic rocks may present extremely different values with respect to uranium content. While basic volcanic rocks are very low in U content, it is relatively higher in acidic volcanic rocks. Volcanic rocks within the area in this study were simplified and presented without considering their origin (Figure 3). While volcanic rocks extending in the northern parts of the region are basic, the Kötüdað volcanite extending in the southern parts are mainly acidic volcanic products (Section 2.2.4). U anomaly in figure 11c might be showing that samples were collected more preferably from acidic volcanites.

RESULTS

This study was performed in area which covers the largest part of the Kýrþehir Massif in the Central Anatolia (Figures 1 and 2). The shallowest area of the Curie point depth which is 580°C takes place around Kýrþehir with 11 km's, the deepest part occurs around Nevþehir with 15 km's (Figure 6). Effective anomaly directions on Curie point depth map is approximately in E - W. When this and the geological maps were compared (Figure 3), it was seen that the shallowest anomaly was on the Kýrþehir - Yozgat line. It was also observed that rocks spreading on this area consist of granitoids in west and east and of metamorphic rocks around Kýrþehir. Both rock groups possess sufficient thermal conductivity to permit heat flow to approach the surface. Besides, regional tectonomagmatic events also have a significant role for the Curie depth to be shallow in addition to the thermal conductivity. These two maps are generally compatible with each other (Figure 3 and Figure 6).

Heat flow (Figure 7) and radiogenic heat production maps (Figure 8) of the study area were produced by using data of previously performed aeromagnetic, on land regional scaled gravity and aerial gamma ray spectrometry studies in the region. The heat flow of the region showed an anomaly which is dominant in north - south directions (Figure 7). On the heat flow map, there was observed a variation between 50 mW/m² and 110 mW/m² and the average value was estimated as 72 mW/m². The anomaly of the region which its heat flow is high overlaps on granitoids spreading approximately in NW - SE directions along Aksaray - Þ. Koçhisar - Kaman - Keskin line on the geological map shown in figure 3. However; anomaly regions that have low heat flow correspond with areas where there are sedimentary and volcanic rocks on the geological map. In spite of the fact that there is morphologically considered a close relationship between the heat flow map and the Curie point depth map, a positive correlation could not be attained in this study. It was seen that effective anomaly directions on the Curie point depth map and the effective anomaly direction on the heat flow map had developed perpendicular to each other. On the other hand, looking at the tectonic position of the region (Figure 2), it can be seen that common directions of main structural elements are compatible to some extent with effective anomaly directions on the Curie point depth map. This

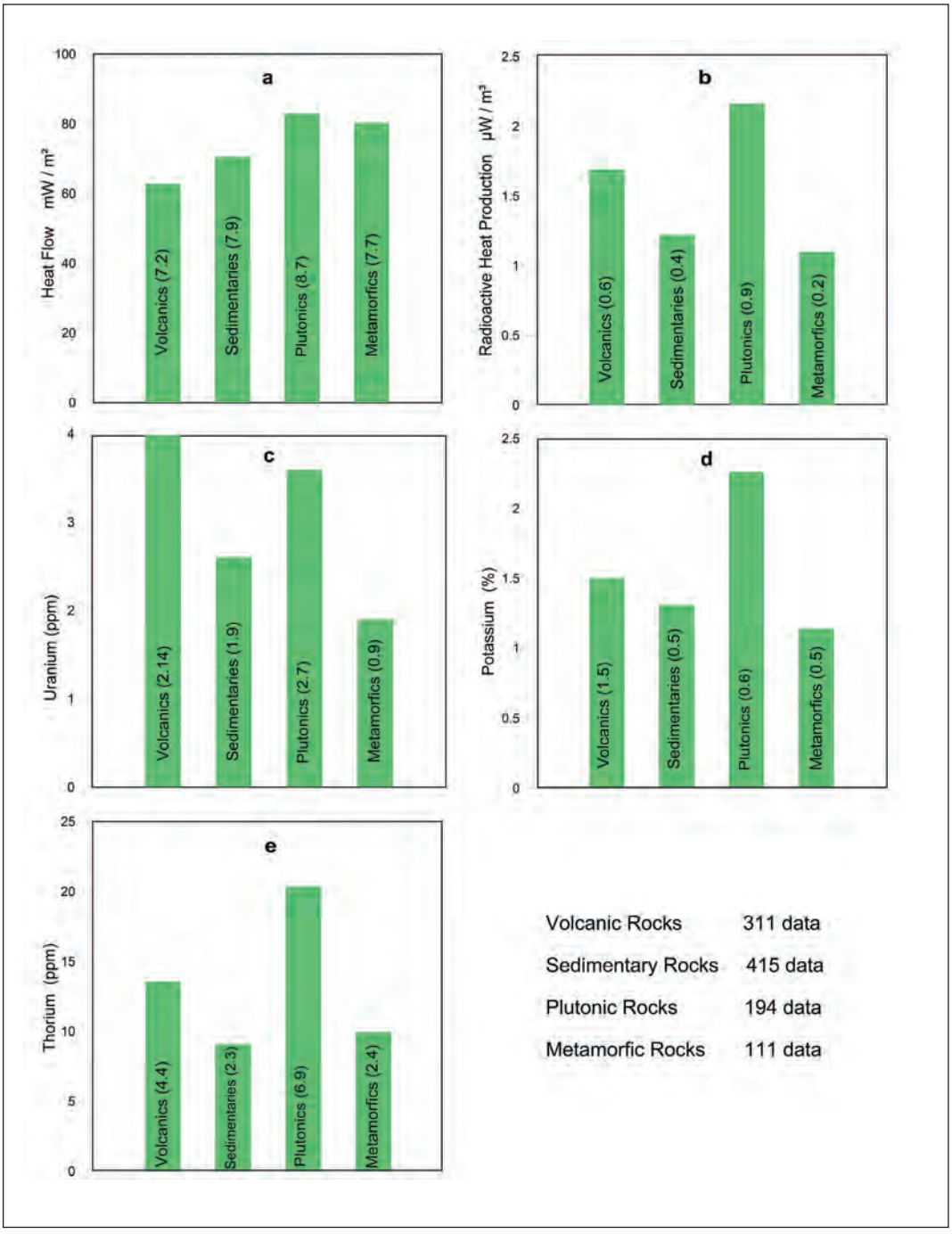

Figure 11- Average and standard deviation values of rocks within the study area a) heat flow, b) radiogenic heat production, c) Uranium, d) Potassium and e) Thorium.

compatibility suggests that, deep fault systems control the Curie depth at the same time as well.

In this study, the percentage ratios of the heat derived from two different heat sources (from mantle and the layer where the radiogenic heat production had occurred) were calculated and the map showing the distribution of percentage ratio of the mantle source heat was produced (Figure 10). According to this map, the heat originating from mantle in the study area shows variation in between 60% and 92%. When the mantle + radiogenic heats are accepted as 100%, the complementary ratios of the heat distribution originating from mantle will give us the distribution of the radiogenic heat. In this case, regions in which the radiogenic heat is the highest will correspond to the regions where the mantle source heat is the lowest. In accordance with this approach, when figure 10 is studied again, it will be seen that, regions where the radiogenic heat is the highest, are around Nevþehir, NE of Kaman and the zone enlarging over NW of Yozgat which is arranged along a thin line starting from the center of Kayseri. Geologically; Neogene aged volcanic and volcano sedimentary deposits with terrigenous clastics and carbonate deposits are successively observed as widespread in these regions. The radiogenic heat production in these parts rises up to 5.68 μWm^{-3} (Figure 8). These high radiogenic heat production zones generally overlaps granitoid areas on the western side of the study area and this is meaningful to a certain extent. Although volcanic and volcano sedimentary series are extensively seen around Nevsehir, occurring the highest radiogenic heat production values here indicates that concentrations of radioactive element in these rocks are rather high. Thus, when Figure 11b is studied, it could be seen that the heat production values of volcanic are not as much as plutonic rocks. Similarly; the heat production in terrigenous clastics and carbonates reaching high values suggest that there are high radioactive element concentrations in the source areas of these clastics and conclude sporadic enrichments in some basins (Figure 3).

Plutonic rocks in the study area (as average values) possess 2.16 μWm^{-3} radiogenic heat production; 82 mWm^{-2} heat flow; %2.26 potassium / 20.36 ppm Thorium / 3.29 ppm Uranium as being relatively higher compared to the average values of other rocks (Figure 11). Volcanites in radiogenic heat production follow up plutonites with 1.68 μWm^{-3}. Radiogenic heat productions of both sedimentary and metamorphics rocks are very close to each other and are successively around 1.25 μWm^{-3} and 1.20 μWm^{-3}. These values actually indicate that the radiogenic heat production heavily generated in magmatic and volcanic rocks and these values were not reached in other derived rocks although there had been enrichment processes. Hence; this case is clearly observed when looking at the concentration distribution of radioactive element. Although the uranium has a different behavior, almost all radioactive elements reach their peak values in plutonic rocks (however uranium gives a peak value in volcanic rocks). This case is followed by volcanic rocks. Both sedimentary and metamorphic rocks too take their places in succession having approximate half values.

Human health and environmental conditions should also be carefully treated since radiogenic heat production is rather high in magmatic and volcanic rocks in the region. Within this scope, this scientific finding would be useful both to differentiate mantle and radiogenic heats in geothermal energy surveys, to define reservoirs in the region and to reduce probable radioactive effects to human settlements and food chain to a minimum.

ACKNOWLEDGEMENTS

We would like to thank to Assist. Prof. Dr. Ünal Dikmen and to Research Ass. M. Özgü Arýsoy for their contributions in preparing some package programs that was needed during the

study. We also would like to thank to Geological Eng. (M.S.) Kerem Mustafa Avcý for his helps during the translation of this paper into English. Dr. Mehmet Duru passed away soon before had also significant contributions into this study. We proud of knowing Dr. Duru who was a model engineer with his endless interest to all areas of Earth Sciences, and will be always remembered with mercy and respect.

Manuscript received May 4, 2011

REFERENCES

Akçay, A.E., Dönmez, M., Kara, H., Yergök, A.F. and Esentürk, K., 2007. 1/100.000 ölçekli Türkiye Jeoloji Haritalarý, Kýrþehir Ý-33 paftasý, No:80, General Directorate of Mineral Research and Exploration, Ankara.

_____, _____, _____, _____, and _____, 2008. 1/100.000 ölçekli Türkiye Jeoloji Haritalarý, Kýrþehir Ý-34 paftasý, No:81, General Directorate of Mineral Research and Exploration, Ankara.

Akýn, U. and Çiftçi, Y., 2010. Kýrýkkale-Kýrþehir-Nevþehir-Kayseri-Yozgat Arasýndaki Bölgenin Isý Akýsý ve Radyoaktif Isý Üretimi Araþtýrma Raporu, Mineral Research and Exploration Report No: 11307, (unpublished) Ankara.

_____ and Duru M., 2006. Türkiye Isý Akýsý Haritasý (manyetik verilerden) Raporu, General Directorate of Mineral Research and Exploration Report No. 10840, (unpublished), Ankara.

_____ Duru, M., Kutlu, S. and Ulugergerli, E.U., 2006. Heat Flow Map of Turkey (from magnetic data), 17 Geophysical Congress, General Directorate of Mineral Research and Exploration, Ankara (in Turkish). Extended Abstract CD.

_____, Iþýkdeniz Þerifoðlu, B. and Duru, M., 2011. Gravite ve Manyetik Yöntemlerde Tilt Açýsýnýn Kullanýlmasý. Bulletin of the Mineral Research and Exploration no. 143.

_____ and Çiftçi, Y., 2011. Structural discontinuities of Turkey: Geological and Geophysical Analysis (Gravity and Magnetic), Monography Series No. 6, General Directorate of Mineral Research and Exploration, 156p, Ankara, Turkey.

Andreoli, M.A.G., Hart, R.J., Ashwal, L.D. and Coetzee, H., 2006. Correlations between U, Th Content and Metamorphic Grade in the Western Namaqualand Belt, South Africa, with implications for radioactive heating of the crust. Journal of Petrology 47(6), pp.1095-1118.

Arslan, S., Akýn, U. and Alaca, A., 2010. Investigation of Crustal Structure of Turkey by means of Gravity Data. Bulletin of the Mineral Research and Exploration no. 140.

Atabey, E., Tarhan, N., Akarsu, B. and Taþkýran, A., 1987. Þerflikoçhisar, Panlý (Ankara) - Acýpýnar (Niðde) Yöresinin Jeolojisi, General Directorate of Mineral Research and Exploration report no: 8155 (unpublished), Ankara.

_____, 1989. 1/100.000 ölçekli açýnsama nitelikli Türkiye Jeoloji Haritalarý serisi, Aksaray H18 Paftasý, General Directorate of Mineral Research and Exploration, Ankara.

Ataman, G., 1972. Ankara Güneydoðusundaki Granitik-Granodiyoritik Kütlelerden Cefalik Daðýn Radyometrik Yaþý Hakkýnda Ön Çalýþma. Hacettepe Fen ve Mühendislik Bilimleri Dergisi, 2, pp.44-49.

Ayan, M., 1963. Contribution a, l'etude petrographique et geologique de la region situee au Nord-Est de Kaman : General Directorate of Mineral Research and Exploration Publications, 115, 332 p.

Aydýn, I., 1990. Orta Anadolu Uranyum Aramalarý Havadan gamma ray Spektrometre Etüdü Raporu, General Directorate of Mineral Research and Exploration report no. 9146. (unpublished), Ankara.

Bailey, E.B. and McCallien, W.C., 1950. Ankara Melanjý ve Anadolu Þariyajý. Bulletin of the Mineral Research and Exploration, 40, pp.12-17.

Bal, A., 2004. Aydýn Ýzmir Civarýnýn Havadan Manyetik Verilerinden Isý Akýsý Deðerlerinin Belirlenmesi ve Isý Akýsý Daðýlýmýnýn Ýncelenmesi, Ankara

Üniversitesi Fen Bilimleri Enstitüsü Jeofizik Mühendisliði Anabilim Dalý.

Baykal, F., 1943. Kýrýkkale-Kalecik ve Keskin-Bala Mýntýkasýndaki Jeolojik Etütler, General Directorate of Mineral Research and Exploration, Report No: 1448 (unpublished), Ankara.

Bea, E., Montero, P. and Zinger, T., 2003. The Nature, Origin and Thermal Influence of the Granite Source Layer of Central Iberia. Journal of Geology 111, pp.579-552.

Bilgin, Z. R., Akarsu, B., Arbas, A., Elibol, E., Yaþar, T., Esentürk, K., Güner, E. and Kara, H., 1986. Kýrýkkale - Kesikköprü - Çiçekdað Alanýnýn Jeolojisi, General Directorate of Mineral Research and Exploration, Report No: 7876 (unpublished), Ankara.

Bingöl, E., 1989. Geological Map of Turkey at 1:2.000.000 scale. Mineral Research and Exploration Institute of Turkey Publications, Ankara.

Birch, F., 1947. Crustal Structure and Surface Heat Flow near the Colorado Front Range, Transaction, American, Geophysical, Union, 28 (5), pp.792-797.

_____, Roy, R.F. and Decker, E.R., 1968. Heat Flow and Thermal History in New England and New York, in studies of Appalachian Geology: Northern and Maritime, Edited by E-an Zen, White, W.S., Hadley, J.B. and Thompson, J.B. Jr.,pp. 437-451, Interscience, New York.

Birgili, Þ., Yoldaþ, R. and Ünalan, G., 1975. Çankýrý - Çorum Havzasýnýn Jeolojisi ve Petrol Olanaklarý: General Directorate of Mineral Research and Exploration, Report No: 5621 (unpublished), Ankara.

Blackwell, D.D., 1971. The thermal structure of the continental crust. The Structure and Physical Properties of the Earth's Crust, Geophysical Monograph 14, Editor: John G. Heacock, pp. 169-184.

Bozkurt, E., 2000. Timing of extension on the Büyük Menderes Graben, western Turkey, and its tectonic implications, in: Bozkurt E., Winchester J.A., Piper J.D.A. (Eds.), Tectonics and magmatism in Turkey and the surrounding area, Geological Society Special Publication no. 173, Geological Society, London, pp. 385-403.

Bozkurt, E., 2001. Neotectonics of Turkey: a synthetis. Geodinamica Acta 14, pp.3-30.

_____ and Koçyiðit, A., 1996. The Kazova basin: an active negative flower structure on the Almus Fault Zone, a splay fault system of the North Anatolian Fault Zone, Turkey, Tectonophysics, 265, pp.239-254.

Dirik, K. and Göncüoðlu, M.C., 1996. Neotectonic characteristics of the Central Anatolia: International Geology Review, 38/9, pp.807-817.

Dönmez, M., Akçay, A.E. and Türkecan, A., 2005*a*. 1/100.000 ölçekli Türkiye Jeoloji Haritalarý, Kayseri K-34 paftasý, No:49, General Directorate of Mineral Research and Exploration, Ankara.

_____, Bilgin Z.R., Akçay, A.E., Kara, H., Yergök, A. F. and Esentürk, K., 2005*b*. 1/100.000 ölçekli Türkiye Jeoloji Haritalarý, Kýrþehir i-31 paftasý, No:46, General Directorate of Mineral Research and Exploration, Ankara.

Ericson, A.J., 1970. The measurement and interpretation of heat flow in the Mediterranean and Black Sea. Ph. D. Thesis, Massachussetts ýnstitute of Technology, Department of Earth and Plaetary Sciences, Massachusetts.

Fytikas, M.D., 1980. Geothermal exploration in Greece. 2nd. International Seminar on the Results of E.C.

Göncüoðlu, M. C., 1977. Geologic des westlichen Niðde massivs. Bonn Üniversity, PhD Thesis, 181 p.

_____, 1981. Niðde masifinde viridin-gnaysýnýn kökeni, Türkiye Jeoloji Kurumu Bülteni C.24/1, pp.45-50.

_____, 1982. Niðde masifi paragnayslarýnda zirkon U/Pb yaþlarý, Türkiye Jeoloji Kurumu Bülteni Sayý :25/1, pp.61-66.

_____, 1986. Orta Anadolu Masifi'nin güney ucunda jeokronolojik yaþ bulgularý, Bulletin of the Mineral Research and Exploration, No: 105-106, pp. 27-28.

Göktürkler, G., 2002. Yerbilimlerinde, Isý Transferi Modellemesi: Kararlý-Hal Kondüktif Isý Ýletimi.

Dokuz Eylül Üniversitesi Mühendislik Fakültesi Fen ve Mühendislik Dergisi Vol: 4, No: 3 pp. 67-80.

_____, Þalk, M. and Sarý, C., 2003. Numerical modeling of the conductive heat transfer in western Anatolia. Journal of the Balkan Geophysical Society, Vol. 6, No.1, pp. 1-15.

ÝIkýþýk, O. M., 1992. Silica heat flow estimates and lithospheric temperature in Anotolia. Proceedings of XI.Conference of World Hydrothermal Organization 13-185. 1992 Ýstanbul-Pamukkale, pp.92-106.

_____, 1995. Regional heat flow in western Anatolia using silica temperature estimates from thermal springs: Tectonophysics, 244, pp.175-184.

Jaupart, C. and Mareschal, J.C., 2003. Constraints on crustral heat production from heat flow data. In Rudnick, R.L., (ed.), The Crustal Treatise on Geochemistry 3, pp.65-84. Elsevier-Pergamon, Oxford.

Jongsma, D., 1974. Heat flow in the Agean Sea. Geophysics J.R. Astr. Soc., 37, pp.337-346.

Kara, H., 1997. 1/100.000 ölçekli, Açýnsama Nitelikli Türkiye Jeoloji Haritalarý Serisi, Yozgat G19 Paftasý, No:54,General Directorate of Mineral Research and Exploration, Ankara.

_____ and Dönmez, M., 1990. 1/100.000 ölçekli, Açýnsama Nitelikli Türkiye Jeoloji Haritalarý Serisi, Kýrþehir G17 Paftasý, No:34, General Directorate of Mineral Research and Exploration, Ankara.

Karlý R., Öztürk, S. and Destur, M. 2006. Türkiye Isý Akýsý Haritasý projesi raporu, General Directorate of Mineral Research and Exploration, Report No. 10937, (unpublished), Ankara.

Ketin, Ý., 1955. Yozgat bölgesinin jeolojisi ve Orta Anadolu Masifi'nin tektonik durumu, TJK Bulletin, C. VI, Sayý 1, pp.1-40, Ankara.

_____, 1963. 1/500.000 ölçekli Türkiye jeoloji haritasý, Kayseri paftasý ve açýklamasý, Mineral Research and Exploration Bulletin., Ankara.

Koçyiðit, A., 2000. Güneybatý Türkiye'nin depremselliðinin BADSEM 2000 Batý Anadolu'nun Depremselliði Sempozyumu, Proceedings, 24-27 Mayýs 2000, Izmir, 2000, pp. 30-39 (in Turkish with English abstract).

Koçyiðit, A., Ünay, E. and Saraç, G., 2000. Episodic graben formation and extensional neotectonic regime in west Central Anatolia and the Isparta Angle: a case study in the Akþehir-Afyon graben, Turkey, in: Bozkurt E., Winchester J.A., Piper J.D.A. (Eds.), Tectonics and magmatism in Turkey and the surrounding area, Geological Society Special Publication no. 173, Geological Society, London, pp. 405-421.

_____ and Erol, O., 2001, A tectonic escape structure: Erciyes pull-apart basin, Kayseri, Central Anatolia, Turkey. Geodynamica Acta, 14, pp.1-13.

McLennan, S.M. and Taylor, S.R., 1996. Heat Flow and the chemical composition of continental crust: Jour. Geol., v. 104, no.4, pp.369-377.

MTA, 2002. 1:500.000 Ölçekli Türkiye Jeoloji Haritalarý (Kayseri Paftasý), No:9, General Directorate of Mineral Research and Exploration, Ankara.

Norman, T., 1972. Ankara Yahþýhan bölgesinde Ü. Kretase-A. Tersiyer istifinin stratigrafisi, Türkiye Jeoloji Kurultayý Bulletin, XV, 2, pp.180-276.

Okay, A.I. and Tüysüz, O., 1999. Tethyan sutures of northern Turkey. In: Durand, B., Jolivet, L., Horvath, F., Seranne, M. (Eds.), Mediterranean Basins: Tertiary extension within the Alpine Orogen. Geological Society of London Special Publication, vol. 156, pp.475-515.

Okubo, Y., Graf, R. J., Hansen, R. O., Ogawa, K. and Tsu, H., 1985. Curie point depths of the island of Kyushu and surrounding areas, Japan, Geophysics, 50, pp.491-494.

Özcan, A., Erkan, A., Keskin, A., Keskin, E., Oral, A., Özer, S., Sümengen, M. and Tekeli, O., 1980. Kuzey Anadolu Fayý - Kýrþehir Masifi arasýnýn temel jeolojisi. General Directorate of Mineral Research and Exploration, Report No: 6722 (unpublished), Ankara.

Pasquare, G., 1968. Geology of the Cenozoik volcanic area of the Central Anatolia, Atti. Della. Accad. Naz. Deiline, 40, 1077-1085.

Rudnick, R.L. and Fountain, D.M., 1995. Nature and composition of the continental crust: A lower

crustal perspective: Review Geophysics, v.33, no. 3, pp. 267-309.

Rybach, L. and Buntebarth, G., 1982. Relationships between the petrophysical properties density, seismic velocity, heat generation, and mineralogical constitution, Earth and Planetary Science Letters, 57, pp.367-376.

Sandiford, M. and McLaren, S., 2006. Thermomechanical controls on heat production distributions and the long-term evolution of the continents. In Brown, M. and Rushmer, T. (eds), Evolution and Differantiation of the Continental Crust, pp.67-91. Cambridge University Press.

Seyitoðlu, G., 1997. Late Cenozoic tectono-sedimentary development of the Selendi and Uþak-Güre basins: a contribution to the discussion on the development of E-W and north trending basins in western Turkey, Geological Magazine 134, pp.163-175.

Seymen, I., 1981*a*. Kaman (Kýrþehir) dolayýnda Kýrþehir Masifi'nin metamorfizmasý. Ýç Anadolu' nun Jeoloji Sempozyumu. Türkiye Jeoloji Kurumu, pp.12-15.

_____, 1981*b*. Kaman (Kýrþehir) dolayýnda Kýrþehir Masifi'nin stratigrafisi ve metamorfizmasý. Türkiye Jeoloji Kurumu Bülteni, 24, pp.7-14.

_____, 1982. Kaman dolayýnda Kýrþehir Masifinin jeolojisi. Assist. Prof. Thesis (unpublished), ÝTÜ, Mining Fac., 164 p.

Spector, A. and Grant, F.S., 1970. Statistical models for interpreting aeromagnetic data, Geophysics, 35, pp.293-302.

Þaroðlu, F., Emre, Ö. and Kuþçu, Ý., 1992. The East Anatolian fault zone of Turkey, Annales Tectonieae 6, pp.99-125.

Tanaka, A., Okubo, Y. and Matsubayashi, O., 1999. Curie point depth based on spectrum analysis of the magnetic anomaly data in East and Southeast Asia, Tectonophysics, 306, 461-470.

Temel, A., 1992. Kapadokya eksplozif volkanizmasýnýn petrolojik ve jeokimyasal özellikleri. Hacettepe Üniversitesi Fen Bilimleri Enstitüsü PhD Thesis (unpublished), Ankara.

Tezcan, A.K. and Turgay, I., 1989. Türkiye ýsý akýsý haritasý. General Directorate of Mineral Research and Exploration, Geophysics Research Department, Ankara.

Turcotte, D. and Schubert, G., 1982. Geodynamics; Application of Continuum Physics to Geological Problems. John Wiley and Sons Inc., New York, 464 p.

Waples, D.W., 2001. A new model for heat flow in extensional basins: Radiogenic heat, asthenospheric heat and the McKenzie model: Natural Resourches Res., 10, 3, 227-238.

Yemen, H., 1999. Ege bölgesi ýsý akýsý daðýlýmý yüksek lisans tezi Süleyman Demirel Üniversitesi, Fen Bilimleri Enstitüsü. 101p, Isparta (unpublished).

Yýlmaz, Y., Genç, S.C., Gürer, O.F., Bozcu, M., Yýlmaz, K., Karacýk, Z., Altunkaynak, Þ. and Elmas, A., 2000. When did the western Anatolian grabens begin to develop? in: Bozkurt E., Winchester J.A., Piper J.D.A. (Eds.), Tectonics and magmatism in Turkey and the surrounding area, Geological Society Special Publication 173, Geological Society, London.

Mineral Res. Expl. Bull., 143, 75-94, 2011

MINERALOGICAL, PETROGRAPHICAL AND GEOCHEMICAL CHARACTERISTICS OF ELDIVAN OPHIOLITE (ÇANKIRI) HARZBURGITIC TECTONITES

Tijen ÜNER* and Üner ÇAKIR**

ABSTRACT.- The Eldivan Ophiolite is located at the central part of the Ýzmir-Ankara-Erzincan Ophiolitic Belt which is between Þabanözü, Eldivan and Korgun towns. From bottom to top, units forming the ophiolite consist of volcano sedimentary and metamorphic series, tectonites, cumulates and sheeted dikes. Tectonites, which are the main subject of the study, are generally represented by harzburgites and occassionally consist of dunite, pyroxenolite and chromitite levels. In harzburgites which have traces of plastic deformation (foliation, lineation and folding), the minerals display a distinct orientation as a result of intra crystallographic dislocation and grinding mechanism. The degree of deformation decreases upwards. Less amount of clinopyroxene is encountered at lower levels of harzburgites which are composed of olivine (60-90%) and orthopyroxene (10-35%). There is also observed a decrease in the amount of orthopyroxene and an increase in chromite ratio towards upper levels. The composition of olivines is usually forsteritic and orthopyroxene is enstatitic and display a slight impoverishment in Mg content towards upper levels. However, there is observed a decrease in the amount of chrome but an increase in aluminum amount in upward direction. This situation can be explained as a result of primary composite of upper mantle and partial melting processes.

Key Words: Eldivan Ophiolite, harzburgite, chromite, olivine, tectonite.

INTRODUCTION

Ophiolites representing the segments exposing on the continent of oceanic lithosphere are important in terms of determining the petrological descriptions of the oceanic crust and the upper mantle which is difficult to investigate and to get information about the geodynamic evolution of the region which they occur.

Ýzmir - Ankara - Erzincan Suture Zone is the residual of Ýzmir - Ankara - Erzincan Ocean which occurs amongst Sakarya, Pontides and Kýrþehir Blocks and Anatolide - Tauride platforms (Þengör and Yýlmaz, 1981). This zone which starts from the north of Ýzmir at west and extends approximately 2000 km until the Georgian border at east (Okan and Tüysüz, 1999), continues namely as the Sevan-Akera Suture Zone at Caucasians (Khain, 1975; Adamia et al., 1977; Knipper, 1980). The NE-SW trending Eldivan Ophiolite occurring within the central parts of Ýzmir - Ankara - Erzincan Suture Zone (Figure 1a) represents the fragments of lithosphere belonging to the Neothethys Ocean which has started to rift towards the ends of Triassic and closed within the Upper Cretaceous - Lower Paleocene and there are several studies about its stratigraphy, tectonical environment and geochemical properties (Bailey and McCallien, 1953; Akyürek, ,1981; Tankut, 1984; Tankut and Gorton, 1990; Floyd, 1993; Önen and Hall 1993; Rojay et al 1995; Yalýnýz et al. 1998; Rojay et al. 2001; Rojay et al. 2004; Göncüoðlu et al. 2006; Dangerfield, 2008; Gökten and Floyd 2007; Çakýr, 2009;). Units in the region are the rocks belonging to the Eldivan Ophiolites, Cenomanian and after Cenomanian aged cover rocks cropping out on them (Figure 1b).

* Yüzüncü Yýl Üniversitesi, Jeoloji Mühendisliði Bölümü, Zeve Kampüsü, 65080, Van.
** Hacettepe Üniversitesi, Jeoloji Mühendisliði Bölümü, Beytepe Kampüsü, 06800, Ankara.

Eldivan Ophiolitic deposit from bottom to top is represented by volcano sedimentary series (basalt, radiolarite - chert - mudstone) and the overlying metamorphic series (amphibolite, epidosite, quartzite), tectonites (dunite, harzburgite, chromite), cumulates (dunite, pyroxenite, gabbro, diorite, plagiogranite) and plate dykes (Figure 2). All units within the deposit except volcanic series are cut by isolated diabase dykes. Among these units, volcano sedimentary series and metamorphics which crop out around close vicinity are not observed on the map (Figure 1) but were shown on the generalized columnar section (Figure 2). Mart, Karakoçaþ and Hançýlý formations which directly lie on the Eldivan Ophiolite and shown as cover units in figure 2 represent a tectonical relationship with this ophiolite. The unit named by Akyürek et al (1979, 1981) starts with conglomerate and sandstone layers forming by the sediments of the Eldivan Ophiolites at bottom and continues with the alternation of siltstone, sandstone, conglomerate and marn layers. Limestone layers are sporadically observed at the uppermost layers. Mart formation is the first unit that directly overlies the Eldivan Ophiolite. The age of the unit has been detected as Cenomanian - Turonian due to its fossil content (Akyürek et al., 1979). The other unit, Karakoçaþ Formation is generally composed of reddish colored, coarse grained conglomerates and sandstones. The age of the units has been determined as Late Miocene due to its stratigra-

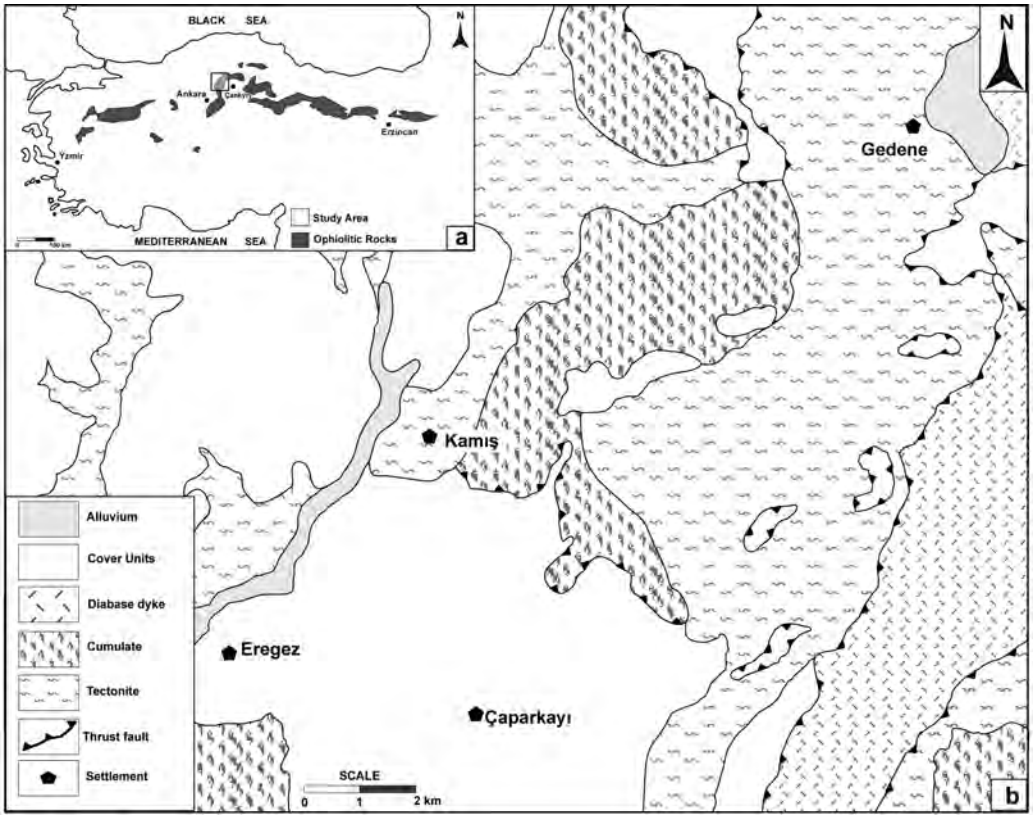

Figure 1- a) Map showing the location of study area in Ýzmir-Ankara-Erzincan belt, b) the simplified geological map of Eldivan Ophiolite and cover rocks observed in the study area (modified from Akyürek et al., 1979; Hakyemez et al., 1986).

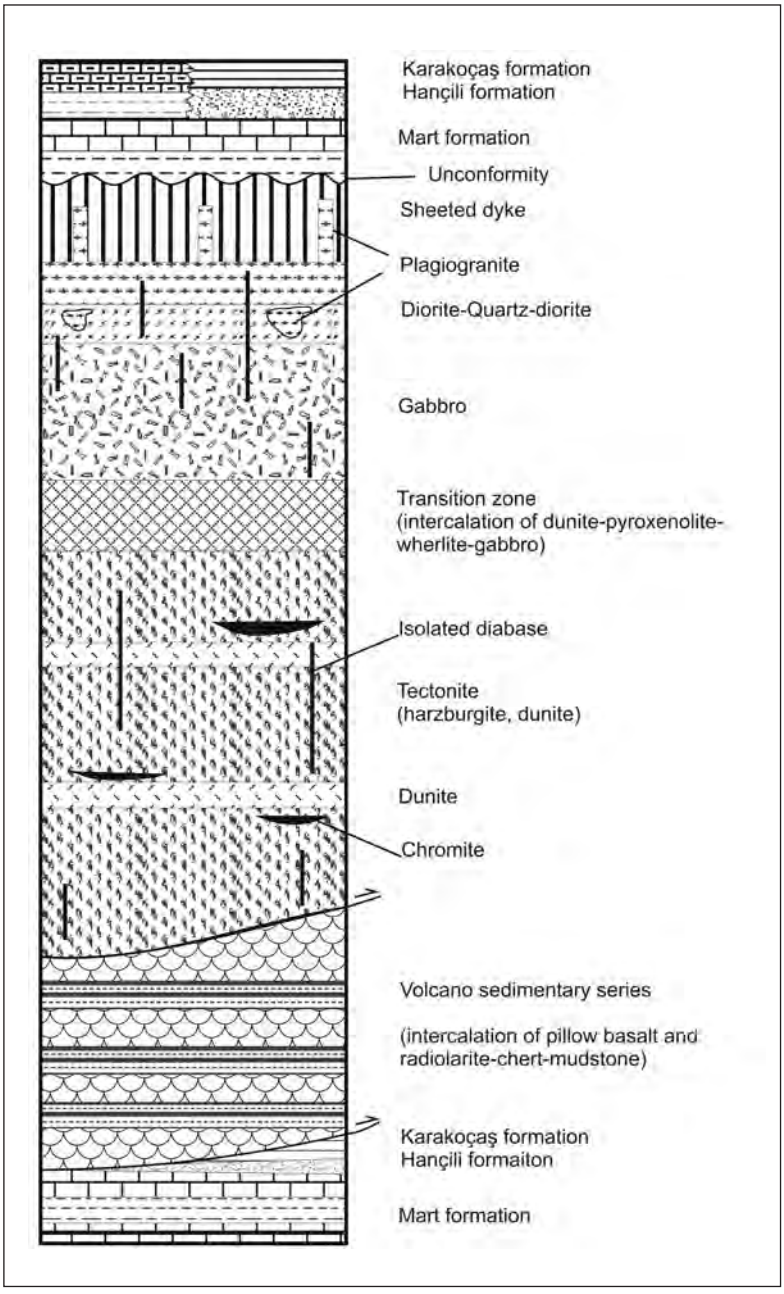

Figure 2- The tectono-stratigraphic columnar section of the Eldivan Ophiolite and units (after the settlement) (not to scale).

phical position. However, The Hançýlý formation is composed of alternation of siltstone, marn, clayey limestone and tuff - tuffite. Sporadically, gypsium and coal layers were encountered. The Late Miocene age were detected from the samples taken from some coal layers by performing the pollen analysis (Akyürek et al., 1979). Mart, Karakoçaþ and Hançýlý formations

unconformably overlie the Eldivan Ophiolite. Due to the post Miocene tectonism developed, it is observed that Eldivan Ophiolite had thrusted over Mart, Karakoçaþ and Hançýlý formations at some places (Figure 1 and 2).

In this study, it was aimed at detecting the geological and geochemical properties of peridotites of the Eldivan Ophiolite which have less been investigated so far. Within this scope, the geological map of the region was prepared and environments of formation of these rocks were determined analyzing the geochemistry of olivine, orthopyroxene and spinel minerals in samples taken from tectonites of the Eldivan Opholite.

TECTONITES OF THE ELDÝVAN OPHIOLITES

Peridotites with tectonite texture form the most significant part of the Eldivan Ophiolite. Mylonitic and schistositic serpentines are clearly observed within the contact zone of tectonites that had thrusted over volcano sedimentary series. Tectonites are generally composed of harzburgites and sporadically constitute dunitic, chromitic and pyroxenolitic layers and have traces of plastic deformation. The rock has gained a distinctively foliated and lineated form due to gliding, grinding and recrystallization of intra crystals of minerals. Towards the upper levels the degree of deformation decreases, despite that; dunitic levels and chromite ores were frequently encountered. Harzburgite and dunitic tectonites were serpentinized at high levels.

As a result of petrographical studies of samples taken from tectonites, it was investigated that these units were formed by serpentinized harzburgites in general. Harzburgites forming tectonites constitute olivine (60-70%) (forsterite), orthopyroxene (enstatite) (20-30%), chromite ((3 -5%) and clinopyroxene (1-2%). Textural properties observed here are same as the common textural properties observed in harzburgites. Rocks are generally granoblastic in structure (Figure 3a) and in mosaic texture which small olivine minerals (product of recrystallization) have formed especially around peripheral zones of coarse olivine and pyroxene minerals were sporadically observed (Figure 3b). Tiny olivine crystals showing mosaic texture are in the form of surrounding the coarse crystals. Tiny olivine crystals that are the product of recrystallization show wavy extinction around some of the coarse olivine crystals that have the same extinction. This phenomenon indicates that the plastic deformation causing the wavy extinction continues after recrystallization too (Engin et al., 1980). Along cracks that have developed within olivines the serpentinization is obviously observed (Figure 3d). Olivines that are present as disseminated in small dimensions within the grain sizes of orthopyroxenes enclose orthopyroxene grains (See Figure 3a). Orthopyroxene minerals are generally in medium to coarse grained and disintegration along cleavages (Figure 3c) and thin clinopyroxene exsolution lamellae that have developed parallel to the planes of cleavage were sporadically observed (Figure 3d). Deformation lamellae (kink banding) were seldom observed in enstatite minerals that showed slight elongation (Figure 3e, 3f). Magnetisation at different proportions was observed around chromite minerals that had variable crystal sizes (Ferric chromite). Serpentinization along crack systems that developed in one or sometimes two ways was evident in minerals that had disintegrated as a result of deformation.

Within upper layers of tectonites, generally veins that have thickness in centimeter or decimeter scale and often pyroxenolites that are observed as phyllonite cut harzburgites in such a way to make a small angle with foliation plane. Pyroxenolite phyllonite made by solutions of the partial melting product have been folded during plastic deformation forming the foliation (Figure 4a).

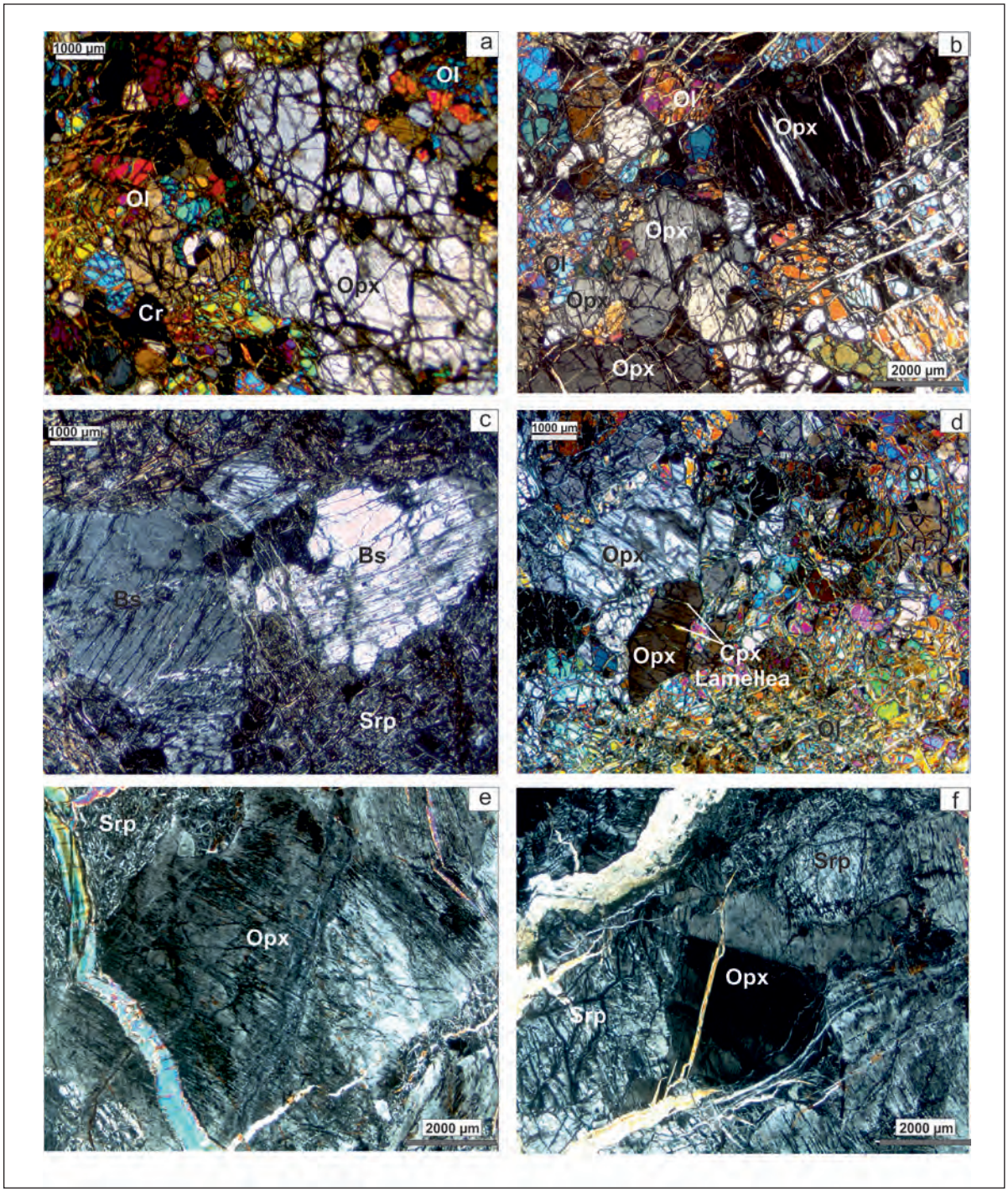

Figure 3- Thin-section images of harzburgites, a) granoblastic texture observed in harzburgites, b) tiny olivine minerals observed around the orthopyroxene, c) orthopyroxene minerals alterated to the bastite, d) exsolution lamellae of clinopyroxene among orthopyroxene minerals, e) and f) deformation lamellae observed in enstatite minerals (Ol: olivine, Opx: orthopyroxene, Cpx: clinopyroxene, Serp: serpentinite minerals, Cr: chromite, Bs: bastite).

Dunitic zones are observed as in lenses and bands at variable thicknesses generally in the upper layers of tectonites (Figure 4b). Olivine (90 -96%), orthopyroxene (1-3%) and chromite (3-5%) minerals are present in dunites. While olivines are observed as residuals in some thin sections (Figure 5a), these are seen as in tiny particles in nucleic parts of the sieve textured high level serpentinized samples. It is considered that the sieve structure that are widely observed in thin sections have developed in this way. Chromite minerals within dunites are available at higher proportions than harzburgites. It is accepted that the pull apart texture observed in chromites within dunites have developed as a result of tensional forces during plastic deformation (Engin et al., 1980) (Figure 5b).

Chromites that are present generally in dunitic and sometimes in harzburgitic zones show massive, nodular and dispersive distributions in rock. Typical elongation and orientation seen in chromite minerals can be observed in the rock (Figure 6). Flattening and elongation that could macroscopically be distinguished in minerals such as orthopyroxene and chromite indicate the presence of foliation planes in the rock.

Peridotites of the Eldivan ophiolite were largely serpentinized. Serpentines that generally show massive structure are covered by brown to yellow colored crust in centimeter thickness which has formed due to atmospheric leaching. These rocks that can be described by their massive and green to black colored views when broken represent a schistosic appearance at fault zones and along margins of diabase dikes. After serpentinization, the rock gains a mottled green colored, slippery and shiny view as a result of the period that has occurred in tectonically active zones.

Petrographical studies and X-RD analyses were performed in order to describe serpentine minerals. Chrysotile-γ, chrysotile-α and lizardite minerals were encountered during petrographical investigations of the samples taken (Figure 7). While chrysotiles are distinguished according to the crystallographic structures of minerals, lisardites are detected due to their massif form and are in the form of sieve texture. Due to the results of X-RD analyses, chromite, orthoserpentinite, forsterite and pyroxene minerals were encountered in addition to the minerals mentioned above (Figure 8). The presence of chrysotile, lizardite and antigorite minerals

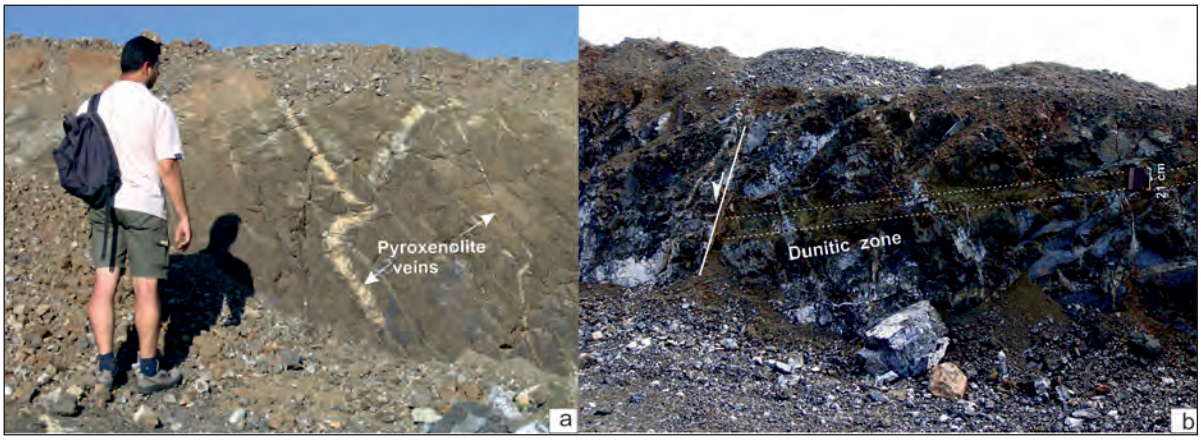

Figure 4- Within the tectonites of the Eldivan Ophiolite; a) folded pyroxenolite vein observed in harzburgite and b) Dunitic bands.

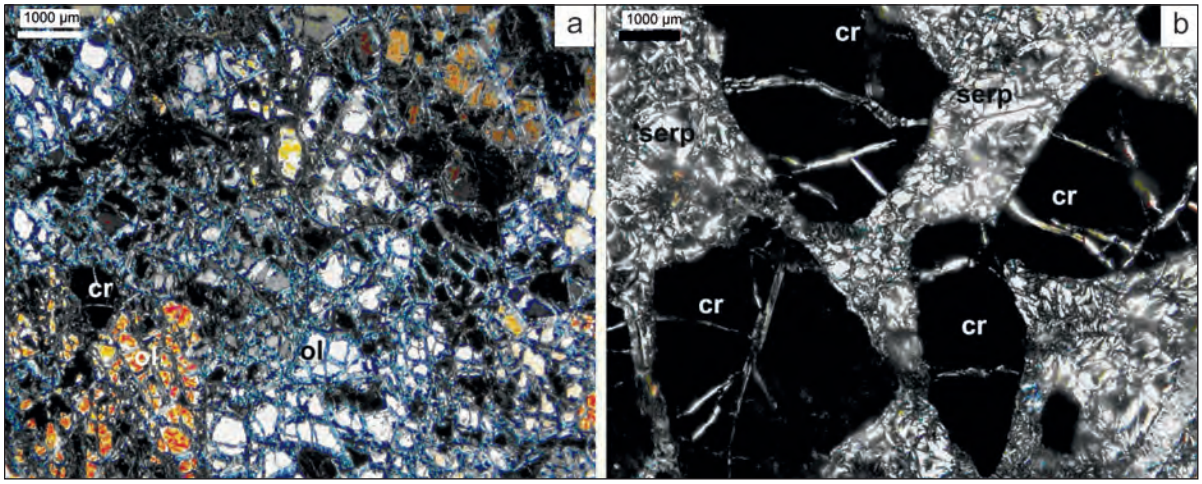

Figure 5- Minerals and textures observed in dunites, a) sieve texture, b) pull-apart structures in chromites (ol: olivine, serp: serpentinite, cr: chromite).

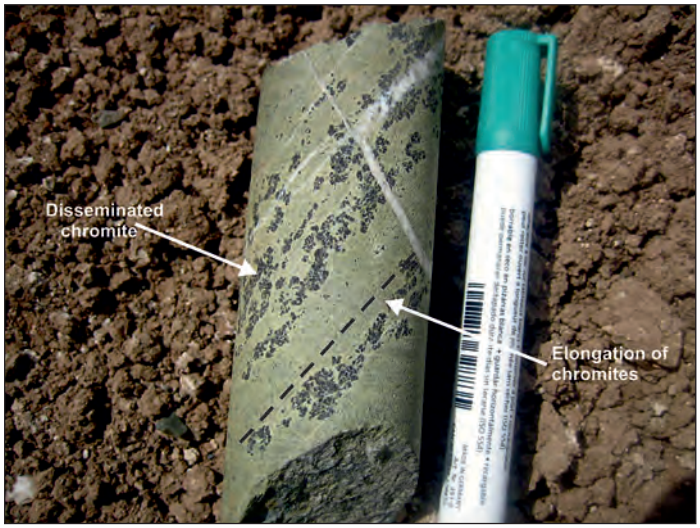

Figure 6- Flattened and elongated chromite minerals within dunitic zones in the Eldivan Ophiolite.

altogether indicates that the serpentinization has formed at a temperature of up to 500°C (Coleman, 1977).

MINERAL CHEMISTRY OF PERIDOTITES

As a result of mineralogical investigations point analyses were performed by means of EDS (Energy Dispersive Spectrometer) device on two fresh harzburgite samples (showing no alteration) belonging to Eldivan formation. In order to perform these analyses, JEOL - 6490 electron microscope, SQ analysis program and ZAF correction program have been used which are available at the Directorate of Sedimantology and Reservoir Geology of Turkish Petroleum

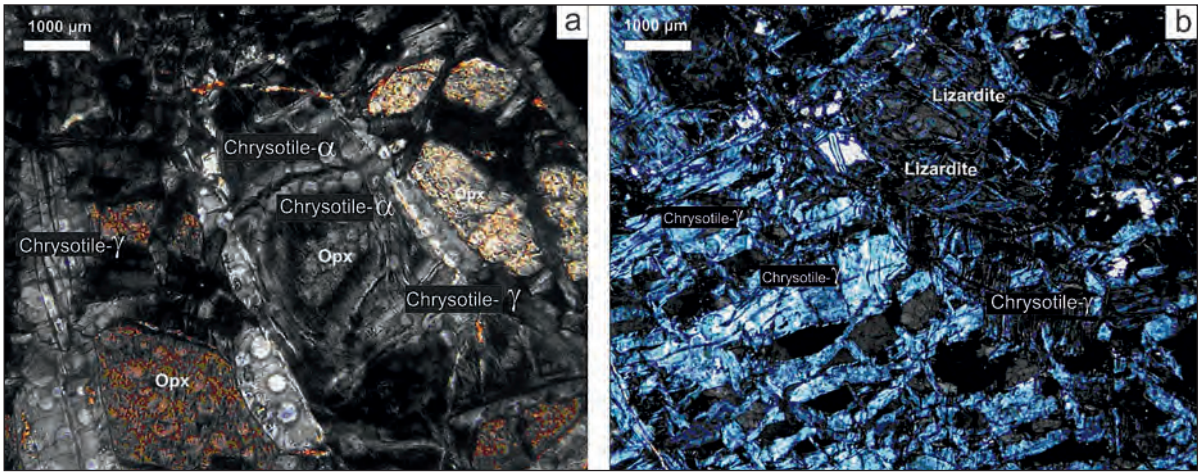

Figure 7- Thin-section views of serpentine group minerals, a) chrysotile - α ve chrysotile - γ minerals surrounding the orthopyroxene mineral, b) chrysotile - γ and lizardite minerals.

Corporation (TPAO). By this technique, the chemistry of minerals (olivine, orthopyroxene, clinopyroxene, spinel) in the rock were defined and their structural formulae were calculated by CALCMIN software.

Olivine minerals

According to the mineralogical chemistry analysis performed on olivine minerals in harzburgite samples belonging to Eldivan Ophiolite, forsterite constituents (Fo) of olivines and Mg# (100*(Mg/(Mg+Fe^{+2}))) values range in between 88 - 92% and 90 - 94%, respectively (Table 1). Olivine minerals that have Fo_{88}-Fo_{92} values indicate excessively depleted harzburgite and dunite (Uysal et al., 2007).

Pyroxene minerals

Results of analyses obtained from orthopyroxene (Table 2) and clinopyroxene (Table 3) in harzburgites were assessed according to the En - Wo - Fs classification prepared by Morimoto (1989). According to this, it was determined that orthopyroxene minerals showed an abundance on behalf of enstatite due to their Mg contents (Figure 9a). However, clinopyroxene minerals were detected as in the character of diopside (Figure 9b).

Cr - Spinel minerals

Cr - spinels are accepted as one of the best indicators of partial melting period of mantle peridotites (Matsukage and Kubo, 2003; Tamura and Arai, 2006; Uysal et al., 2007). Cr_2O_3 values were detected as 32.09-48.43%, Al_2O_3 values as 12.14-19.89%, Fe_2O_3 values as 1.95-23.78%. However; MgO values were detected as 9.26-15.05% in chemical analyses of Cr- spinel minerals within harzburgites (Table 4). The large range observed in Fe_2O_3 and Al_2O_3 values indicate that chromites were subjected to alteration (Uysal et al., 2007 and Singh, 2009).

Cr - spinels were plotted on Al-(Fe^{+3}+2Ti)-Cr ternary diagram (Figure 10a) and on 100*Mg/(Mg+Fe^{+2})-100*Cr/(Cr+Al) diagram (Figure 10b) in order to understand its character. As a result it was seen that these samples fell into Alpine type peridotites. Chemical changes determined in Cr - spinels might be due to magmatic alterations or regional metamorphism (Cameron, 1975; Kimball, 1990). However, it was observed that Cr - Spinel minerals belonging to Eldivan

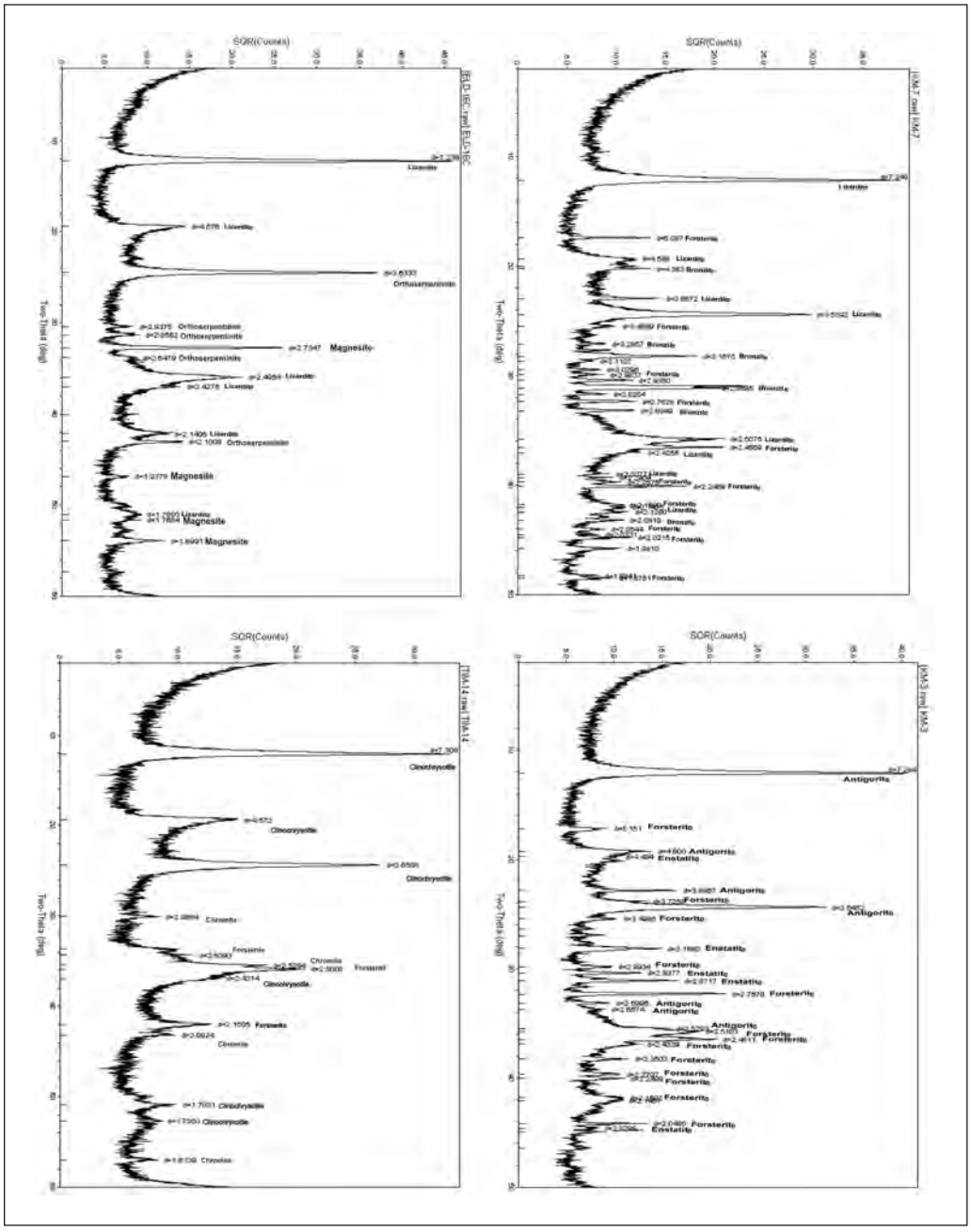

Figure 8- X-RD results taken from serpentine minerals of the Eldivan ophiolite. Chrysotile, lizardite, chromite, ortho-serpentine, forsterite and pyroxene minerals occur in ophiolitic rocks.

Table 1- The results of analysis and cation values of olivine mineral in harzburgites belonging to the Eldivan Ophiolite.

	KM-2			Mİ-13		
X	1.00	2.00	3.00	4.00	5.00	6.00
SiO_2	42.50	39.89	41.76	41.93	41.40	38.14
TiO_2	0.14	0.23	0.11	0.14	0.13	0.26
Al_2O_3	0.01	0.04	0.09	0.17	0.02	0.05
Cr_2O_3	0.11	0.14	0.00	0.00	0.00	0.00
FeO	7.44	9.19	9.11	9.12	8.77	5.42
Fe_2O_3	0.00	0.35	0.00	0.00	0.00	6.11
MgO	48.37	48.31	48.41	48.36	49.34	49.60
CaO	0.15	0.25	0.21	0.13	0.12	0.20
Total	98.72	98.38	99.69	99.85	99.79	99.78
Cation=3, Fe^{2+}/Fe^{3+}, valance=8						
	KM-2			Mİ-13		
Fe_2	0.1539	0.1908	0.1871	0.1871	0.1793	0.1114
Mn	0.0030	0.0092	0.0064	0.0032	0.0044	0.0077
Mg	1.7832	1.7883	1.7712	1.7696	1.7980	1.8183
sum6	1.9400	1.9883	1.9647	1.9600	1.9818	1.9375
Si	1.0508	0.9907	1.0250	1.0292	1.0121	0.9380
Ti	0.0025	0.0042	0.0021	0.0025	0.0024	0.0048
Al	0.0003	0.0011	0.0026	0.0048	0.0006	0.0013
Cr	0.0022	0.0027	0.0000	0.0000	0.0000	0.0000
Fe_3	0.0000	0.0065	0.0000	0.0000	0.0000	0.1130
V	0.0000	0.0000	0.0000	0.0000	0.0000	0.0000
Ca	0.0041	0.0066	0.0055	0.0035	0.0032	0.0053
sum4	1.0600	1.0117	1.0353	1.0400	1.0182	1.0625
Fo	92.0571	90.0368	90.4480	90.4376	90.9323	88.4677
Fa	7.9429	9.9632	9.5520	9.5624	9.0677	11.5323
Mg#	92.0551	90.3593	90.4458	90.4380	90.9321	94.2271

Ophiolites fell into MORB type peridotite region in Al_2O_3-Fe^{+2}/Fe^{+3} diagram (Kamenetsky et al., 2001) (Figure 11).

GEOCHEMICAL PROPERTIES OF TECTONITES

Total rock analyses for 5 samples taken from harzburgites were performed by XRF and ICP - MS devices in ACME laboratories (Canada). When results of major oxide analyses were investigated, it was observed that SiO_2 values and MgO values had ranged in between 44- 47% and 41 - 45%, respectively. However, FeO values were determined as ranging in between 8 - 9% (Table 5). It is seen that all samples are rich in Mg and were clustered in metamorphic peridotite

Table 2- The results of analysis and cation values of orthopyroxene minerals in harzburgite samples belonging to the Eldivan Ophiolite.

	K-02									Mİ-13				
	1-3	1-1	2-3	4-2	4-3	4-4	4-5	5-1	5-2	1-3	2-5a	4-1	6-1	6-3
SiO_2	55.38	52.67	55.98	55.40	51.58	49.09	55.15	51.19	52.82	50.90	52.37	50.33	51.36	51.30
TiO_2	0.11	0.30	0.22	0.15	0.12	0.22	0.11	0.11	0.20	0.00	0.16	0.28	0.00	0.00
Al_2O_3	2.66	2.43	2.12	2.55	2.39	0.41	2.64	2.30	2.93	1.67	2.49	2.39	1.62	1.80
Cr_2O_3	0.67	1.40	0.46	0.30	0.80	0.14	0.53	0.77	0.69	0.69	0.90	0.59	0.83	0.47
FeO	4.09	6.00	5.41	2.23	3.42	4.20	1.55	4.81	1.19	3.68	2.02	2.82	2.41	2.40
Fe_2O_3	2.35	4.78	1.02	3.38	5.25	8.95	3.85	6.59	6.31	6.12	6.04	5.50	5.95	5.22
MnO	0.16	0.13	0.22	0.00	0.00	0.00	0.24	0.31	0.20	0.00	0.24	0.11	0.30	0.42
MgO	33.13	29.80	33.04	34.65	35.50	37.10	34.62	32.47	35.38	36.23	35.50	36.92	37.63	38.32
NiO	0.00	0.00	0.00	0.00	0.00	0.00	0.00	0.00	0.00	0.00	0.00	0.00	0.00	0.00
CaO	1.05	1.63	0.67	0.67	0.72	0.20	0.71	1.36	0.99	0.21	0.65	0.28	0.39	0.33
Na_2O	0.36	0.41	0.38	0.33	0.33	0.39	0.35	0.00	0.00	0.29	0.00	0.61	0.00	0.40
Total	99.97	99.54	99.52	99.65	100.10	100.69	99.76	99.92	100.69	99.78	100.37	99.84	100.49	100.64
Valences = 12, cations = 4, Fe^{2+}/Fe^{3+}- All calculations made of with modelling OPX (Brandelik and Massonne, 2004)														
	1-3	1-1	2-3	4-2	4-3	4-4	4-5	5-1	5-2	1-3	2-5a	4-1	6-1	6-3
Si	1.9152	1.8717	1.9439	1.9075	1.7767	1.6447	1.8982	1.7988	1.8184	1.7223	1.8030	1.6778	1.7240	1.7239
Al_T	0.0848	0.0000	0.0561	0.0925	0.0000	0.0000	0.1018	0.0000	0.0000	0.0000	0.0000	0.0000	0.0000	0.0000
sum4	2.0000	1.8717	2.0000	2.0000	1.7767	1.6447	2.0000	1.7988	1.8184	1.7223	1.8030	1.6778	1.7240	1.7239
Al_O	0.0235	0.1017	0.0308	0.0111	0.0969	0.0162	0.0053	0.0952	0.1188	0.0666	0.1167	0.1147	0.0642	0.0785
Ti	0.0028	0.0081	0.0057	0.0038	0.0031	0.0056	0.0030	0.0029	0.0052	0.0000	0.0042	0.0070	0.0000	0.0000
Cr	0.0183	0.0392	0.0126	0.0081	0.0218	0.0036	0.0144	0.0214	0.0188	0.0720	0.0244	0.0156	0.0344	0.0389
Fe_3	0.0613	0.1278	0.0267	0.0876	0.3435	0.7046	0.0997	0.2801	0.2152	0.4359	0.2445	0.5394	0.4534	0.4607
Fe_2	0.1183	0.1784	0.1572	0.0641	-0.1274	-0.5099	0.0445	-0.1414	-0.0342	-0.3021	-0.0582	-0.4410	-0.3670	-0.3657
Mn	0.0046	0.0038	0.0065	0.0000	0.0000	0.0000	0.0070	0.0093	0.0059	0.0000	0.0069	0.0032	0.0086	0.0118
Mg	1.7081	1.5790	1.7102	1.7786	1.8226	2.1027	1.7763	1.5439	1.8156	1.9788	1.8218	2.0338	2.0684	2.0142
Ni	0.0000	0.0000	0.0000	0.0000	0.0000	0.0000	0.0000	0.0000	0.0000	0.0000	0.0000	0.0000	0.0000	0.0000
Ca	0.0391	0.0620	0.0248	0.0249	0.0412	0.0073	0.0263	0.3899	0.0364	0.0075	0.0367	0.0101	0.0140	0.0117
sum6	2.0000	2.1283	2.0000	2.0000	2.2233	2.3553	2.0000	2.2012	2.1816	2.2777	2.1970	2.3222	2.2760	2.2761
components	1-3	1-1	2-3	4-2	4-3	4-4	4-5	5-1	5-2	1-3	2-5a	4-1	6-1	6-3
X-ENS_ORTHO	0.8085	0.6957	0.8348	0.8398	0.7029	0.5919	0.8297	0.3898	0.7674	0.6965	0.7509	0.6768	0.7292	0.7106
X-FERROSILITE	0.0560	0.0786	0.0767	0.0303	0.0491	0.1435	0.0208	0.0357	0.0144	0.1064	0.0240	0.1468	0.1294	0.1290
X-Al_ENS_B	0.0118	0.0133	0.0154	0.0055	0.0632	0.1696	0.0026	0.0530	0.0314	0.1055	0.0402	0.1037	0.1059	0.0988
X-CPX	0.0391	0.0620	0.0248	0.0249	0.0412	0.0073	0.0263	0.3899	0.0364	0.0075	0.0367	0.0101	0.0140	0.0117
X-NA_CPX	0.0239	0.0283	0.0255	0.0219	0.0217	0.0251	0.0235	0.0000	0.0000	0.0191	0.0000	0.0394	0.0000	0.0259
X-REST	0.0608	0.1487	0.0228	0.0776	0.3466	0.6887	0.0971	0.3090	0.2421	0.4888	0.2766	0.5243	0.4920	0.4796

Table 3- The results of analysis and cation values of the clinopyroxene minerals in harzburgites belonging to the Eldivan Ophiolite (valence=12, cation=4).

	K-02						Mİ-13		
Comment	1-2	1-6	2-1	2-5	2-6	5-3	1-7	2-8	5-8
SiO_2	53.02	51.28	50.27	47.96	50.84	53.54	47.69	46.55	47.54
TiO_2	0.15	0.20	0.14	0.30	0.22	0.10	0.16	0.30	0.38
Al_2O_3	2.90	2.56	2.15	2.12	2.25	2.84	2.71	2.06	2.65
Cr_2O_3	0.95	1.00	0.87	0.73	1.03	0.65	0.93	0.97	0.00
Fe_2O_3	0.05	2.51	2.27	3.24	3.04	0.00	2.93	3.28	3.03
FeO	2.08	0.00	0.00	0.00	0.00	2.16	0.00	0.00	0.00
MnO	0.17	0.13	0.29	0.27	0.24	0.10	0.12	0.22	0.36
MgO	16.91	16.01	16.28	15.54	16.95	18.69	17.68	14.75	16.09
CaO	23.56	25.84	27.27	29.23	25.13	20.68	27.44	31.99	29.92
Na_2O	0.20	0.46	0.21	0.29	0.22	0.44	0.00	0.07	0.00
K_2O	0.02	0.02	0.02	0.19	0.08	0.00	0.08	0.13	0.00
Total	100.00	100.00	99.78	99.87	100.00	99.19	99.73	100.33	99.96
Si	1.9267	1.8701	1.8366	1.7564	1.8541	1.9427	1.7359	1.7052	1.7353
Al_T	0.0733	0.0000	0.0000	0.0000	0.0000	0.0573	0.0000	0.0000	0.0000
sum4	2.0000	1.8701	1.8366	1.7564	1.8541	2.0000	1.7359	1.7052	1.7353
Al_O	0.0509	0.1100	0.0927	0.0915	0.0969	0.0641	0.1162	0.0890	0.1139
Ti	0.0042	0.0055	0.0037	0.0084	0.0061	0.0027	0.0044	0.0082	0.0105
Cr	0.0273	0.0288	0.0252	0.0213	0.0297	0.0187	0.0266	0.0282	0.0000
Fe3	0.0013	0.0688	0.0624	0.0894	0.0834	0.0001	0.0803	0.0903	0.0831
Fe2	0.0632	0.0000	0.0000	0.0000	0.0000	0.0654	0.0000	0.0000	0.0000
Mn	0.0053	0.0040	0.0090	0.0083	0.0075	0.0031	0.0036	0.0069	0.0110
Mg	0.9161	0.8702	0.8868	0.8482	0.9215	1.0110	0.9591	0.8056	0.8758
Ca	0.9171	1.0097	1.0676	1.1472	0.9819	0.8039	1.0702	1.2557	1.1703
Na	0.0137	0.0322	0.0149	0.0207	0.0152	0.0310	0.0000	0.0049	0.0000
K	0.0008	0.0007	0.0010	0.0088	0.0038	0.0000	0.0037	0.0060	0.0000
sum6	2.0000	2.1299	2.1634	2.2436	2.1459	2.0000	2.2641	2.2948	2.2647
Na_start	0.0137	0.0322	0.0149	0.0207	0.0152	0.0000	0.0000	0.0049	0.0000

(ultramafite tectonite) zone when these were plotted in order to define the differentiation grades of samples at Al_2O_3-CaO-MgO diagram made by Coleman (1977) (Figure 12). The term "metomorphic peridotite" can also be named as "tectonic harzburgite", "harzburgite type", "Alpine type ultramafic" (Jackson and Thayer, 1972).

When Cr_2O_3-NiO values obtained as a result of geochemical analyses of tectonites in the study area were plotted on the discrimination diagram of Irvine and Findlay (1972), it was seen that all samples were condensed over the region of "Alpine type peridotite" (Figure 13). When major oxide analysis results obtained from rocks in the region were plotted on Ringwood's (1975)

Table 4- The results of analysis of chromite minerals samples in peridotites of the eldivan Ophiolites (chrome spinel analyzes and Fe^{+2} and Fe^{+3} value were standardized using Droop (1984) equation. Cation number were taken as 24 in all analyses).

sample	KM-2						MI-13				
Probe No	1-1	2-2	2-4	2-6	3-2	4-5	1-3	1-4	2-3	3-5	4-2
Cr_2O_3	37.14	27.91	33.98	31.87	26.11	33.55	39	34.43	38.34	37.85	34.11
Al_2O_3	27.91	40.96	31.56	36.64	41.08	34.01	27.74	31.73	23.01	29.01	26.32
TiO_2	0.14	0.12	0.05	0.093	0.09	0.07	0.14	0.08	0.06	0.08	0.04
FeO	11.34	13.44	13.71	11.35	15.46	18.61	11.37	13.38	16.8	15.6	12.06
Fe_2O_3	7.25	0.23	5.91	1.86	1.03	0.96	4.24	4.95	9.26	3.73	11.59
MgO	16.72	16.17	15.28	17.27	14.25	12.37	15.26	15.43	12.63	13.24	15.27
MnO	0.05	0.24	0.25	0.03	0.34	0.12	1.99	0.11	0.13	0.38	0.6
NiO	0	0	0	0	1.13	0	0	0	0	0.57	1.39
Total	100.69	99.13	100.74	99.24	99.67	99.9	99.92	100.05	100.49	100.41	101.77
Cr	6.8825	4.9862	6.2587	5.7479	4.6989	6.2628	7.3328	6.3652	7.4512	7.1456	6.3751
Al	7.7146	10.9116	8.6695	9.8531	11.0252	9.4661	7.778	8.7454	6.6694	8.167	7.3369
Ti	0.0485	0.0316	0.0088	0.0395	0.0497	0.0503	0.0608	0.0035	0.0593	0.0054	0.0774
Fe3+	1.2792	0.0389	1.037	0.3185	0.1761	0.1702	0.7584	0.8702	1.7123	0.6695	2.0622
Fe2+	2.249	2.5393	2.6887	2.1676	2.9435	3.6755	2.2706	2.6293	3.5007	3.1219	2.4539
Mg	5.8418	5.4457	5.3045	5.87	4.8356	4.3509	5.4084	5.3766	4.6273	4.7119	5.3793
Mn	0.0105	0.0467	0.05	0.005	0.0648	0.0247	0.4001	0.0217	0.0269	0.0767	0.1202
Ni	0	0	0	0	0.2067	0	0	0	0	0.1091	0.2638
Total	24.0261	24	24.0171	24.0016	24.0005	24.0005	24.0091	24.012	24.0471	24.0071	24.0687
Mg/Mg+Fe2+	0.5863	0.4049	0.467	0.4883	0.3462	0.3311	0.5382	0.4727	0.455	0.4174	0.5494
Cr/Cr+Al	0.4715	0.3136	0.4193	0.3684	0.2988	0.3982	0.4853	0.4212	0.5277	0.4666	0.4649
Fe3+/ (Cr+Al+Fe3+)	0.0806	0.0024	0.065	0.02	0.0111	0.0107	0.0478	0.0545	0.1082	0.0419	0.1307

Al_2O_3-MgO diagram, it was seen that all samples were clustered over less depleted pyrolite zone (Figure 14).

In MgO/SiO_2-Al_2O_3/SiO_2 diagram (Figure 15), the MgO/SiO2 value in abyssal peridotites systematically decreases due to loss in MgO during the degradation period at the sea bottom (Snow and Dick, 1995; Niu, 2004, Paulick et al., 2006). MgO/SiO_2 decrease with Al_2O_3 increase can be explained by the process of suction of the melt at the thermal boundary layer (Niu, 2004; Paulick et al., 2006).

DISCUSSION AND RESULTS

As a result of geological, mineralogical and geochemical studies carried out in harzburgitic tectonites belonging to Eldivan Ophiolites, it was determined that these units represented the residual mantle after partial melting. Within tectonites, the increase in dunitic zones, gabbro and pyroxenolith phyllonites from bottom to top was interpreted as the partial melting grade had increased towards top. As a result of assessment of the chemical and all rock analyses of minerals forming peridotites of the Eldivan Ophiolite, it was considered that these rocks had been

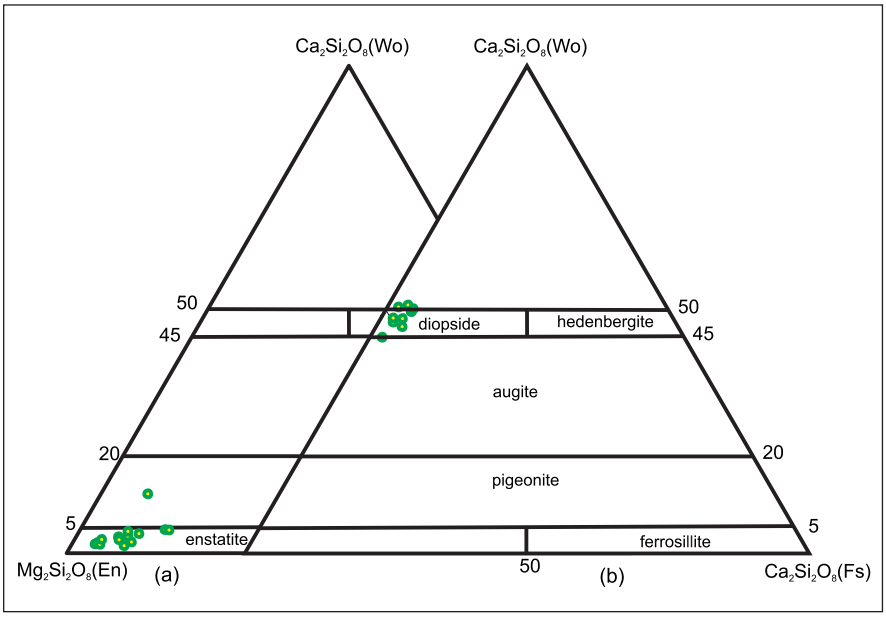

Figure 9- En-Wo-Fs distribution diagrams of (a) orthopyroxene and (b) clinopyroxene minerals in harzburgite samples of the Eldivan Ophiolite (after Morimoto, 1989

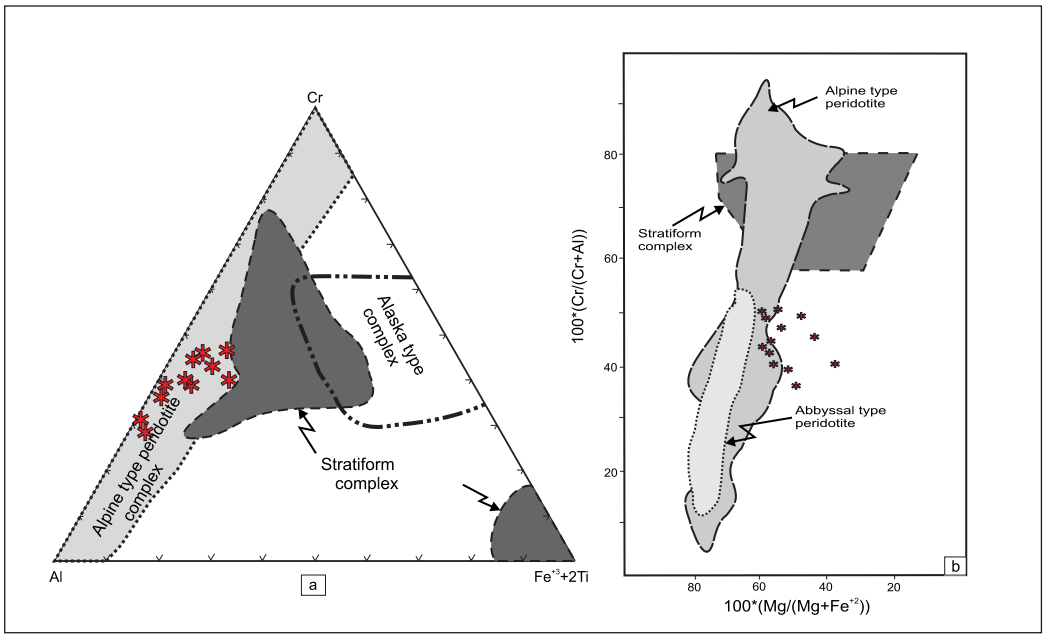

Figure 10- Plot diagrams of Cr-spinels of the Eldivan Ophiolite. a) Al-(Fe^{+3} + 2Ti)-Cr (modified from Jan and Windley, 1990), b) 100*Cr/(Cr+Al) ile 100*Mg/(Mg+Fe^{+2}) (modified from Dick and Bullen, 1984).

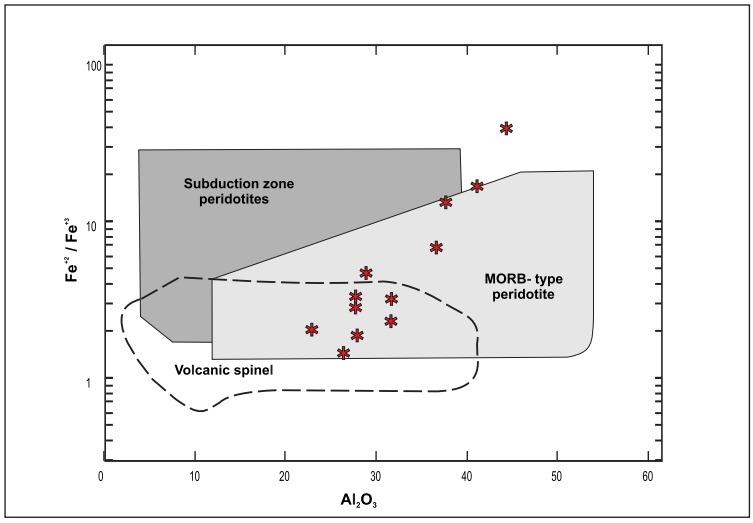

Figure 11- Display of Cr-spinel minerals on Fe^{+2}/Fe^{+3} - Al_2O_3 diagram (modified from Kamenetsky et al., 2001).

Table 5- The resutls of major oxide analyses of peridotites of the Eldivan Ophiolite.

	KM-1	KM-2	KM-3	KM-5	KM-7	KM-9	SB-3	SB-6
SiO_2	41.32	37.65	41.79	37.99	42.49	43.21	40.38	42.21
Al_2O_3	1.07	0.15	1.18	0.14	1.45	0.98	1.25	0.73
Fe_2O_3	8.15	8.55	8.2	8.9	7.79	8.24	6.98	8.55
MgO	38.1	38.92	37.83	37.26	37.46	38.23	39.11	38.79
CaO	1.46	0.59	1.34	0.39	1.41	1.41	0.62	0.81
Na_2O	<0.01	<0.01	<0.01	<0.01	<0.01	<0.01	<0.01	<0.01
K_2O	<0.01	<0.01	<0.01	<0.01	<0.01	<0.01	<0.01	<0.01
TiO_2	0.01	0.03	0.01	0.02	0.03	0.03	0.03	0.04
P_2O_5	<0.01	<0.01	0.01	<0.01	<0.01	<0.01	<0.01	<0.01
MnO	0.12	0.11	0.12	0.11	0.12	0.12	0.16	0.15
NiO	0.27	0.31	0.26	0.31	0.25	0.28	0.35	0.38
Cr_2O_3	0.398	0.222	0.409	0.206	0.423	0.362	0.182	0.218
LOI	8.41	12.8	8.18	14.01	7.92	8.14	7.44	7.61
H_2O-	0.47	0.97	0.55	1.17	0.7	1.01	0.41	0.89
H_2O+	8.56	11.24	8.35	11.61	8.19	8.59	9.13	8.63
Ba	<5	<5	<5	<5	<5	<5	<5	<5
Sr	2	23	2	15	<2	2	18	21
Zr	<5	10	<5	<5	<5	<5	5	5
Y	<3	<3	<3	<3	<3	<3	<3	<3
Sc	12	5	12	5	13	12	12	12
Cu	0.003	<0.001	0.001	<0.001	0.002	0.002	0.003	0.004
Co	0.01	0.012	0.01	0.011	0.009	0.012	0.009	0.016

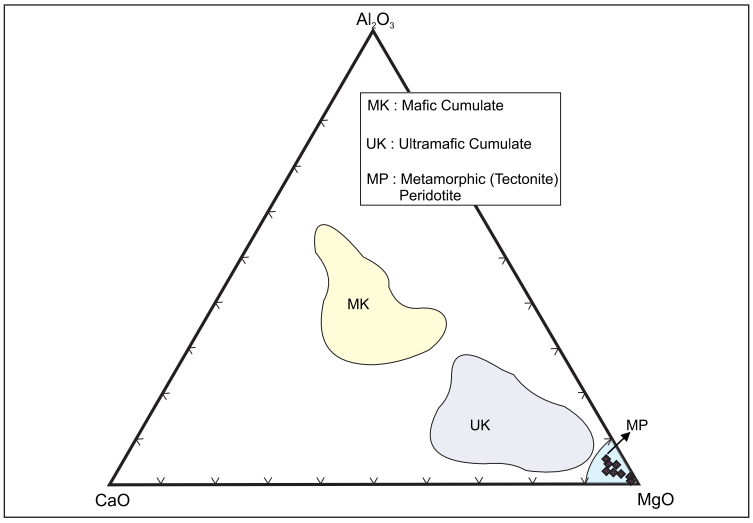

Figure 12- The plots of ultramafic rocks on $CaO-Al_2O_3-MgO$ ternary diagrams belonging to the Eldivan Ophiolite (after Coleman, 1977).

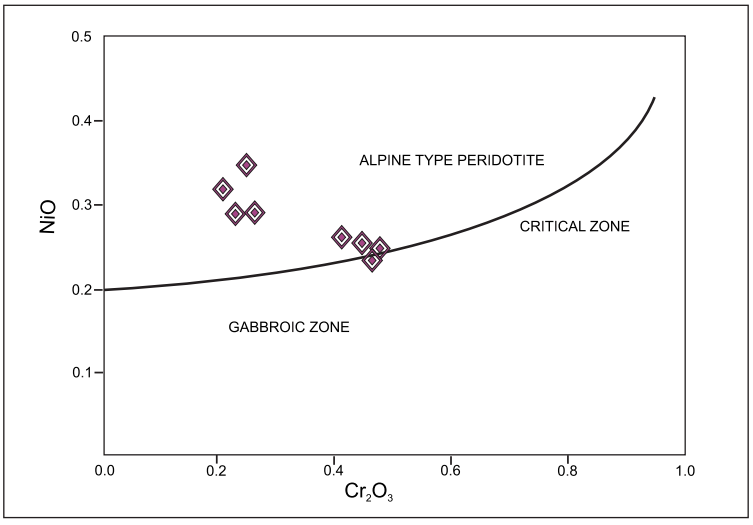

Figure 13- The plots of tectonite samples of the Eldivan Ophiolite on Cr_2O_3 - NiO diagram (after Irvine and Findlay, 1972).

derived by a low grade partial melt from a tholeiitic melt (for instance MORB). As a result of all rock chemical analyses, Mg proportions to be in high and Al and Ca proportions to be in low values show that rocks developed by the low grade partial melting of the primary mantle source and by its excess consumption. The percentage of Mg# in olivine minerals to be approximately 90 - 94% interval indicates that the origin of olivines occurring in peridotites is also mantle source.

When the formation of depleted harzburgite and dunites have reasons such as melting,

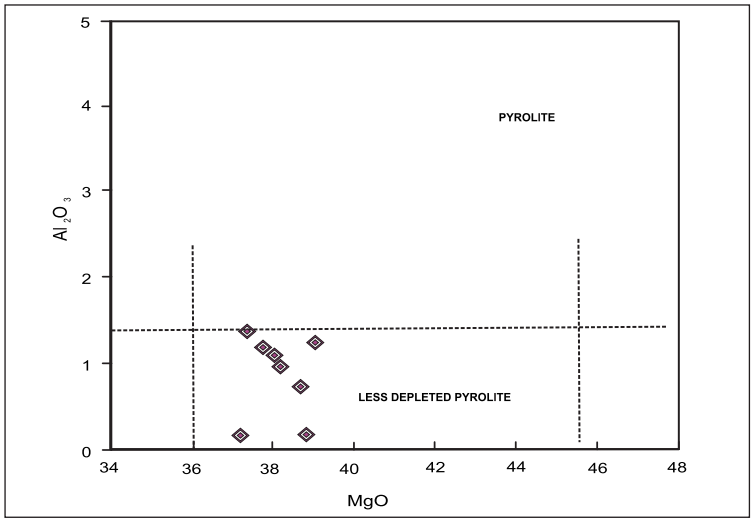

Figure 14- The distribution tectonites of the Eldivan Ophiolite on Al_2O_3-MgO diagram (after Ringwood, 1975).

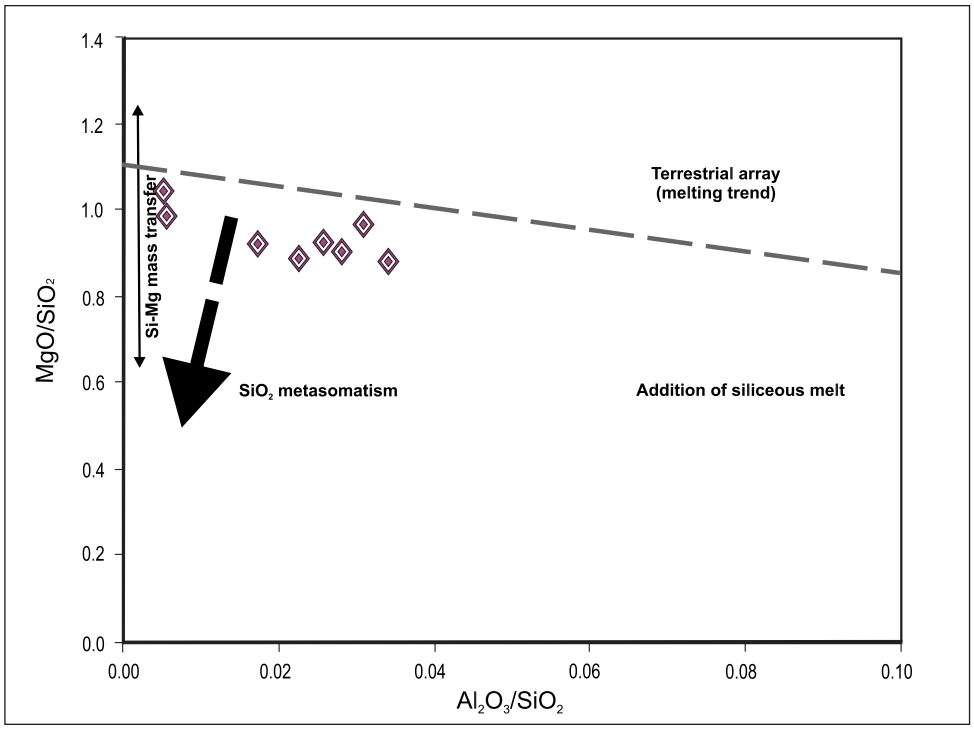

Figure 15- The diagram showing the plots of harzburgitic tectonites of the Eldivan Ophiolites on MgO/SiO_2 - Al_2O_3/SiO_2 diagram. Examples shown in the diagram present a parallelism with the boundary shown as dotted line and defined by the terresterial region (Jagoutz et al., 1979). The geochemistry of the samples is controlled by their modal mineralogical compositions and hydrothermal alterations (from Paulick et al., 2006).

mantle - melting interaction and mantle metasomatism are considered (Kelemen et al, 1992; Zhou et al., 1996; Uysal et al., 2007), it is inferred that harzburgite and dunite samples of the Eldivan Ophiolite were depleted rocks at different grades. Besides, number of Cr# in tectonite samples to be at variable proportions is one the best examples of he partial melting grade in mantle peridotites (Dick and Bullen, 1984; Arai, 1994; Tamura and Arai, 2006; Uysal et al., 2007).

Dunite and harzburgites are typical residuals of mantle melting in pyrolitic model (Wilson, 1993; Blatt and Tracy, 1996). The occurrence of residual type harzburgite and dunites depleted by Al_2O_3 in mid oceanic ridges too (Bacak and Uz, 2003) indicates that tectonites of the Eldivan Ophiolites were formed by depleted mantle.

ACKNOWLEDGEMENTS

This study has been supported by project number 2008-FBE-D006 of the Department of Scientific Research Projects of Yüzüncü Yýl University. The authors are kindly indebted to Ýrem Arat, E. Merter Bilgin and to Kerem Mustafa Avcý for their helps, discussions and suggestions during the improvement of this aricle.

Manuscript received March 24, 2011

REFERENCES

Adamia, S. A., Lordkipanidze, M. B. and Zakariadze, G. S., 1977, Evolution of an active continental margin as exemplified by the Alpine history of the Caucasus, Tectonophysics, 40, pp: 183-199.

Akyürek, B., 1981, Ankara Melanjýnýn Kuzey Bölümünün Temel Jeoloji Özellikleri, Türkiye Jeoloji Kurumu 35. Bilimsel ve Teknik Kurultayý, "Ýç Anadolu Jeolojisi Sempozyumu", Tebliðler kitabý, pp: 41-45.

_____, Bilginer, E., Çatal, E., Daðer, Z., Soysal, Y. and Sunu, D., 1979, Eldivan Þabanözü (Çankýrý) Dolayýnda Ofiyolit yerleþmesine Ýliþkin Bulgular, Jeoloji Mühendisliði, 9, pp: 5-11.

Arai, S., 1994, Characterization of spinel peridotites by olivine - spinel compositional relationships: review and interpretation, Chem. Geol., 113, pp: 191-204.

Bacak, G. and Uz, B., 2003, Daðardý güneyi (Kütahya) Ofiyoliti'nin jeolojisi ve jeokimyasal özellikleri: Istanbul Technical University, Mühendislik Dergisi, 2, (4), pp: 86-98.

Bailey, E.B. and McCallien, C., 1953, Serpentine lavas, the Ankara melange and the Anatolian thrust, Transactions Royal Society, Edinburgh, 62, pp: 403-442.

Blatt, H. and Tracy, J. R., 1996, Petrology: Igneous, sedimentary and metamorphic: W.H. Freeman Company Pres, New York, USA, 350 p.

Cameron, E. N., 1975, Post cumulus and subsolidus equilibration of chromite and coexisting silicates in the Eastern Bushveld Complex. Geochimica et Cosmochimica Acta, 39, pp: 1021-1033.

Coleman, R.G., 1977, Ophiolites: Ancient Oceanic Lithosphere?, Springer-Verlag, Berlin, Heidelberg, 229 p.

Çakýr, Ü., 2009, Structural and geochronological relationships of metamorphic soles of eastern Mediterranean ophiolites to surrounding units: indicators of intraoceanic subduction and emplacement, International Geology Rewiev, 51, 3, pp: 189-215.

Dangerfield, A., 2008, Geochemistry, structure and tectonic evolution of the Eldivan Ophiolite, Ankara Melange, central Turkey, Department of Geological Sciences, Brigham Young University, Master of Science, 51 p.

Dick, H. J. B. and Bullen, T., 1984, Chromian spinel as a petrogenetic indicator in abyssal and alpine-type peridotites and spatially associated lavas. Contribution of Mineralogy Petrology, 86, pp: 54-76.

Droop, G.T.R., 1987, A general equation for estimating Fe^{+3} concentrations in ferromagnesian silicates and oxides from microprobe analyses using

stoichiometric criteria. Mineralogical Magazine, 51: pp: 431-435.

Engin, T., Balcý, M., Sümer, Y. and Özkan, Y.Z., 1980, Guleman (Elazýð) krom yataklarý ve peridotit biriminin genel jeolojik konumu ve yapýsal özellikleri, Maden Tetkik ve Arama Dergisi, 95-96, pp: 77-101.

Floyd, P.A., 1993, Geochemical discrimination and petrogenesis of alkali basalt sequences in part of the Ankara melange, Central Turkey. J. Geol. Soc., London, 150, pp: 541-550.

Gökten, E. and Floyd, P.A., 2007, Stratigraphy and geochemistry of pillow basalts within the ophiolitic melange of the Izmir-Ankara-Erzincan suture zone: implications for the geotectonic character of the northern branch of Neotethys: International Journal Of Earth Sciences, 96, pp: 725-741 (Geology Rundsch).

Göncüoðlu, M.C., Yalýnýz, K. and Tekin, U.K., 2006, Geochemistry, Tectono - Magmatic Discrimination and Radiolarian Ages of Basic Extrusives within the Izmir-Ankara Suture Belt (NW Turkey): Time Constraints for the Neotethyan Evolution, Ofioliti 31, pp: 25-38.

Hakyemez, Y., Barkurt, M.Y., Bilginer, E., Pehlivan, Þ., Can, B., Daðer, Z. and Sözeri, B., 1986, Yapraklý - Ilgaz - Çankýrý - Çandýr Dolayýnýn Jeolojisi. General Directorate of Mineral Research and Exploration (MTA), Report No: 7966, 114 p., Ankara (unpublished)

Irvine, T. A. and Findlay, T. C., 1972, Alpine type peridotite with particular reference to the bay of island igneous complex: Publications of the Earth Physics Brach, Department of Energy, Mines and Resources, Ottowa, Canada, 42, pp: 97-128.

Jackson, E. D. and Thayer, T. P., 1972, Some criteria for distinguishing between stratiform concentric and Alpin peridotite - gabbro complexes: 24th International Geological Congress, Montreal, Canada, pp: 289-296.

Jagoutz, E., Palme, H., Baddenhausen, H., Blum, K., Cendales, M., Dreibus, G., Spettel, B., Lorenz, V. and Waenke, H., 1979. The abundance of major, minor and trace elements in the Earth's mantle as derived from primitive intramafic modules. In: Merrill, R. B., Bogard, D. D., Hoerz, F., Mc Kay, Dç S. And Robetson, D. C. (Eds.) Proceeding of the Lunar and Planetary Science Conference, 2:2, 031-2, 050, Pergamon New York.

Jan, M.Q. and Windley, B.F., 1990, Chromian Spinel - Silicate Chemistry in Ultramafic Rocks of the Jijal Complex, NW - Pakistan, Journal of Petrology, 31, pp: 666-715.

Kamenetsky, V. S., Crawford, A. J. and Meffre, S., 2001, Factors controlling chemistry of magmatic spinel: an empirical study of associated olivine, Cr-spinel and melt inclusions from primitive rocks, Journal of Petrology, 42, pp: 655-671.

Kelemen, P.B., Dick, H. J. B. and Quick, J.E., 1992, Formation of harzburgite by pervasive melt rock reaction in the upper mantle, Nature, 358, pp: 635-641.

Khain, V., 1975, Structure and main stages in the tectono - magnetic development of the Caucasus: an attempt at geodynamic interpretation. American Journal of Science, 275-A, pp: 131-156.

Kimball, K. L., 1990, Effects of hydrothermal alteration on the compositions of chromian spinels, Contributions to Mineralogy and Petrology, 105 (3), pp: 337-346.

Knipper, A.L., 1980, The tectonic position of ophiolites of the Lesser Caucasus in Panayiotou, A. (ed), Ophiolites, Proceeding of International Ophiolite Symposium, Cyprus, 1979, pp: 372-376.

Matsukage, K. and Kubo, K., 2003, Chromian spinel during melting experiments of dry peridotite (KLB.1) at 1.0.2.5 GPa. Am. Mineral, 88, pp: 1271-1278.

Morimoto, N.,1989, Nomenclature of pyroxenes. Canadian Mineralogist, 27, pp:143-156.

Niu, Y., 2004, Bulk-rock major and trace element com position of abyssal peridotites: implications for mantle melting, melt extraction and post-melt-

ing processes beneath mid-ocean ridges, Journal of Petrology, 45, pp: 2423-2458.

Okay, A. I. and Tüysüz, O., 1999, Tethyan sutures of northern Turkey: In B. Durand, L. Jolivet, E. Horvath and M. Serrane (Eds.), The Mediterranean Basins, extension within the Alpine Orogen, Geological Society London Special Publication, 156: pp: 475-515.

Önen, P and Hall, R., 1993, Ophiolites and related metamorphic rocks from the Kütahya region, north- west Turkey, Geological Journal, 28, pp: 399-412.

Paulick, H., Bach, W., Godard, M., De Hoog, J.C.M., Suhr, G. and Harvey, J., 2006 Geochemistry of abyssal peridotites (Mid-Atlantic Ridge, 15°20' N, ODP Leg 209): Implications for fluid/rock interaction in slow spreading environments, Chemical Geology, 234, pp:179-210.

Ringwood, A. E., 1975, Composition and petrology of the earth's mantle: McGraw Hill, New York, USA, 618 p.

Rojay, B., Yalýnýz, K. and Altýner, D., 1995, Age and Origin of Some Spilitic Basalts from Ankara Melange and their Tectonic Implications to the Evolution of Northern Branch of Neotethys. Cenral Anatolia, International Earth Sciences Colloquium on the Aegean Region, Abstracts, 82 p.

_____, _____ and _____, 2001, Age and Origin of some Pillow Basalts from Ankara Melange and Their Tectonic Implications to the Evolution of Northern Branch of Neotethys, Central Anatolia. Turkish Journal of Earth Sciences, 10, pp: 93-102.

_____, Altýner, D., Özkan-Altýner, S., Önen, A. P., James, S. and Thirlwall, M. F. 2004, Geodynamic significance of the Cretaceous pillow basalts from North Anatolian Ophiolitic Melange Belt (central Anatolia, Turkey), Geodinamica Acta, pp: 349-361.

Singh, A.K., 2009, High-Al chromian spinel in peridotites of Manipur Ophiolite Complex, Indo-Myanmar Orogenic Belt: implication for petrogenesis and geotectonic setting, Current Science, 96, 7, pp: 973-978.

Snow, J. E. and Dick, H. J. B., 1995, Pervasive magnesium loss by marine weathering of peridotite, Geochim, Cosmochim, Acta 59, pp: 4219-4235.

Þengör, A.M.C. and Yýlmaz, Y., 1981, Tethian evolution of Turkey: A plate tectonic approach, Tectonophysics, 75, pp: 181-241.

Tamura, A. and Arai, S., 2006, Harzburgite - dunite - orthopyroxenite suite as a record of supra-subduction zone setting for the Oman ophiolite mantle, Lithos, 90, pp: 43-56.

Tankut, A., 1984. Basic and ultrabasic rocks from the Ankara melange, Turkey. In: Dixon. J.E. and Robertson A.H.F. (Eds.) The geological evolution of eastern Mediterranean. Geological Society of London, Special Publication 17, 441-447.

_____ and Gorton, M.P., 1990. Geochemistry of a mafic-ultramafic body in the Ankara melange, Anatolia, Turkey; evidence for a fragment of oceanic lithosphere. Ophiolites, oceanic crustal analogues, Troodos 1987 Symp. Proc. 339-349.

Uysal, Ý., Kaliwoda, M., Karslý, O., Tarkian, M., Sadýklar, M.B. and Ottley, C.J., 2007, Compositional variations as a result of partial melting and melt-peridotite interaction in an upper mantle section from the Ortaca Area, Southwestern Turkey, The Canadian Mineralogist, Vol: 45, pp:1471-1493.

Yalnýz, K., Göncüoðlu, M. C. ve Floyd, P.A., 1988. Geochemistry and geodynamic setting of basic volcanics from the northernmost part of the Ýzmir-Ankara branch of Neotethys. Central Sakarya Region, Turkey. 3 Int. Turkish Geology Symposium 31 August - 4 September 1998 Ankara, Abstracts, 174.

Wilson, M., 1993, Igneous petrogenesis: A global tectonic approach, Chapman & Hall Pres, New York, USA, 446 p.

Zhou, M., Robinson, P.T., Malpas, J. and LI, Z., 1996, Podiform chromitites in the Luobusa ophiolite (Southern Tibet): implications for melt rock interaction and chromite segregation in the upper mantle, Journal of Petrology, 37, pp; 3-21.